JAERI-M
86-063

A USER'S MANUAL FOR SCOPERS-2;
A STATIC CORE PERFORMANCE SIMULATOR FOR LIGHT WATER REACTORS [VERSION2]

March 1986

Takanori SHIMOOKE* and Masafumi ITAGAKI

日本原子力研究所
Japan Atomic Energy Research Institute

JAERI-Mレポートは，日本原子力研究所が不定期に公刊している研究報告書です。
入手の問合わせは，日本原子力研究所技術情報部情報資料課（〒319-11茨城県那珂郡東海村）あて，お申しこしください。なお，このほかに財団法人原子力弘済会資料センター（〒319-11 茨城県那珂郡東海村日本原子力研究所内）で複写による実費頒布をおこなっております。

JAERI-M reports are issued irregularly.
Inquiries about availability of the reports should be addressed to Information Division Department of Technical Information, Japan Atomic Energy Research Institute, Tokai-mura, Naka-gun, Ibaraki-ken 319-11, Japan.

©Japan Atomic Energy Research Institute, 1986

編集兼発行　日本原子力研究所
印　　刷　いばらき印刷㈱

JAERI-M 86-063

A User's Manual for SCOPERS-2, A Static Core Performance Simulator for Light Water Reactors [Version 2]

Takanori SHIMOOKE* and Masafumi ITAGAKI

Department of Nuclear Ship Engineering
Japan Atomic Energy Research Institute
Toranomon, Minato-ku, Tokyo

(Received March 11, 1986)

SCOPERS-2 is a new version to the FLARE program which had been developed to simulate the core physical characteristics of boiling water reactors. A generalized FLARE type nodal equation is used in SCOPERS-2 together with the nodal-form neutron migration kernel which is derived in a relatively rigorous theoretical way and replaces the empirical kernel used in the FLARE. The effort was also made to expand the flexibility of the original FLARE program. The resultant program, SCOPERS-2, has reliable theoretical basis and can be applied to both PWR and BWR with wider options than before.

Present report describes the code performance, the physical model used in SCOPERS-2, and describes in detail the format of the input data required to execute various options available in this program. The input and output of sample problems for both PWR and BWR are represented to help user's understanding. Derivation of the new migration kernel is also shown in Appendix.

Keywords: Manual, SCOPERS-2 Code, BWR, PWR, Nodal Equation, Migration Kernel, Core Physical Characteristics, Nuclear Ship Mutsu

---

* Nuclear Power Engineering Test Center, Institute of Nuclear Safety

JAERI－M 86－063

軽水炉核特性シミュレーション計算コードSCOPERS－2
使　用　手　引　書

日本原子力研究所むつ事業所原子力船技術部
下桶　敬則*・板垣　正文

（1986年3月11日受理）

SCOPERS－2は，沸騰水型原子炉の炉心特性シミュレーション用に開発されたFLAREプログラムをさらに発展させたプログラムである。SCOPERS－2では，FLAREの場合よりも一般化されたノード方程式を用いており，またFLAREで用いられた経験的なノード間中性子移動カーネルもより厳密に導出されたものに変更されている。さらに，FLAREのもっていた諸シミュレーション機能が広く拡充されている。これらの結果，計算モデルの信頼性が理論的に裏づけられ，かつ，BWRのみならずPWRへも適用できるようになった。

本報告書では，SCOPERS－2の機能，物理モデルについて記述すると共に，入力データの作成法について詳細に記述してある。利用者の理解を助けるためにBWRとPWR両方の例題につきサンプル入出力を示してある。新しい中性子移動カーネルの導出についても付録に示してある。

原子力船部門分室　〒105 東京都港区虎の門一丁目15番16号
*㈱原子力工学試験センター，原子力安全解析所

CONTENTS

目　　次

I. Introduction

SCOPERS-2 program is a new version to the FLARE program[1] which solved first but intuitively a three-dimensional coarse-mesh neutronic-balance equation to determine reactor core reactivity and core power distributions for scoping evaluations of the physical characteristics of the boiling water reactor.

Some basic studies have been made so far by one of the authors to improve the physical model employed in the FLARE program. In the previous report[2], the nodal-form neutron migration kernel was newly derived in a relatively rigorous theoretical way and the so-called FLARE kernel used in the FLARE program was shown not to be "the best kernel that can be obtained" just as so claimed by Delp et al.[1], the authors of FLARE program. It is also suggested that the FLARE equation given in the program has to be modified if the original FLARE kernel is replaced by a proper migration kernel.

Afterward, starting from the general nodal equation derived by Z. Weiss[3], one of the authors showed[2),4] that the degeneration of thermal and epithermal neutrons into one-energy-group under appropriate assumptions in coarse node system resulted in a generalized FLARE-type nodal equation which includes the original FLARE equation as a special case of the application.

This generalized FLARE-type nodal equation together with the migration kernels are incorporated into the FLARE's original program-logics and input-output format. The effort has also been made to improve the flexibility of the program. The resultant program, SCOPERS-2, has the reliable theoretical basis and can be applied to both types of Light Water Reactors, i.e. BWR and PWR, with wider options than before.

SCOPERS (or SCOPERS-2) was written by one of the author (T. Shimooke) for Japan Nuclear Ship Development Agency in March, 1972. This forerunner version of SCOPERS-2 was referred to in the report, JAERI-M 5805[2]. Later, change is made at JAERI so that the revised version, SCOPERS-2 is obtained.

II. GENERAL DESCRIPTION

SCOPERS-2 is a computer program that can perform following calculations for both boiling water reactor (BWR) and pressurized water reactor (PWR);

- three-dimensional (XYZ) steady-state nodal power distribution in the core,
- core reactivity,
- axial void distribution (for BWR) or coolant temperature distribution (for PWR) at any fuel positions in the core, which are compliance with the power distribution,
- three-dimensional burnup distribution in the core and core total burnup.

SCOPERS-2 is designed to perform these calculations by a rather simple model. A neutronic balance is solved by a "generalized FLARE-type nodal equation"[2),4)]. In the framework of a coarse mesh representation of a XYZ core geometry, the equation describes the one-group representative Ψ that is essentially proportional to a fission rate (called hereafter neutron source), in terms of an infinite multiplication constant k_∞ and a "migration kernel" $K_{i\to j}$. An additional simplification includes the replacement of the reflector by an albedo at the core surface so that only mesh points within the active fueled region are considered. In SCOPERS-2, a reactor core can be described by, for example, one horizontal mesh point at the center of each fuel element, and about a dozen of vertical points along the height of the fuel element. This small number of mesh points and the one-group representation of neutrons allow us to have a fast throughput for a three-dimensional core calculation.

The neutron source Ψ at each node is calculated as a function of k_∞ at the node, the sources at the eighteen neighboring nodes, and a "migration kernel" $K_{i\to j}$ which is a measure of the probability that a neutron born at node i is absorbed at node j. This migration kernel is a given function of the noding space L_x, L_y, L_z, the Fermi age τ of thermal neutron and the thermal neutron diffusion area $1/k^2$. These age and area are calculated at each node based on a fit to the moderator void ratio or to the moderator temperature. The infinite multiplication constant is also given by a simple fitting equation which includes the following effects:

(a) Presence (or absence) of a control rod or a rod-cluster.
(b) Local moderator void ratio or temperature.
(c) Power-dependent equilibrium xenon and Doppler reactivity.
(d) Local fuel exposure.

The void (or coolant temperature) calculation consists of a determination of the average steam quality (or coolant enthalpy) at each node based on the inlet mass flow rate, inlet enthalpy, and power integrated from the bottom of the channel to the node of interest. The void (or coolant temperature) is calculated by a numerical fit to a void-quality (or temperature-enthalpy) correlation curve. The inlet mass flow rate is calculated as a simple function of the channel power.

The effects of the loss in reactivity resulting from fuel burnup are included by a simple fit of k_∞ to exposure, exposure-weighted voids, and exposure-weighted local control. The data from which these fits are generated must come from independent, complex calculations, or experimental data.

SCOPERS-2 program involves many portions of FLARE program which are still valid to use. In other words, SCOPERS-2 follows FLARE in its program resources such as basic subroutines and the logic structure, while many modifications and improvements are also included in SCOPERS-2.

Main improvements on the physical model are:

(1) One-group, coarse mesh, neutron balance equation is completely revised from the semi-empirical one to the generalized FLARE-type nodal equation[2),4)] that has a firm foundation.
(2) The nodal interaction is considered between a node and the neighbouring 18 ones. In the old program only 6 neighbouring nodes were considered.
(3) The migration kernel used in the program is given beforehand by analytically integrating the point migration kernel by six-multiple space variables (Reference (2) or see Appendix) so that there is no need to input any adjusting parameter for a kernel as requested by FLARE.
(4) Albedo for the reflector effect is given by the program. A user can input only nuclear constants λ, D, κ and τ_e for top, bottom and peripheral reflectors.

The effect of reflector geometry on albedo is also considered

automatically by built-in logic in the program, so that the user is free from adjusting input of albedo as was at FLARE.

Main improvements on the code flexibility are:

(5) A PWR as well as a BWR can be calculated now under a consistent model and logic.

(6) The relative allocation of control rods to the core nodal assignment is enlarged from four patterns in original to seven for input modeling.

(7) The cross sectional core symmetry conditions in combination with the boundary condition at an axis of symmetry are of 11 varieties for code users (It was 6 at FLARE.).

(8) A critical search option has been completed in the code; a rod-withdrawal search for BWR and a boron-concentration search for PWR.

SCOPERS-2 can make any of the following calculations for BWR and PWR. Each of these are one run which can be performed by one submission of the job if a combination of options is properly selected by the user.

For BWR

1) calculates the three-dimensional power distribution within the core under any of the control rod pattern at an arbitrary reactor power (Power Distribution Calculation).

2) calculates the three-dimensional void distribution in moderator under any of the control rod pattern at an arbitrary reactor power (Void Calculation).

3) calculates the critical withdrawal patterns and length of control rods for a given reactor power (Critical Search).

4) calculates the (thermal) power output of a reactor in compliance with the control rods patterns given (Power Search).

5) calculates the final burnup attained by each fuel element loaded in the core, taking into account the changes of power distribution with the various control patterns encountered during the course of reactor operation (Burnup Trace).

6) takes into consideration the fuel shuffling and the removal of poison curtains during the calculation described in 5) (Burnup Trace with Fuel-Shuffling).

7) predicts the final core burnup to be attained, calculating the power and exposure distributions at each burnup step for which the control rods positioning is searched automatically in accordance with a given priority for the withdrawal, to maintain the power level against the exposure (Critical-Exposure Iteration).

8) performs the above-stated calculation 7) with the predetermined plan on the fuel shuffling (Critical-Exposure Iteration with Fuel-Shuffling).

For PWR

1) calculates the three-dimensional power distirbution within the core at any reactor power under any control program including the part length rod-cluster and boron dilution in the moderator (Power Distribution Calculation).

2) calculates the coolant temperature distributions along the core height at any location of the core under any control program and reactor power (Coolant Temperature Calculation).

3) determines the position of the regulating rod-clusters for a given reactor power and boron concentration (Critical Search).

4) determines the concentration of boron for a given reactor power and position of rod-clusters (Boron Search).

5) calculates the (thermal) power output of a reactor in compliance with the rod-clusters position and the boron concentration given (Power Search).

6) calculates the final burnup attained by each fuel element loaded in the core, through changes of power distribution affected by the rod-clusters position and the boron dilution during the course of reactor operation (Burnup Trace).

7) takes into consideration the fuel shuffling during the calculation described in 6) for PWR (Burnup Trace with Fuel-Shuffling).

8) (Critical-Exposure Iteration).

9) (Critical-Exposure Iteration with Fuel-Shuffling).

The present version of the code will handle a maximum array of $15 \times 15 \times 20$ nodes with mirror, or diagonal, or 90°/180° rotational symmetry. A full-core, half-core, or quarter-core representation is possible with either symmetry, each with or without a central fuel bundle. It needs a core memory of 572 k-byte and File 5 for input, 6 for output and 7 for card punch output. By utilizing a mirror symmetry with a quarter core, a 32-bundle Nuclear Ship Mutsu reactor core can be represented by 432 mesh points; 4 mesh points in each bundle with 12 points along height. Typical CPU time on FACOM M-380 is 8.6 second for a solution of this problem with converged power and moderator temperatures but fixed control rod position and burnup.

III. PHYSICAL MODEL

3.1 Nodal Equation for Source

Presently starting from the general nodal equation derived by Z. Weiss[3], which was based on the response matrix theory, it will be shown that the degeneration of thermal and epithermal neutrons into one-energy-group under appropriate assumptions in coarse node system results in a generalized FLARE-type nodal equation[4] that includes the original FLARE equation as an extreme example of the application.

Being with the two neutron-energy-groups in the Weiss theory in one-dimension, some assumptions are made on the partial incident-neutron current components $j_i^{(1)}$ and $j_i^{(2)}$ of node i for group 1 and 2. It is supposed, for example, that epithermal neutrons incident by $j_i^{(1)}$ into node i complete slowing down within the node and will be all absorbed during diffusion in the same node. Once fission occurs after absorption, the multiplied neutrons will partially leak from node i to the adjacent nodes i-1 and i+1 as an epithermal group. The rest of the multiplied neutrons will leak from the node i as a thermal group. On the contrary, thermal neutrons incident by $j_i^{(2)}$ into node i are all absorbed in the node without producing any new current. The epithermal and thermal neutrons are thus treated in an asymmetric way, which is a feature of the present model.

The final form of the equation derived for the fission rate multiplied by η_{th}, i.e., for $\bar{\Psi}_i \equiv \eta_{th}^i \bar{k}_\infty^i J_i^{(1)}$ of node i is,

$$[1 - k_\infty^i (1 - \sum_m \eta^i K_{i\to m} - \frac{\eta_t^i}{\eta_{th}^i} K_s^i)]\bar{\Psi}_i = k_\infty^i \sum_m \eta^m K_{m\to i} \bar{\Psi}_m, \qquad (1)$$

where $\eta^i \equiv \eta_t^i/\eta_{th}^i + \eta_e^i/(\bar{k}_\infty^i \eta_{th}^i)$.

$\eta_e^i K_{i\to m}$ and $\eta_t^i K_{i\to m}$ are fractions of the migration kernel, $K_{i\to m}$, for epithermal and thermal neutron, respectively. The factors η_e^i and η_t^i are always normalized so that $\eta_e^i + \eta_t^i = 1$. η_{th}^i is the probability that a fission neutron is thermalized in the native node where it is born. k_∞^i and $\bar{k}_\infty^i$ are the infinite multiplication factors for the node i with and without resonance escape probability correction, respectively. K_s^i is

given as $\sum_{m} K_{i\to m}$. Strictly, the equation is derived in one-dimension because the original Weiss equation is not proved rigorously for more than one-dimension. In the application hereafter, however, it is supposed valid also for two- and three-dimension.

The equation (1) is reduced to the original FLARE equation when $\eta_t \simeq 0$ and $\eta \simeq 1$. This implies physically that

(a) the unit node in consideration is relatively small ($\to \eta_t \simeq 0$), and

(b) there is a condition that $(\nu\Sigma_f/\Sigma_a)\cdot\eta_{th} \simeq \eta_e \simeq 1$)

($\to$ the node itself is just or nearly critical in neutron multiplication). It must be noticed that these two conditions (a) and (b) are never satisfied simultaneously in a slightly enriched uranium-fueled thermal reactor.

3.2 Migration Kernel from Node to Node

Migration kernels are shown in Table 3.1 in the form of equation which are used for calculation in the code. These are the probabilities that a neutron born in a node be absorbed in one of the neighbouring nodes during its migration. They are derived by integrating a point migration kernel analytically by using the method described in Appendix in this report.

Table 3.1 A Summary of the Kernels Used in SCOPERS-2

Direction	Nodal Migration Kernel
for the x- or y-direction	$K_{xx} \equiv \frac{q}{V}\sqrt{\frac{\tau}{\pi}}\left[\left\{L_y L_z - \frac{8}{3\pi}L_x(L_y+L_z) + \left(\frac{67}{12\pi}-1\right)L_x^2\right\}\cdot A_1(L_x) + \left\{\frac{4\alpha}{3\pi}\frac{L_y+L_z}{L_x} - \left(\frac{67}{12\pi}-1\right)\right\}\tau\cdot A_2(L_x)\right]$
for the z-direction	$K_{zz} \equiv \frac{q}{V}\sqrt{\frac{\tau}{\pi}}\left[\left\{L_x L_y - \frac{8}{3\pi}(L_x+L_y)L_z + \left(\frac{67}{12\pi}-1\right)L_z^2\right\}\cdot A_1(L_z) + \left\{\frac{4\alpha}{3\pi}\frac{L_x+L_y}{L_z} - \left(\frac{67}{12\pi}-1\right)\right\}\tau\cdot A_2(L_z)\right]$
for the diagonal direction in x-y plane	$K_{xy} \equiv \frac{1}{2}\frac{q}{V}\sqrt{\frac{\tau}{\pi}}\left[\left\{\frac{8}{3\pi}L_x L_z - \left(\frac{67}{12\pi}-1\right)L_x^2\right\}\cdot A_1(L_x) + \left\{-\frac{4\alpha}{3\pi}\frac{L_z}{L_x} + \left(\frac{67}{12\pi}-1\right)\right\}\tau\cdot A_2(L_x)\right]$
for the diagonal direction in x-z plane	$K_{xz} \equiv \frac{1}{2}\frac{q}{V}\sqrt{\frac{\tau}{\pi}}\left[\left\{\frac{8}{3\pi}L_x L_z - \left(\frac{67}{12\pi}-1\right)L_z^2\right\}\cdot A_1(L_z) + \left\{-\frac{4\alpha}{3\pi}\frac{L_x}{L_z} + \left(\frac{67}{12\pi}-1\right)\right\}\tau\cdot A_2(L_z)\right]$
Notes	$V = L_x L_y L_z$, $\alpha = 1.1681$, $A_1(L_x) =$ Eq. (46), $A_2(L_x) =$ Eq. (48) $K_{11} = 1 - 4K_{xx} - 2K_{zz} - 4K_{xy} - 8K_{xz}$ $q \equiv \dfrac{\left\{\frac{2}{R_0}f\left(\frac{R_0}{2\sqrt{\tau}}\right) + \frac{R_0(2\kappa^2\tau+1)}{(2\kappa\tau)^2 - R_0^2}\right\}e^{-R_0^2/4\tau}}{\left\{\frac{2}{R_0}f\left(\frac{R_0}{2\sqrt{\tau}}\right) + \frac{R_0(2\kappa^2\tau+1)}{(2\kappa\tau)^2 - R_0^2}\right\}e^{-R_0^2/4\tau} - \left\{\frac{2}{R_1}f\left(\frac{R_1}{2\sqrt{\tau}}\right) + \frac{R_1(2\kappa^2\tau+1)}{(2\kappa\tau)^2 - R_1^2}\right\}e^{-R_1^2/4\tau}}$ $R_0 = 0.3582\sqrt{L_x^2 + L_y^2 + L_z^2}$, $R_1 = R_0 + L_x$

IV. Input Data Requirements

4.1 Node and the Numbering

A node is supposed in this program to be a rectangular prism with a square base. Moreover the height Lz is not much greater or smaller than Lx(=Ly). It is not recommended that Lz $\geq$ 1.5Lx or Lz $\leq$ 0.5Lx. The node numbering used in the program is shown in Fig. 4.1 where Node 1,1,1 is in the far left corner at the bottom. Where it is necessary to specify a particular edge or corner of a node (such as control rods when they are not in the center of a node), the following convention is used: The far left-hand corner at the top of each node is given the same index as the node itself.

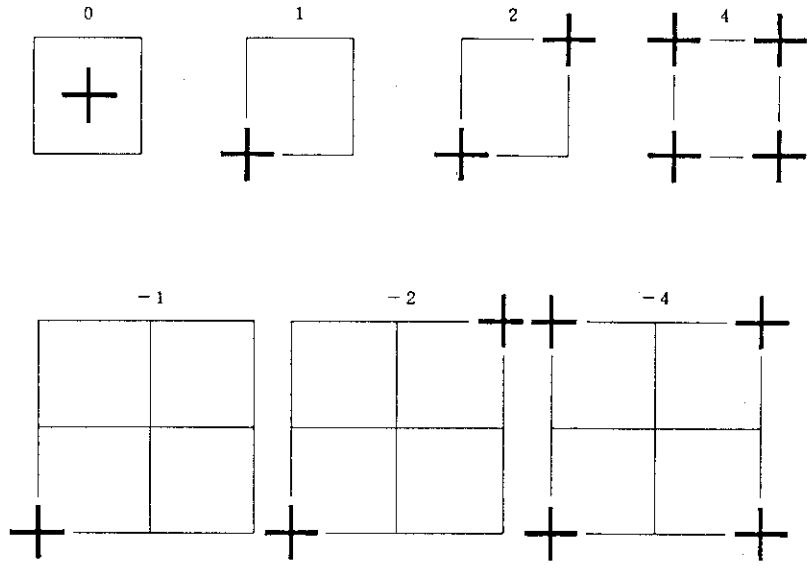

Fig. 4.1 Rod/Cell options.

4.2 General Input Philosophy

Every card carries three 2-digit descriptors and 64 columns of free-form data. The descriptors always replace any descriptors previously read from this card type. Since descriptors are sometimes used to designate running options, options to be continued must be repeated on overlay cards of that type. In other words, a blank descriptor is interpreted as a zero and is so stored.

General data on the remainder of the cards, however, are always

considered as overlay and skipped values remain unchanged from their previous setting. Therefore, no card need be read in if the data from this card are already contained in memory.

The effect of an Independent Case Card is to clear memory to zero and then to initialize three arrays to unity. The three arrays set to one are the source-guess, S, the fractional-flow, F, and the partial-fuel factor, XK. Input to these arrays then need include only changes from unity. Input to other arrays need include only changes from zero. If any source values are read in, the source array is renormalized to one. No other input array is ever normalized.

In general, no cards of a type need to be read if no change in that type of data is to be made. However, it is imperative that all cards which are used be ordered by card type from smallest to largest.

4.3 Card Order

The first card must be a CASE Card (see Section 4.5). The card following a CASE Card must be Type 01 for an independent case. Subsequent data cards must be ordered by card type. A Terminal Card, Type 99, must follow data cards to initiate calculation.

It is possible to use a basic input deck and follow it with a modification or overlay deck pertinent to a particular problem. The overlay deck must be preceded by a Reorder Card, Type 33. The effect of this card is to reset the counters to accept a new sequence of ordered card types so that the overlay deck need not be merged with the basic deck to maintain a single ordered sequence of card types. A Reorder Card must be inserted before every card whose type is lower than or equal to the preceding card.

Following every Terminal Card, Type 99, either a CASE Card or a LAST Card must be used. The CASE Card will leave input and calculated values unchanged from the previous case if it carries a left parenthesis in Column 1, designating a dependent case.

4.4 Card Format

All data input cards have the same format (except when ID cards are used, see card type 10A). Any characters may be punched in columns 1-10 for user identification. Three 2-column descriptors are punched in columns 11-16. The first descriptor is the Card Type, punched in columns

11-12. The other two descriptors are used for further identification and for running options.

The general data supplied on each data card is punched in free form in columns 17 through 80. Free form requires that each number be separated by one or more spaces or commas from its neighbors. Thus, no spaces may occur between the characters of a single value. Decimal points are not required unless the value is non-integer. Exponential scaling is optional with or without an E and followed by a signed integer scaling factor. (Thus, minus pi may be punched as -314.159-2 where the 10 characters are contiguous). +10.2 and 10.2 are both allowed.

Additional flexibility is possible by the use of bSnb for spacking by or skipping n values in the input array and by the use of bRnb for repeating the last given number n MORE times. (Thus, b1bR12bS2b3b would store unity in the first thirteen elements of the array designated by card type, would leave the 14th and 15th values unchanged, and would store 3.0 in the 16th). Note that a maximum of 16 words per card is allowed. This applies to repeats and skips also (bR10b counts as ten additional words).

It is possible that the required data will not fit on a single card. Sequential data can be continued on successive cards without limit. Numbers may not be split between cards, and blanks are never required in Columns 17 and 80. Each continuation card, however, must have punches in Columns 11-16 which are identical with those on the preceding card.

It is recommended for ease of reading and checking of the input that decimal points not be used with integers and that the configuration of geometrically dependent quantities be arranged in a regular form similar to the reactor core shape. It is usually better to repeat integers and zeros explicitly than to use repeat and skip options.

4.5 Input Descriptions by Card Type

Type CASE

Columns	Content	Description
1 ∿ 5	)bbbb	This is an independent case, input data shall be all initialized.
	or	
	(bbbb	This case is dependent on the preceding case, and the revised and/or newly added data are only required.
	or	
	)LAST	terminates a batch of runs of calculations.
6 ∿ 69		Any alphanumeric statement, edited as a heading on every page of output.

Type 01

Columns	Content	Description
11 ∿ 12	01	
13 ∿ 14	B/P	=0; selects BWR type calculation. =1; selects PWR type calculation.
15 ∿ 16	BRN-LST	=0; the program will calculate a source for the exposure distribution up to and including $E=E_{max}$. =1; an extra exposure distribution is calculated for $E=E_{max} + \Delta E$ after the last source calculation is over for $E=E_{max}$.
17 ∿ 80		FREE FORM DATA

Columns	Content	Description
	E_o	Initial average core exposure in 1000MWD/T.
	E_{max}	Maximum average core exposure (in 1000MWD/T) for which a source is to be calculated.
	ΔE	Amount (in 1000MWD/T) that the program is to advance the average core exposure for every source recalculation until E_{max} is reached.
	p^{th}	Thermal power of the reactor in MW. The program assumes the constant†) power level p^{th}

†) For different power level calculation, use the "dependent case" option, specifying E_o and E_{max} for each power level.

during calculation for E_o through E_{max}.
This is also used as the initial guess for the power level, when the power search option is chosen.

p^{rated} Rated power of the reactor in MW.

ΔX Node width (cm) = ΔY.

ΔZ Node length in axial direction (cm).

Rod/Cell This number specifies the relative location of control rods to a node, and therefore their effect to the node. These are specified as shown below.

=0; a node has a control rod in it and is affected directly and fully by the rod when inserted.

=1; a node has a control rod at the corner and is affected by 1/4 worth of the rod inserted.

=2; a node has two control rods at the two corners, and is exerted separately by 1/4 worth of each rod

=4; a node has four control rods at the all corners, and is governed separately by any rod, each by 1/4 control-worth.

=-1; a four-node group is exerted an equal effect in the member node by a control rod positioned at the group corner.

=-2; a four-node group is controlled equally in the member node by each of two control rods which are at the two corners of the group and act separately.

=-4; a four-node group is controlled equally in the member node by one of four control rods which are located at the group corners and have a separate effect.

See also Figure 4.1.

NOTE: If Rod/Cell > 0, then a control rod positioned at a corner is thought to govern the nearest 4 nodes. If Rod/Cell < 0, then a control rod at a node corner is supposed to have an effect also on the peripheral 12 nodes beyond the nearest 4 nodes.

BC — Boundary condition indicator. Figures 4.2 through 4.3 illustrate the following table. (See also the foot note††)

=9; 1/4 core, diagonal mirror symmetry, with a center node.

=8; 1/4 core, diagonal mirror symmetry, no center node.

=7; 1/4 core, mirror symmetry, with central nodes.

=6; 1/4 core, 90° rotational symmetry, with central nodes.

=5; 1/4 core, mirror symmetry, no central node.

=4; 1/4 core 90° rotational symmetry, no central node.

=3; 1/2 core, mirror symmetry, with central nodes.

=2; 1/2 core, 180° rotational symmetry, with central nodes.

=1; 1/2 core, mirror symmetry, no central node.

=0; 1/2 core, 180° rotational symmetry, no central node.

=-1; Full core.

Each figure shows an x-y plane, and the type of boundary condition is the same for all z.

Any input model requires the symmetric boundaries are placed at the top and left sides just illustrated in Figures 4.2 and 4.3. When BC = 8 and 9, put the symmetric boundaries obliquely at the right and left (not at the upper and lower sides).

I_{max} — Number of nodes in y-direction (≤15).

J_{max} — Number of nodes in x-direction (≤15).

K_{max} — Number of nodes in z-direction (≤20).

β — Boron concentration in primary cooling water for PWR calculation (in 1000ppm).

Leave blank or put zero for BWR calculation.

---

††) To specify BC, one must take into consideration control rod withdrawal pattern and core flow distribution as well as fuel loading pattern.

Type 02

Columns	Content	Description
11 ∿ 12	02	
13 ∿ 14	IPCH	=n; S_{ijk}, E_{ijk}, and V_{ijk} are punched onto cards after every n exposure steps if KPCH = 1.
		=0; S_{ijk}, E_{ijk}, and V_{ijk} are punched at the end of the final exposure step if KPCH = 1.
15 ∿ 16	KPCH	=0; no card punching is done.
		≠0; card punching is done according to IPCH, and KPCH is punched in columns 1 ∿ 2 of S, E and V Cards for identification of run.
17 ∿ 80		FREE FORM DATA
	DSIJK	Convergence criterion for source convergence. If $$\frac{\text{Maximum } \left|S_{ijk}^{n} - S_{ijk}^{n-1}\right|}{S_{ijk}^{n-1}} \leq \text{DSIJK},$$ the source loop is terminated.
	NS	Maximum number of source iterations per moderator void (for BWR) or temperature (for PWR) calculation. Two iterations will be run even if NS < 2.
	DL(S)	Another source convergence criterion. Loop is terminated if $$\left|\lambda_n - \lambda_{n-1}\right| \leq \text{DL(S)}.$$
	NV	Maximum number of void (or temperature) loops per exposure step. If NV = 0, V_{iik} and $k_{\infty ijk}$ are re-calculated but S_{ijk} is not, so that input Source (or Source from previous case) will be used in burnup calculation. On the other hand, if NV ≠ 0, source-void iteration begins.
	DL(V)	If λ from the final source iteration of the previous void loop is less than DL(V) from the λ of the last source iteration of the present void loop, then the void loop is terminated (converged). $$\left|\lambda_v - \lambda_{v-1}\right| \leq \text{DL(V)}$$

DL(SH) This is another void convergence criterion on the quantity labeled SHANK. The source-void iteration is thought to be converged if

$$|\mathrm{SHANK} - \lambda_v| \leq \mathrm{DL(SH)}$$

where

$$\mathrm{SHANK} \equiv \frac{\lambda_v\lambda_{v-2} - \lambda_{v-1}^2}{\lambda_v - 2\lambda_{v-1} + \lambda_{v-2}} .$$

See the next input.

DSHNK One more void convergence criterion, which is back up to the above-stated DL(SH) criterion. The void loop may be converged if

$$|\mathrm{SHANK} - \mathrm{SHANKSQ}| \leq \mathrm{DSHNK}$$

where

$$\mathrm{SHANKSQ} \equiv \frac{\mathrm{SHANK}_v \cdot \mathrm{SHANK}_{v-2} - \mathrm{SHANK}_{v-1}^2}{\mathrm{SHANK}_v - 2\mathrm{SHANK}_{v-1} + \mathrm{SHANK}_{v-2}}$$

Both DL(SH) and DSHNK criteria must be satisfied to terminate the loop.

LMBDA λ_o; the initial guess on λ. It is <u>also</u> the value of λ to converge on for the critical search, the power search, and the fuel reload option.
Zero-input assumes $\lambda = 1.0$.

NOTE: In a sequential burnup calculations, the calculated λ in the previous exposure step will be used as an initial guess for λ for the new step.

JP	Output control for S_{ij}	*
JS	Output control for S_{ijk}	
JV	Output control for V_{ijk}	
JK	Output control for $k_{\infty ijk}$	

* =n: prints them every n iterations in void loop.
=0; doesn't print.

Type 03

Columns	Content	Description
11 ∿ 12	03	
13 ∿ 14	Blank	
15 ∿ 16	ICH	Option for search =-1; Power Search =+1; Critical Search (control rod positioning search). =+2; Boron Search. =0 ; no search at all.
17 ∿ 80		FREE FORM DATA

(When ICH=-1 or +2, the following data should be input in columns 17 ∿ 80.)

NC — >0 ; Maximum number of iterations for Power Search or Boron Search.

DL(C) — Convergence criterion for Power or Boron Search. If

$$|\lambda_c - \lambda_0| \leq DL(C),$$

Power or Boron Search is terminated, where λ_0 is given in input and usually 1.0 (but not limited to).

Δp^{th} ($\Delta\beta$) — Adjusting band to be used for the first guess of power or boron concentration during Power of Boron Search. Δp^{th} must be given a variation in MW per 1% reactivity change. The program guesses first a power according to the equation:

$$p^{th} = p^{th}(\text{initial guess}) + \Delta p^{th}(\lambda - \lambda_0) \times 100,$$

after it has calculated the eigenvalue λ for the p^{th} (initial guess) of the input. At the second guess and thereafter, the program interpolates or extrapolates the two or three previous values to search a power with no input-assistance.
$\Delta\beta$ is given in 1000ppm/1% $\Delta k/k$ and used in the program just as the same way as Δp^{th} is.

Columns	Content	Description

NOTE: With ICH = -1, boron concentration and control rod position are fixed as given in input. With ICH = +2, power level and control rod position are fixed.

(When ICH = +1, the following data should be input in columns 17 ∿ 80).

NC — >0 ; maximum number of iterations for Critical Search.

DL(C) — Convergence criterion for Criterical Search. If

$$|\lambda_c - \lambda_0| < DL(C),$$

Critical Search is terminated, where λ_0 is given in input and normally 1.0 (but not limited to).

$\Delta\beta$ — =0.

NOTE: The following data are a prority assignment and related data for withdrawing control rods until the criticality is reached.

NGR1 — The group number of control rods (or a rod) which are (is) to be withdrawn first in a gang.

RLL1 — Minimum length of insertion of NGR1 rods.

RUL1 — Maximum length of insertion of NGR1 rods.

ΔZ_{rod1} — A differential insertion length (in bank) of NGR1 rods which is used for the first guess of the position being

$$R_{ij} = R_{ij}(\text{initial guess}) \pm \Delta Z_{rod}$$

during the course of control rod positioning for NGR1 rods. The length is in tips and fractions of nodes.

NGR2, RLL2, RUL2, ΔZ_{rod2} — The group number of control rods (or a rod) which are (is) to be withdrawn after NGR1 rods come to the limit position, and the relevant data.

NGRn, RLLn, RULn, ΔZ_{rodn} — The group number of control rods (or a rod) which are (is) searched finally, and the relevant data.

Columns	Content	Description

NOTE: The control rod group numbers are not necessarily sequential. The location in a core is assigned in Type 07 Card.

NOTE: RLL and RUL are given in terms of the inserted length (in tips and fractions of nodes) within a core. Hence, RLL=0 means a rod is fully out of a core.

NOTE: Control rods will be inserted in a sequence just opposite to that described in input (i.e. from NGRn to NGR1) when the criticality is searched with $\lambda>1$.

NOTE: Guess ΔZ_{rod} as precisely as possible, or use so large value for it that over-criticality may be attained (when approaching it from a sub-critical state) and vice versa. This helps the code to get a quick and correct answer.

NOTE: If the input R_{ij} for the initial guess of control rod position, or the R_{ij} calculated by the Critical Search in the previous step of Burnup Trace, goes beyond the range RLL $\sim$ RUL, then, the R_{ij} is reset within the range.

NOTE: If a user wants to change the control rod pattern (e.g. a pattern swapping) during Critical-Exposure Iteration, use Type 03 Card as many times as desired together with Type 01 Card where E_0 and E_{max} are re-input for the pertinant exposure period.

Type 04

Columns	Content	Description
11 $\sim$ 12	04	
13 $\sim$ 14	Blank	
15 $\sim$ 16	IBR	$\neq$0; outputs the albedos used for calculation.
		=0 or Blank; doesn't output.
17 $\sim$ 80		FREE FORM DATA
	λ^t	A constant (cm).
	D^t	Diffusion coefficient for water (cm).
	κ^t	Inverse diffusion length in water (cm^{-1}).
	τe^t	Effective Fermi age of fast neutron in reflector (cm^2).

NOTE: These four parameters are given for Core Top Reflector.

λ^b
D^b
κ^b
τe^b

The same as above for Core Bottom Reflector.

λ^p
D^p
κ^p
τe^p

The same as above for Core Peripheral Reflector.

Type 05 (for BWR type calculation)

Columns	Content	Description
11 ∿ 12	05	
13 ∿ 14	KZ	=1; denotes upper section of a core. =0; middle section of a core. =-1; lower section of a core.

NOTE: This input specifies the material constants dependent on core axial height.
If there is no variation of material in axial direction, then put KZ=0.

Columns	Content	Description
15 ∿ 16	T	Fuel type ($\leq$13).
17 ∿ 80		FREE FORM DATA
	$B_n(T,KZ)$	Material constants for fuel type T, specified by the axial dependence KZ. There are 28 constants (n=1 ∿ 28) needed to specify each material type, which have the following definitions. For convenience the superscripts T and KZ have been dropped.
	$B_1 \sim B_3$	$\tau=B_1(1+B_2V+B_3V^2)$ where τ is the Fermi age (cm^2) of fission neutrons and V is the moderator void fraction.
	$B_4 \sim B_6$	$1/\kappa^2=B_4\ (1+B_5V+B_6V^2)$ where $1/\kappa^2$ is the thermal neutron diffusion area (cm^2).

Columns	Content	Description
	$B_7 \sim B_{15}$	These are used to determine k_∞ as a function of void ratio and control. There are three equations which evaluate k_∞ as a function of V: one for uncontrolled k_∞, one for half-control, and one for full-control. If the node being considered is less than half-controlled the program does a straight line interpolation using the results of the first two equations. Similarly, for more than half-control it uses the results of the second and third equations. $k_\infty^{\text{uncontrolled}} = B_7(1+B_8V+B_9V^2)$ $k_\infty^{1/2\ \text{controlled}} = B_{10}(1+B_{11}V+B_{12}V^2)$ $k_\infty^{\text{full-controlled}} = B_{13}(1+B_{14}V+B_{15}V^2)$
	B_{16}, B_{17}	These constants are used to define the xenon reactivity effect $(\Delta k/k)_{\text{xenon}}$ by the following equation; $(\frac{\Delta k}{k})_{\text{xenon}} = -\frac{S_{ijk}P(1+B_{16})B_{17}}{S_{ijk}P + B_{16}}$ where $P \equiv P^{\text{th}}/P^{\text{rated}}$. This is in turn used to modify the nodewise k_∞ given above. $k_{\infty ijk} \leftarrow k_{\infty ijk}[1+(\frac{\Delta k}{k})_{\text{xenon}}+(\frac{\Delta k}{k})_{\text{Doppler}}]$ See below for $(\Delta k/k)_{\text{Doppler}}$.
	$B_{18} \sim B_{20}$	Used to define the Doppler reactivity effect $(\Delta k/k)_{\text{Doppler}}$; $(\frac{\Delta k}{k})_{\text{Doppler}} = -S_{ijk}PZ_2$ where $Z_2 \equiv B_{18}[1+B_{19}(B_{20}V-1)]$.

$B_{21} \sim B_{25}$ These constants are used to specify the exposure dependence of k_∞ in terms of the following equation;

$$\frac{k_\infty(E)}{k_\infty(0)} = 1 + B_{21} - B_{22}(1+B_{25}U)E - B_{23}\cdot e^{-(E/B_{24})}.$$

B_{26} used in summing up the nodewise exposure through burnup step;

$$E^{e+1}_{ijk} = E^{e}_{ijk} + B_{26}S_{ijk}\cdot\Delta E.$$

Usually put = 1.0.

B_{27}, B_{28} used to define the exposure-weighted average void fraction U in a node;

$$U^{e+1}_{ijk} = [U^{e}_{ijk}E^{e}_{ijk}+B_{27}(V_{ijk}+B_{28}C_{ijk})S_{ijk}\cdot\Delta E]/E^{e+1}_{ijk}$$

where V_{ijk} and C_{ijk} are a temporary void fraction and a fraction of control in node ijk, respectively.

ZR Height (in unit of the nodal axial length) of the upper or lower section of a core (if KZ=1 or KZ=-1). Leave blank when KZ=0.

NOTE: Redundant Material Constants can be input for the fuel type that is not assigned in Type 06 Card.

NOTE: Only B_1 and B_4 have the dimension of cm^2, the others all dimensionless.

Type 05 (for PWR type claculation)

Columns	Content	Description
11 ∿ 12	05	
13 ∿ 14	KZ	=1; denotes upper section of a core. =0; middle section of a core. =-1; lower section of a core.

NOTE: See the corresponding NOTE in 05 Card for BWR.

15 ∿ 16 T — Fuel type (≤13).

17 ∿ 80 — FREE FORM DATA

$B_n(T,KZ)$ — Material constants for fuel type T, specified by the axial dependence KZ.
There are 30 constants (n=1 ∿ 30) required to specify each fuel type for PWR calculation, which have the following definitions. For convenience the superscripts T and KZ have been dropped.

B_1, B_2 — $\tau = B_1+B_2(t-t_0)$

where τ is the Fermi age (cm^2) of fission neutrons and t, t_0 are the moderator temperature (°C) and its reference value, respectively.

B_3, B_4 — $1/\kappa^2 = B_3+B_4(t-t_0)$

where $1/\kappa^2$ is the thermal neutron diffusion area (cm^2).

$B_5 \sim B_{22}$ — These constants are used to determine k_∞ as a function of boron concentration β, moderator temperature and control. β is given in 1000ppm.
See the corresponding description for k_∞ in BWR case for more detail.

$$k_\infty^{\text{uncontrolled}} = B_5+B_6\beta+B_7\beta^2+(B_8+B_9\beta+B_{10}\beta^2)(t-t_0)$$

$$k_\infty^{1/2\text{controlled}} = B_{11}+B_{12}\beta+B_{13}\beta^2+(B_{14}+B_{15}\beta+B_{16}\beta^2)(t-t_0)$$

$$k_\infty^{\text{full-controlled}} = B_{17}+B_{18}\beta+B_{19}\beta^2 +(B_{20}+B_{21}\beta+B_{22}\beta^2)(t-t_0)$$

B_{23}, B_{24} — used to define the zenon reactivity effect $(\Delta k/k)_{\text{xenon}}$ by the following equation;

$$\left(\frac{\Delta k}{k}\right)_{\text{xenon}} = -\frac{S_{ijk}P(1+B_{23})B_{24}}{S_{ijk}P+B_{23}}$$

where $P \equiv P^{th}/P^{rated}$.

B_{25} — defines the Doppler reactivity effect by the following equation for PWR calculation:

$$\left(\frac{\Delta k}{k}\right)_{Doppler} = -S_{ijk}{}^{P} \cdot B_{25}$$

NOTE: The xenon and Doppler reactivity effects are incorporated into k_∞ calculation;

$$k_{\infty ijk} \leftarrow k_{\infty ijk}\left[1 + \left(\frac{\Delta k}{k}\right)_{xenon} + \left(\frac{\Delta k}{k}\right)_{Doppler}\right]$$

where the righthand side k_∞'s are given by constants B_5 through B_{22}.

$B_{26} \sim B_{29}$ used to specify the reactivity loss due to exposure by following equation for PWR calculation;

$$\frac{k_\infty(E)}{k_\infty(0)} = 1 + B_{26} - B_{27}E - B_{28}e^{-E/B_{29}}$$

B_{30} a weight for fuel type T in summing up the nodewise exposure through burnup step;

$$E_{ijk}^{i+1} = E_{ijk}^{e} + B_{30}S_{ijk} \cdot \Delta E.$$

Usually put 1.0.

ZR Height (in unit of ΔZ) of the upper or lower section of a core (if KZ=1 or KZ=-1).
Leave blank when KZ=0.

Type 06

Columns	Content	Description
11 ∿ 12	06	
13 ∿ 14	Blank	
15 ∿ 16	I	Row designation
17 ∿ 80		FREE FORM DATA
	$T_{i,j}$ ($j=1$ to j_{max})	Fuel type in j^{th} position of i^{th} row (put zero at no-fuel positions).

Type 07

Columns	Content	Description
11 ∿ 12	07	
13 ∿ 14	Blank	
15 ∿ 16	I	Row designation
17 ∿ 18		FREE FORM DATA
	$GR_{i,j}$	Group number to which a control rod is classified.
	(j=1 to j_{max})	Identify the same group members by a number.
		The group numbers are not necessarily in sequence.

NOTE: 07 Card is only needed when "critical search" option is selected.

Type 08

Columns	Content	Description
11 ∿ 12	08	
13 ∿ 14	Blank	
15 ∿ 16	I	Row designation
17 ∿ 18		FREE FORM DATA
	$R_{i,j}$	Axial insertion length of control rod given in tips and fractions of nodes. It has been assumed in
	(j=1 to j_{max})	the program that the control rods entered from the core bottom for the BWR case, and from the top for the PWR case. With the "critical search" option, this input is used as the initial guess for the control rod position search.

NOTE: The data $GR_{i,j}$ and $R_{i,j}$ input at the node position (i,j) should be related to the control rod which is

(1) positioned in the same node, when Rod/Cell=0, or

(2) positioned at the left-top corner of the node specified, when Rod/Cell≠0.

Input Example:
(for GR_{ij} & R_{ij})

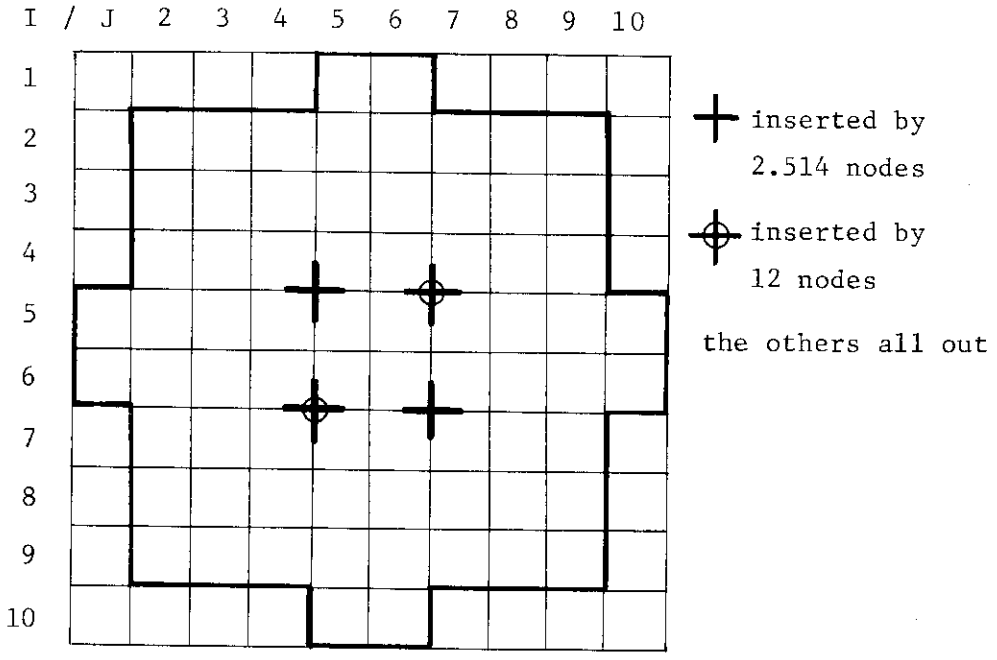

GR_{ij}

```
0  0  0  0  0  0  0  0  0  0
0  0  0  0  0  0  0  0  0  0
0  0  0  0  0  0  0  0  0  0
0  0  0  0  0  0  0  0  0  0
0  0  0  0  1  0  2  0  0  0
0  0  0  0  0  0  0  0  0  0
0  0  0  0  2  0  1  0  0  0
0  0  0  0  0  0  0  0  0  0
0  0  0  0  0  0  0  0  0  0
0  0  0  0  0  0  0  0  0  0
```

R_{ij}

```
S 10  (a special input technique which stands for;
S 10       skip 10 places; equivalent to 10 zeros)
S 10
S 10
S 4  12.00      S 1  2.514     S 3
S 10
S 4  2.514      S 1  12.00     S 3
S 10
S 10
S 10
```

Type 09

Columns	Content	Description
11 ∿ 12	09	
13 ∿ 14	Blank	
15 ∿ 16	I	Row designation
17 ∿ 80		FREE FORM DATA
	$XK_{i,j}$ (j=1 to j_{max})	Partial fuel factors by i,j location. This is another multiplier on k_∞ but is only i,j dependent. It may represent Δk of poison curtains or any other fudge factor the user requires.

$$k_{\infty i,j,k} \leftarrow k_{\infty i,j,k} \cdot XK_{i,j}$$

NOTE: Skipping 09 Card leads to all $XK_{ij}=1$.

Type 10

Columns	Content	Description
11 ∿ 12	10	
13 ∿ 14	Blank	
15 ∿ 16	I	Row designation
17 ∿ 80		FREE FORM DATA
	$F_{i,j}$ (j=1 to j_{max})	Relative flow up each channel, normalized to 1.0 in full-core basis.

NOTE: Skipping 10 Card leads to all $F_{i,j}=1$.

NOTE: The input of $F_{i,j}$ shall be given for the center and the central nodes just as the same basis as for the ordinary node. That is, the volume fraction of the center and the central nodes need not be taken into account.

Type 11

Columns		Content	Description
11	12	11	
13	14	I	Row designation
15	16	J	Column designation
17	80		FREE FORM DATA
		$S_{i,j,k}$ ($k=1$ to k_{max})	Source guess: $k=1$ to k_{max} for this I,J. Increment J by 1 for the next set of sources and so on until $J=j_{max}$, then increment I by 1 and repeat the next set of J's (and their associated k's) until $I=i_{max}$. The values of the source guess are normalized to an average value of 1.0 by the program.

NOTE: Skipping 11 Card leads to all $S_{i,j,k}=1$ in Independent Case. In Dependent Case, on the other hand, the source guess is set automatically by program identical to the source solution of just a previous run. Give the explicit data both in Independent and Dependent Cases if the user has the special purpose.

NOTE: In practice, cards disorder in I's and J's is immaterial.

Type 12A (ID Card)

Columns	Content	Description	Description
11 ∿ 12	12		
13 ∿ 14	I	Row designation	
15 ∿ 16	00	Zero	
17 ∿ 20	$ID_{i,1}$	Four alpha-numeric characters. Notice this is not free format data. $ID_{i,j}$ is the identification label of each bundle (i,j location) in the problem; use blanks where there is no fuel.	
21 ∿ 24	$ID_{i,2}$		
25 ∿ 28	$ID_{i,3}$		
etc.			
73 ∿ 76	$ID_{i,15}$		

The purpose of the fuel ID is to facilitate fuel shuffling and to maintain records of the rearrangement. It has three functions, labeling, fuel

shuffling, and exposure data relocating functions.

Normally, Exposure Cards (Type 12B) will be read in originally for each i,j location with non-zero exposure, followed by the ID cards (Type 12A) to label each fuel bundle (Labeling function).

In Dependent Cases thereafter, ID cards of any row for a bundle to be replaced will be ordered to precede the Exposure Cards for the new bundles (Fuel shuffling function).

NOTE: An ID card is required only for the row where there are fuels to be replaced. In this case, the label for all bundles in the row must be given.

Once one or more ID cards have been read in, all following exposure cards supplied in each case or exposure data in computer core memory with ID label will be assigned to the i,j position whose ID label is equal to that punched in columns 3∿6 of each Exposure Card. Thus, an ID card not only changes the labels in the ID array but also forces all succeeding Exposure data in the case under problem or any following Dependent Case to be stored by the label in columns 3∿6 of 12B Card rather than by the i,j carried in columns 13∿14 and 15∿16 of the Card (Exposure data relocating function).

Type 12B (Exposure Card)

Columns	Content	Description
1 ∿ 2	Run Number	(Punched output contains KPCH from input.)
3 ∿ 6	$ID_{I,J}$	Identification label of a fuel bundle.
7 ∿ 8	Blank	
11∿12	12	
13∿14	I	Row designation
15∿16	J	Column designation
17∿80		FREE FORM DATA

$E_{i,j,k}$ (k=1 to k_{max}) Exposure in 1000 MWD/T in the same manner as the source guess.

NOTE: When $E_{i,j,k}$ Card has been input before going to ID Card (Type 12A), the $E_{i,j,k}$ data will be stored in the i,j position (carried in columns 13∿14 and 15∿16). This setup of cards deck will be used for e.g. calculations of burnup without fuel shuffling.

NOTE: In the above case, a blank can be used in columns 3∿6, and the ID Cards can be skipped.

NOTE: Once ID Card has been read in, the succeeding data punched in $E_{i,j,k}$ Card will be stored at the $ID_{i,j}$ position designated in columns 3∿6 of the $E_{i,j,k}$ Card. In this case, the i, and j position shown in columns 13∿14, and 15∿16, will be ignored.

NOTE: In the above case, the $E_{i,j,k}$ data of the fuel assigned by ID Card must be always input. The $E_{i,j,k}$ data with the fuel lable which is not found in ID Card will be stored separately, so that the data can be used later if the $ID_{i,j}$ position is given by Dependent Card.

NOTE: If the user wants to simulate fuel shuffling during burnup calculation, assign the exposure up to the time when refueling begins by Card 01, and input fuel loading locations by ID Card. (In this case, if there is a change in the map of fuel types, input new fuel types by Card 06.) The $E_{i,j,k}$ Card for newly loaded fuels should be added after ID Card.

NOTE: If the user wants to simulate poison curtain unloading, assign E by Card 01 and input fuel types by Card 06.
(Careful! It is assumed here that fuel locations are unchanged before and after poison curtain unloading.) In this case, the special nuclear constants for fuel must have previously been produced under the condition of no poison curtain. Card 09 is useful when considering these nuclear constants.

NOTE: In case of fuel shuffling without unloading poison curtain, care should be taken about input.

NOTE: An error is not detected when Exposure Card has been input for a fuel which is not loaded in the core.

Type 13

Columns	Content	Description
1 ∿ 10		The same as in Type 12B.
11 ∿ 12	13	
13 ∿ 14	I	Row designation
15 ∿ 16	J	Column designation
17 ∿ 80		FREE FORM DATA
	$U_{i,j,k}$ ($k=1, k_{max}$)	Exposure weighted average void fraction (see card type 05 for BWR) in the same arrangement as $S_{i,j,k}$.

NOTE: These cards are allocated to i,j positions exactly the same manner as Exposure Card (Type 12B) in regard to the Label Card (Type 12A) and corresponding ID array.

Type 14

Columns	Content	Description
11 ∿ 12	14	
13 ∿ 14	Blank	
15 ∿ 16	IACCEL	Type of source acceleration =-1; source over-relaxation =0; point Jacobi =+1; Gauss-Seidel
17 ∿ 80		FREE FORM DATA
	Γ_n	Acceleration factors, n=1 to 16.

Type 15 (for BWR type calculation)

Columns	Content	Description
11 ∿ 12	15	
13 ∿ 14	Blank	
15 ∿ 16	IQ	specifies the quality-void correlation =0; A quadratic function in Q ≠0; Bankoff type correlation

17 ∿ 18 FREE FORM DATA

C_n Thermal-hydraulic constants (n-1 ∿ 18), prepared according to the following definitions.

$C_1 \sim C_4$ These give the total coolant flow in core W (Ton/hr) as a function of reactor power $P \equiv P^{th}/P^{rated}$.

$$W = C_1 + C_2P + C_3P^{-C_4} \qquad (\text{with } C_4 \geq 1).$$

Fitting examples

(1) $C_1 \neq 0$, $C_2 \neq 0$, $C_3 = 0$, $C_4 = 1$

(2) $C_1 = 0$, $C_2 = 0$, $C_3 \neq 0$, $C_4 > 1$

NOTE: The value of W should be the sum of in-channel flows, excluding the leakage flow.

$C_5 \sim C_8$ give the subcool enthalpy Δhs (kcal/kg) as a function of reactor power;

$$\Delta hs = C_5 + C_6P + C_7P^{-C_8} \qquad (\text{with } C_8 \geq 1).$$

Fitting examples

(1) $C_5 \neq 0$, $C_6 \neq 0$, $C_7 = 0$, $C_8 = 1$

(2) $C_5 = 0$, $C_6 = 0$, $C_7 \neq 0$, $C_8 > 1$

NOTE: The Δhs is defined in positive value.

$C_9 \sim C_{14}$ Coefficients in the quality-void correlation. When IQ = 0,

$$V = C_9 + C_{10}Q + C_{11}Q^2 - C_{12}\exp\left(\frac{C_{13} - Q}{C_{14}}\right)$$

or when IQ ≠ 0,

$$V = C_9 + \frac{C_{10}}{1 + C_{11}\left(\frac{1-Q}{Q}\right)} - C_{12}\exp\left(\frac{C_{13} - Q}{C_{14}}\right)$$

where V is the volume fraction of steam voids at quality Q. In the latter equation,

$$C_{11} \equiv \frac{\rho_g}{\rho_f} \cdot s(\text{slip ratio})$$

according to Bankoff.

NOTE: $0 \leq V \leq 1.0$ and $0 \leq Q \leq 1.0$.

C_{15}, C_{16} If these are non-zero, the channel relative flows $F_{i,j}$'s (given in Type 10 Card) will be modified in terms of channel relative power;

$$F_{i,j} \leftarrow F_{i,j}[1+C_{15}(S_{i,j}-1)+C_{16}(S_{i,j}-1)^2].$$

NOTE: The large correction of $F_{i,j}$ by $C_{16}(S_{i,j}-1)^2$ may be not considered because $F_{i,j}$ is not renormalized after the modification.

C_{17} $=h_{fg}$; latent heat for evaporation (kcal/kg) at rated condition.

C_{18} $=\gamma_{in}$; the power fraction to be spent for generating the steam void in channels.

$$H_{exit} - H_{inlet} = 860 \cdot \gamma_{in} \cdot \frac{P^{th}}{W}$$

Type 15 (for PWR type calculation)

Columns	Content	Description
11 ∿ 12	15	
13 ∿ 14	Blank	
15 ∿ 16	Blank	
17 ∿ 80		FREE FORM DATA
	$C_1 \sim C_4$	These constants give the total coolant flow in core, W(Ton/hr), as a function of reactor power $P \equiv P^{th}/P^{rated}$:

$$W = C_1 + C_2P + C_3P^{-C_4} \quad (\text{with } C_4 \geq 1).$$

Fitting examples

(1) $C_1 \neq 0$, $C_2 \neq 0$, $C_3 = 0$, $C_4 = 1$

(2) $C_1 = 0$, $C_2 = 0$, $C_3 \neq 0$, $C_4 > 1$.

$C_5 \sim C_8$ These constants determine the core inlet enthalpy, h_{in}(kcal/kg), as a function of reactor thermal output $P \equiv P^{th}/P^{rated}$:

$$h_{in} = C_5 + C_6P + C_7P^{-C_8} \quad (\text{with } C_8 \geq 1)$$

Fitting examples

(1) $C_5 \neq 0$, $C_6 \neq 0$, $C_7 = 0$, $C_8 = 1$

(2) $C_5 = 0$, $C_6 = 0$, $C_7 \neq 0$, $C_8 > 1$

$C_9 \sim C_{11}$ Coefficients in an enthalpy-temperature correlation equation at rated condition:

$$t = C_9 + C_{10}h + C_{11}h^2,$$

where t is the coolant temperature (°C) and h is the coolant enthalpy (in kcal/kg).

NOTE: If a calculation is going to be done for a low pressure reactor condition, then, this correlation must be given at and around the condition.

C_{12}, C_{13} The same as C_{15} & C_{16} in Type 15 for BWR calculation.

C_{14} $=t_0$; a reference coolant temperature (°C) used in Card Type 05 for PWR calculation.

NOTE: A coolant average temperature may be suitable for C_{14}, but not limited to.

C_{15} $=\gamma_{in}$; put 1.0 for PWR case.

Type 20

Columns	Content	Description
11 ∿ 12	20	
13 ∿ 14	Blank	
15 ∿ 16	T	Fuel Type

17 ∿ 80		FREE FORM DATA The following four inputs given for each fuel type T are used in the present version program to supply the additional data which are required to run the generalized FLARE-type nodal equation.
	η_e	An epi-thermal neutron portion of the migration kernel $K_{i\to m}$. At present, a value 1.0 is recommended for any case.
	η_t	A thermal neutron portion of the migration kernel $K_{i\to m}$. Presently, a zero is recommended for all time.
	η_{th}	This is the probability that a fission neutron is thermalized in the native node where it is born. Program users may give a value for η_{th}, assuming it is proportional to the self-migration kernel K_{ii}. The values 0.3 ∿ 0.5 are recommended for the proportional factor.
	K_s	is definied as $\sum_{m}^{all} K_{i\to m}$. But presently, put 1.0 (or any other non-zero values). This is because, with η_t=0, the K_s term does not work in the nodal equation coded in program.

Type 33

Columns	Content	Description
11 ∿ 12	33	Reorder Card
13 ∿ 14	Blank	
15 ∿ 16	Blank	
17 ∿ 80		Any alphanumeric statements

NOTE: A Reorder Card must be inserted before every card whose type is lower than or equal to the preceding card in the input deck. This makes a user be possible to use a basic input deck and follow it with a modification or overlay deck pertinent to a particular problem.

Type 99

Columns	Content	Description
11 ∿ 12	99	Terminal Card
13 ∿ 14	Blank	
15 ∿ 16	Blank	
17 ∿ 80	Any alphanumeric statements	

NOTE: A Terminal Card signals end of data for this case, starting for calculation. It precedes Case Card or Last Card.

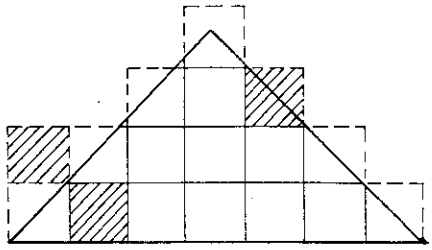

BC = 9

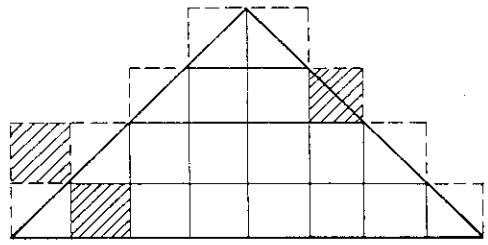

BC = 8

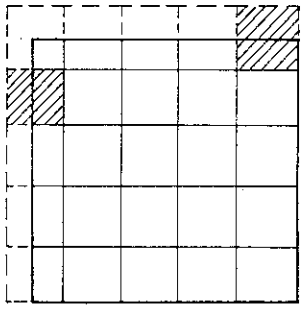

BC = 7

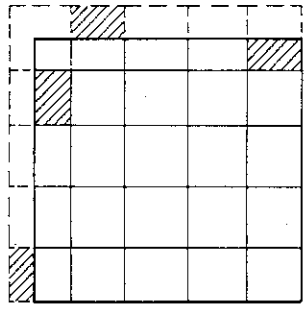

BC = 6

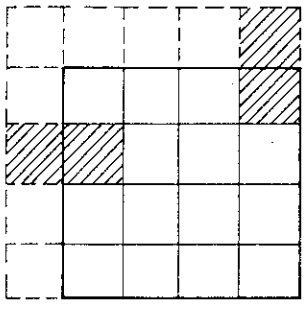

BC = 5

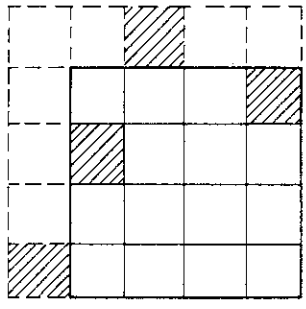

BC = 4

Fig. 4.2 Boundary condition indicators (I).

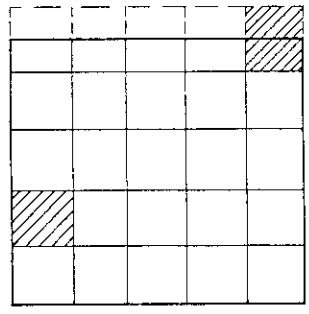

BC = 3

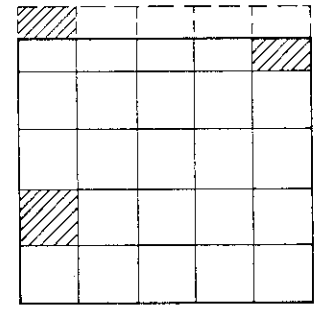

BC = 2

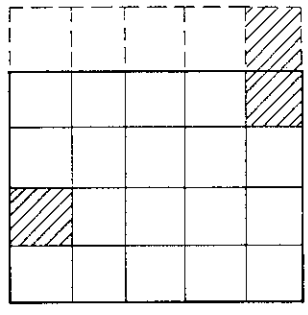

BC = 1

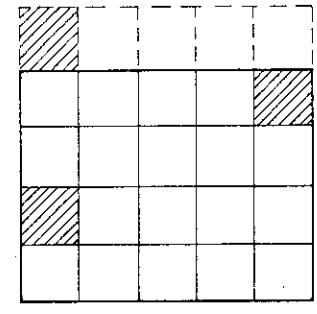

BC = 0

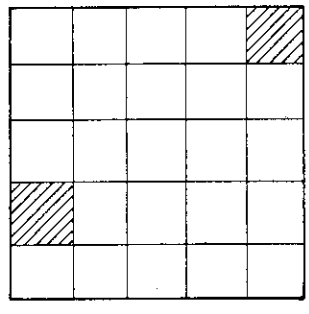

BC = −1

Fig. 4.3 Boundary condition indicators (II).

```
OUTPUT OF SCOPERS-2 PROGRAM     JPDR 100 HR. OPERATION GAMMA PROBED CORE                    PAGE      1

                                                  INPUT CARDS          TIME 20 HRS  14 MIN  19 SEC
                    1     2     3     4     5     6     7     8     9     10    11    12    13    14    15    16

KD B/P BRN-LST    E(O)  EMAX    DE    PTH   PRATED  DX    DZ    RODCEL  BC    IMAX  JMAX  KMAX  BORN
 1  0   1              * 0.0 0.0 0.5 43.5 45.0 13.66 12.23 1 -1 10 10 12                *          (  BWR    )

KD PCH KPCH       DSIJK  NS  DL(S)   NU    DL(U)  DL(SH)  DSHNK  LMBDA   JP  JS  JU  JK
 2  0   0              * 0.00009 4 0.0 12 0.000001 0.001 0.001 1.0 0 0 0 0              *          (         )

KD                      ALBEDO  CONSTANTS  ( TOP , BOTTOM , PERIPHERAL )
 4  0   0              *  2. .508 .1867 36. 2. .359 .236 1. 2. .359 .236 4.            *          (         )

KD KZ   T             CONSTANTS  BY  FUEL  TYPE       B(T,KZ,J)  J=1,28(BWR) , J=1,30(PWR)
 5  0   1              * 53.75 0.836 1.377 5.56 0.836 1.377                            *          (         )
 5  0   1              * 1.19 -0.0262 -0.0676 1.03                                     *          (         )
 5  0   1              * -0.0568 -0.1465 0.9438 -0.0874 -0.2252 3.86 0.0251 4.8E-3     *          (         )
 5  0   1              * 0.0 3.7 0.0235 0.009727 0.0235 1.371 0.0 1.0 1.0 0.0          *          (         )
 5  0   2              * 53.75 0.836 1.377 5.56 0.836 1.377                            *          (         )
 5  0   2              * 1.256 -0.0242 -0.0477 1.103                                   *          (         )
 5  0   2              * -0.0571 -0.1179 1.034 -0.0900 -0.1881 3.86 0.0285 4.8E-3     *          (         )
 5  0   2              * 0.0 3.7 0.0155 0.01142 0.0155 1.255 0.0 1.0 1.0 0.0          *          (         )
 5  0   3              * 53.75 0.836 1.377 5.56 0.836 1.377                            *          (         )
 5  0   3              * 1.32 -0.0336 -0.0129 1.17                                     *          (         )
 5  0   3              * -0.0665 -0.0831 1.111 -0.0993 -0.1533 3.86 0.0300 4.8E-3     *          (         )
 5  0   3              * 0.0 3.7 0.0 0.0124 0.0 1.0 0.0 1.0 1.0 0.0                    *          (         )
 5  0   4              * 53.75 0.836 1.377 5.56 0.836 1.377                            *          (         )
 5  0   4              * 1.327 -0.0336 -0.0129 1.17                                    *          (         )
 5  0   4              * -0.0665 -0.0831 1.111 -0.0993 -0.1533 3.86 0.0300 4.8E-3     *          (         )
 5  0   4              * 0.0 3.7 0.0 0.0124 0.0 1.0 0.0 1.0 1.0 0.0                    *          (         )

KD      I                       FUEL  TYPE        T(I,J)  J=1,JMAX
 6  0   1              *  0 0 0 0 4 4 0 0 0 0                                          *          (         )
 6  0   2              *  0 3 2 2 2 2 2 2 3 0                                          *          (         )
 6  0   3              *  0 2 1 1 1 1 1 1 2 0                                          *          (         )
 6  0   4              *  0 2 1 1 1 1 1 1 2 0                                          *          (         )
 6  0   5              *  4 2 1 1 1 1 1 1 2 4                                          *          (         )
 6  0   6              *  4 2 1 1 1 1 1 1 2 4                                          *          (         )
 6  0   7              *  0 2 1 1 1 1 1 1 2 0                                          *          (         )
 6  0   8              *  0 2 1 1 1 1 1 1 2 0                                          *          (         )
 6  0   9              *  0 3 2 2 2 2 2 2 3 0                                          *          (         )
 6  0  10              *  0 0 0 0 4 4 0 0 0 0                                          *          (         )

KD      I             CONTROL ROD POSITION        R(I,J)  J=1,JMAX
 8  0   1              *    S10                                                       *          (         )
 8  0   2              *    S10                                                       *          (         )
 8  0   3              *    S10                                                       *          (         )
 8  0   4              *    S10                                                       *          (         )
 8  0   5              *    S4 12.00 S1 2.514 S3                                      *          (         )
 8  0   6              *    S10                                                       *          (         )
 8  0   7              *    S4 2.514 S1 12.00 S3                                      *          (         )
 8  0   8              *    S10                                                       *          (         )
 8  0   9              *    S10                                                       *          (         )
```

INPUT CARDS

```
                1    2     3     4     5     6     7     8     9     10    11    12    13    14    15    16
 8  0  10            *  S10                                                    *                 (           )

KD      I             FRACTIONAL FLOW          F(I,J)  J=1,JMAX
10  0   1            *  S4 0.92 0.92 S4                                        *                 (           )
10  0   2            *  S1 0.98 0.98 1.03 R3 0.98 0.98 S1                      *                 (           )
10  0   3            *  S1 0.98 0.98 1.03 R3 0.98 0.98 S1                      *                 (           )
10  0   4            *  S1 1.03 1.03 1.00 R3 1.03 1.03 S1                      *                 (           )
10  0   5            *  0.92 1.03 1.03 1.00 R3 1.03 1.03 0.92                  *                 (           )
10  0   6            *  0.92 1.03 1.03 1.00 R3 1.03 1.03 0.92                  *                 (           )
10  0   7            *  S1 1.03 1.03 1.00 R3 1.03 1.03 S1                      *                 (           )
10  0   8            *  S1 0.98 0.98 1.03 R3 0.98 0.98 S1                      *                 (           )
10  0   9            *  S1 0.98 0.98 1.03 R3 0.98 0.98 S1                      *                 (           )
10  0  10            *  S4 0.92 0.92 S4                                        *                 (           )
12  1   0            *                A61 A66                                  *                 (           )
12  2   0            *    A50 A55 A11 A32 A33 A29 A18 A62                      *                 (           )
12  3   0            *    A73 A64 A06 A48 A05 A31 A28 A35                      *                 (           )
12  4   0            *    A37 A16 A53 A52 A51 A56 A13 A34                      *                 (           )
12  5   0            * A21 A42 A20 A10 A63 X77 A09 A67 A14 A46                  *                 (           )
12  6   0            * A38 A22 A40 A65 A47 X79 A60 A08 A15 A71                  *                 (           )
12  7   0            *    A70 A59 A69 A02 A01 A07 A12 A25                      *                 (           )
12  8   0            *    A39 A45 A23 A26 A36 A57 A68 A76                      *                 (           )
12  9   0            *    A30 A24 A49 A43 A41 A19 A54 A44                      *                 (           )
12 10   0            *                A03 A04                                  *                 (           )

KD   IACCEL       ACCELERATION FACTORS        ACCEL(NS) ,  NS=1,16
14  0   0            * 0.375 0.375 0.09375 0.1875                             *                 (           )

KD  K IED           THERMAL-HYDRAULIC CONST.       C(J)      J=1,18(BWR) , J=1,15(PWR)
15  0   0            * 1116. 432. 0. 1. 2.3 1.6 0. 1. 0.3 3. 0. 0.3 0. 0.0185 0. 0.   *                 (           )
15  0   0            * 373.0 1.0                                              *                 (           )

KD      T           ETA-E ETA-T ETA-TH KS
20  0   1            *   1.0 0.0 0.255 1.0                                    *                 (           )
20  0   2            *   1.0 0.0 0.255 1.0                                    *                 (           )
20  0   3            *   1.0 0.0 0.255 1.0                                    *                 (           )
20  0   4            *   1.0 0.0 0.255 1.0                                    *                 (           )
99  0   0            *                                                        *                 (           )
```

FUEL IDENTIFICATION

I/J	1	2	3	4	5	6	7	8	9	10	11	12	13	14	15
1					A61	A66									
2		A50	A55	A11	A32	A33	A29	A18	A62						
3		A73	A64	A06	A48	A05	A31	A28	A35						
4		A37	A16	A53	A52	A51	A56	A13	A34						
5	A21	A42	A20	A10	A63	X77	A09	A67	A14	A46					
6	A38	A22	A40	A65	A47	X79	A60	A08	A15	A71					
7		A70	A59	A69	A02	A01	A07	A12	A25						
8		A39	A45	A23	A26	A36	A57	A68	A76						
9		A30	A24	A49	A43	A41	A19	A54	A44						
10					A03	A04									
11															
12															
13															
14															
15															

FUEL TYPE

I/J	1	2	3	4	5	6	7	8	9	10	11	12	13	14	15
1	0	0	0	0	4	4	0	0	0	0	0	0	0	0	0
2	0	3	2	2	2	2	2	2	3	0	0	0	0	0	0
3	0	2	1	1	1	1	1	1	2	0	0	0	0	0	0
4	0	2	1	1	1	1	1	1	2	0	0	0	0	0	0
5	4	2	1	1	1	1	1	1	2	4	0	0	0	0	0
6	4	2	1	1	1	1	1	1	2	4	0	0	0	0	0
7	0	2	1	1	1	1	1	1	2	0	0	0	0	0	0
8	0	2	1	1	1	1	1	1	2	0	0	0	0	0	0
9	0	3	2	2	2	2	2	2	3	0	0	0	0	0	0
10	0	0	0	0	4	4	0	0	0	0	0	0	0	0	0
11	0	0	0	0	0	0	0	0	0	0	0	0	0	0	0
12	0	0	0	0	0	0	0	0	0	0	0	0	0	0	0
13	0	0	0	0	0	0	0	0	0	0	0	0	0	0	0
14	0	0	0	0	0	0	0	0	0	0	0	0	0	0	0
15	0	0	0	0	0	0	0	0	0	0	0	0	0	0	0

BASIC ALBEDO FOR TOP 0.26154

BASIC ALBEDO FOR BOTTOM 0.53108

BASIC ALBEDO FOR PERIPHERAL 0.45068

ALBEDOS IN GEOMETRIC CONSIDERATION --- (XBRHL/XBRHLC/AVL/AHS/AHL)

J=	1	2	3	4	5	6	7	8	9	10
I=	1									
	0.0	0.0	0.0	0.0	2.0000	2.0000	0.0	0.0	0.0	0.0
	0.0	0.0	0.0	0.0	1.0000	1.0000	0.0	0.0	0.0	0.0
	0.0	0.0	0.0	0.0	1.9347	1.9347	0.0	0.0	0.0	0.0
	0.0	0.0	0.0	0.0	0.9673	0.9673	0.0	0.0	0.0	0.0
	0.0	0.0	0.0	0.0	0.4507	0.4507	0.0	0.0	0.0	0.0
I=	2									
	0.0	3.0000	2.0000	1.0000	1.0000	1.0000	1.0000	2.0000	3.0000	0.0
	0.0	1.0000	0.0	0.0	1.0000	1.0000	0.0	0.0	1.0000	0.0
	0.0	1.8027	0.9014	1.0333	0.0	0.0	1.0333	0.9014	1.8027	0.0
	0.0	0.9014	0.4507	0.5167	0.0	0.0	0.5167	0.4507	0.9014	0.0
	0.0	0.9014	0.9014	0.4507	0.0	0.0	0.4507	0.9014	0.9014	0.0
I=	3									
	0.0	2.0000	0.0	0.0	0.0	0.0	0.0	0.0	2.0000	0.0
	0.0	0.0	0.0	0.0	0.0	0.0	0.0	0.0	0.0	0.0
	0.0	0.9014	0.0	0.0	0.0	0.0	0.0	0.0	0.9014	0.0
	0.0	0.4507	0.0	0.0	0.0	0.0	0.0	0.0	0.4507	0.0
	0.0	0.9014	0.0	0.0	0.0	0.0	0.0	0.0	0.9014	0.0
I=	4									
	0.0	1.0000	0.0	0.0	0.0	0.0	0.0	0.0	1.0000	0.0
	0.0	0.0	0.0	0.0	0.0	0.0	0.0	0.0	0.0	0.0
	0.0	1.0333	0.0	0.0	0.0	0.0	0.0	0.0	1.0333	0.0
	0.0	0.5167	0.0	0.0	0.0	0.0	0.0	0.0	0.5167	0.0
	0.0	0.4507	0.0	0.0	0.0	0.0	0.0	0.0	0.4507	0.0
I=	5									
	2.0000	1.0000	0.0	0.0	0.0	0.0	0.0	0.0	1.0000	2.0000
	1.0000	1.0000	0.0	0.0	0.0	0.0	0.0	0.0	1.0000	1.0000
	1.9347	0.0	0.0	0.0	0.0	0.0	0.0	0.0	0.0	1.9347
	0.9673	0.0	0.0	0.0	0.0	0.0	0.0	0.0	0.0	0.9673
	0.4507	0.0	0.0	0.0	0.0	0.0	0.0	0.0	0.0	0.4507
I=	6									
	2.0000	1.0000	0.0	0.0	0.0	0.0	0.0	0.0	1.0000	2.0000
	1.0000	1.0000	0.0	0.0	0.0	0.0	0.0	0.0	1.0000	1.0000
	1.9347	0.0	0.0	0.0	0.0	0.0	0.0	0.0	0.0	1.9347
	0.9673	0.0	0.0	0.0	0.0	0.0	0.0	0.0	0.0	0.9673
	0.4507	0.0	0.0	0.0	0.0	0.0	0.0	0.0	0.0	0.4507
I=	7									
	0.0	1.0000	0.0	0.0	0.0	0.0	0.0	0.0	1.0000	0.0
	0.0	0.0	0.0	0.0	0.0	0.0	0.0	0.0	0.0	0.0
	0.0	1.0333	0.0	0.0	0.0	0.0	0.0	0.0	1.0333	0.0
	0.0	0.5167	0.0	0.0	0.0	0.0	0.0	0.0	0.5167	0.0
	0.0	0.4507	0.0	0.0	0.0	0.0	0.0	0.0	0.4507	0.0

ALBEDOS IN GEOMETRIC CONSIDERATION --- (XBRHL/XBRHLC/AVL/AHS/AHL)

J=	1	2	3	4	5	6	7	8	9	10
I=	8									
	0.0	2.0000	0.0	0.0	0.0	0.0	0.0	0.0	2.0000	0.0
	0.0	0.0	0.0	0.0	0.0	0.0	0.0	0.0	0.0	0.0
	0.0	0.9014	0.0	0.0	0.0	0.0	0.0	0.0	0.9014	0.0
	0.0	0.4507	0.0	0.0	0.0	0.0	0.0	0.0	0.4507	0.0
	0.0	0.9014	0.0	0.0	0.0	0.0	0.0	0.0	0.9014	0.0
I=	9									
	0.0	3.0000	2.0000	1.0000	1.0000	1.0000	1.0000	2.0000	3.0000	0.0
	0.0	1.0000	0.0	0.0	1.0000	1.0000	0.0	0.0	1.0000	0.0
	0.0	1.8027	0.9014	1.0333	0.0	0.0	1.0333	0.9014	1.8027	0.0
	0.0	0.9014	0.4507	0.5167	0.0	0.0	0.5167	0.4507	0.9014	0.0
	0.0	0.9014	0.9014	0.4507	0.0	0.0	0.4507	0.9014	0.9014	0.0
I=	10									
	0.0	0.0	0.0	0.0	2.0000	2.0000	0.0	0.0	0.0	0.0
	0.0	0.0	0.0	0.0	1.0000	1.0000	0.0	0.0	0.0	0.0
	0.0	0.0	0.0	0.0	1.9347	1.9347	0.0	0.0	0.0	0.0
	0.0	0.0	0.0	0.0	0.9673	0.9673	0.0	0.0	0.0	0.0
	0.0	0.0	0.0	0.0	0.4507	0.4507	0.0	0.0	0.0	0.0

EXPOSURE 0.0 CYCLE 0 R(I,J) BY CHANNEL

	1	2	3	4	5	6	7	8	9	10	11	12	13	14
(0)														
1	0.0	0.0	0.0	0.0	0.0	0.0	0.0	0.0	0.0	0.0				
2	0.0	0.0	0.0	0.0	0.0	0.0	0.0	0.0	0.0	0.0				
3	0.0	0.0	0.0	0.0	0.0	0.0	0.0	0.0	0.0	0.0				
4	0.0	0.0	0.0	0.0	0.0	0.0	0.0	0.0	0.0	0.0				
5	0.0	0.0	0.0	0.0	12.0000	0.0	2.5140	0.0	0.0	0.0				
6	0.0	0.0	0.0	0.0	0.0	0.0	0.0	0.0	0.0	0.0				
7	0.0	0.0	0.0	0.0	2.5140	0.0	12.0000	0.0	0.0	0.0				
8	0.0	0.0	0.0	0.0	0.0	0.0	0.0	0.0	0.0	0.0				
9	0.0	0.0	0.0	0.0	0.0	0.0	0.0	0.0	0.0	0.0				
10	0.0	0.0	0.0	0.0	0.0	0.0	0.0	0.0	0.0	0.0				
11	0.0	0.0	0.0	0.0	0.0	0.0	0.0	0.0	0.0	0.0				

JAERI-M 86-063

NC	NU	NS	DELTA L S	DELTA L U	DELTA L C	ACCEL S TOT	MAX REL CHG IN SOURCE		SOURCE TOT	LAMBDA
1	1	1	-0.035880	-0.035880	-0.035880	864.029785	0.463078	2 2 12	830.366211	0.964120
1	1	2	0.017749	-0.018132	-0.018132	863.994141	0.179801	2 9 11	871.410400	0.981868
1	1	3	0.008435	-0.009697	-0.009697	863.997070	0.207207	2 9 12	865.175049	0.990303
1	1	4	0.003456	-0.006241	-0.006241	863.997070	0.081872	2 3 11	864.857666	0.993759
1	2	1	0.000322	0.000322	-0.005920	863.995361	0.065425	3 3 12	865.116211	0.994080
1	2	2	0.000764	0.001086	-0.005155	864.001709	0.047054	2 3 12	864.466553	0.994845
1	2	3	0.001215	0.002300	-0.003941	864.003174	0.050548	2 2 12	864.442627	0.996059
1	2	4	0.000836	0.003136	-0.003105	864.003662	0.034446	8 9 12	864.312500	0.996895
1	3	1	-0.000138	-0.000138	-0.003242	864.008545	0.035295	2 2 12	863.523193	0.996758
1	3	2	0.000894	0.000756	-0.002348	864.001465	0.023217	9 9 12	864.300781	0.997652
1	3	3	0.000616	0.001372	-0.001733	863.995850	0.020479	2 2 12	864.250000	0.998267
1	3	4	0.000382	0.001753	-0.001351	863.995850	0.017491	3 2 12	864.181641	0.998649
CONVERGENCE		1	LAMBDA	0.998649	SHANK	1.000991	SHANK SQ	0.0	DEL LMB	0.002342	DEL SH SQ	0.0
1	4	1	-0.000240	-0.000240	-0.001591	864.000244	0.014683	3 3 12	863.992432	0.998409
1	4	2	0.000257	0.000017	-0.001334	864.004639	0.011723	4 4 12	864.219482	0.998666
1	4	3	0.000217	0.000235	-0.001116	863.994873	0.010491	2 2 12	864.206543	0.998884
1	4	4	0.000142	0.000377	-0.000975	864.000244	0.009374	3 3 12	864.173096	0.999025
CONVERGENCE		1	LAMBDA	0.999025	SHANK	0.999653	SHANK SQ	0.0	DEL LMB	0.000628	DEL SH SQ	0.0
1	5	1	-0.000253	-0.000253	-0.001228	864.000000	0.008206	7 7 12	863.978760	0.998772
1	5	2	0.000113	-0.000140	-0.001115	863.991211	0.006785	4 4 12	864.165527	0.998885
1	5	3	0.000091	-0.000049	-0.001024	863.998291	0.005887	3 4 12	864.151611	0.998976
1	5	4	0.000057	0.000008	-0.000967	863.994873	0.005398	4 4 12	864.137207	0.999033
CONVERGENCE		1	LAMBDA	0.999033	SHANK	0.999030	SHANK SQ	0.997162	DEL LMB	0.0	DEL SH SQ	0.001868
1	6	1	-0.000213	-0.000213	-0.001180	863.996094	0.004837	5 5 12	863.998047	0.998820
1	6	2	0.000047	-0.000166	-0.001133	864.001709	0.004062	4 4 12	864.117432	0.998867
1	6	3	0.000031	-0.000136	-0.001103	864.000732	0.003584	6 6 12	864.104004	0.998897
1	6	4	0.000033	-0.000103	-0.001070	863.995117	0.003298	4 4 12	864.100098	0.998930
CONVERGENCE		1	LAMBDA	0.998930	SHANK	1.004324	SHANK SQ	0.999506	DEL LMB	0.0	DEL SH SQ	0.004817
1	7	1	-0.000168	-0.000168	-0.001237	864.001221	0.003000	5 5 12	863.992920	0.998763
1	7	2	0.000024	-0.000144	-0.001213	863.998291	0.002529	4 4 12	864.083740	0.998787
1	7	3	0.000016	-0.000128	-0.001197	863.998291	0.002262	5 5 12	864.073242	0.998803
1	7	4	0.000006	-0.000121	-0.001191	864.002197	0.002091	5 5 12	864.066895	0.998809
CONVERGENCE		1	LAMBDA	0.998809	SHANK	1.040403	SHANK SQ	0.998110	DEL LMB	0.0	DEL SH SQ	0.042293
1	8	1	-0.000106	-0.000106	-0.001297	864.002197	0.001915	6 6 12	863.998047	0.998703
1	8	2	0.000001	-0.000105	-0.001296	863.999023	0.001626	7 7 12	864.053711	0.998704
1	8	3	0.0	-0.000105	-0.001296	864.003174	0.001460	6 6 12	864.047607	0.998704
CONVERGENCE		1	LAMBDA	0.998704	SHANK	0.985965	SHANK SQ	1.018697	DEL LMB	0.0	DEL SH SQ	0.032732
1	9	1	-0.000056	-0.000056	-0.001352	864.002686	0.001344	5 5 12	864.014404	0.998648
1	9	2	0.000011	-0.000045	-0.001341	863.992920	0.001161	4 4 12	864.043945	0.998659
1	9	3	-0.000000	-0.000045	-0.001341	864.003662	0.001059	6 6 12	864.039795	0.998659
1	9	4	0.000007	-0.000038	-0.001334	863.996582	0.000981	5 5 12	864.035400	0.998666
CONVERGENCE		-1	LAMBDA	0.998666	SHANK	0.985866	SHANK SQ	0.985857	DEL LMB	0.0	DEL SH SQ	0.000009

POWER									QUALITY/TEMP.	
THERMAL	RELATIVE	PEAK	I	J	K	S(K)	LEVEL	U(K)	INLET	EXIT
43.5000	0.96667	1.76769	7	4	5				-0.0103	0.0551
						0.31064	12	0.44443		
						0.57043	11	0.43490		
						0.80006	10	0.41944		
						0.99788	9	0.39777		
						1.16248	8	0.36901		
						1.29121	7	0.33140		
						1.37847	6	0.28189		
						1.41351	5	0.21595		
						1.37661	4	0.12827		
						1.21084	3	0.02635		
						0.92813	2	0.0		
						0.56072	1	0.0		
						AVG S		AVG U	AVG K	
						1.00008		0.25412	1.14833	

EXPOSURE 0.0 CYCLE 9 S(I,J) BY CHANNEL

	1	2	3	4	5	6	7	8	9	10	11	12	13	14
(0)														
1	0.0	0.0	0.0	0.0	0.8297	0.8389	0.0	0.0	0.0	0.0				
2	0.0	0.7245	0.8733	1.0071	1.1097	1.1386	1.0761	0.9431	0.7806	0.0				
3	0.0	0.8733	0.9974	1.0680	1.1319	1.1948	1.1887	1.0953	0.9431	0.0				
4	0.0	1.0071	1.0680	0.7619	0.7836	1.1266	1.1733	1.1887	1.0761	0.0				
5	0.8297	1.1097	1.1319	0.7836	0.7752	1.0749	1.1266	1.1948	1.1386	0.8389				
6	0.8389	1.1386	1.1948	1.1266	1.0749	0.7752	0.7836	1.1319	1.1097	0.8297				
7	0.0	1.0761	1.1887	1.1733	1.1266	0.7836	0.7619	1.0680	1.0071	0.0				
8	0.0	0.9431	1.0953	1.1887	1.1948	1.1319	1.0680	0.9974	0.8733	0.0				
9	0.0	0.7806	0.9431	1.0761	1.1386	1.1097	1.0071	0.8733	0.7245	0.0				
10	0.0	0.0	0.0	0.0	0.8389	0.8297	0.0	0.0	0.0	0.0				
11	0.0	0.0	0.0	0.0	0.0	0.0	0.0	0.0	0.0	0.0				

EXPOSURE 0.0 CYCLE 9 S(I,J,K) BY BANK

	1	2	3	4	5	6	7	8	9	10	11	12	13	14
(1)														
12	0.0	0.0	0.0	0.0	0.2359	0.2393	0.0	0.0	0.0	0.0				
11	0.0	0.0	0.0	0.0	0.4581	0.4645	0.0	0.0	0.0	0.0				
10	0.0	0.0	0.0	0.0	0.6462	0.6550	0.0	0.0	0.0	0.0				
9	0.0	0.0	0.0	0.0	0.8062	0.8169	0.0	0.0	0.0	0.0				
8	0.0	0.0	0.0	0.0	0.9395	0.9516	0.0	0.0	0.0	0.0				
7	0.0	0.0	0.0	0.0	1.0455	1.0584	0.0	0.0	0.0	0.0				
6	0.0	0.0	0.0	0.0	1.1216	1.1348	0.0	0.0	0.0	0.0				
5	0.0	0.0	0.0	0.0	1.1616	1.1742	0.0	0.0	0.0	0.0				
4	0.0	0.0	0.0	0.0	1.1527	1.1639	0.0	0.0	0.0	0.0				
3	0.0	0.0	0.0	0.0	1.0686	1.0777	0.0	0.0	0.0	0.0				
2	0.0	0.0	0.0	0.0	0.8355	0.8422	0.0	0.0	0.0	0.0				
1	0.0	0.0	0.0	0.0	0.4846	0.4881	0.0	0.0	0.0	0.0				
(2)														
12	0.0	0.2042	0.2574	0.3011	0.3432	0.3545	0.3274	0.2837	0.2243	0.0				
11	0.0	0.3966	0.4815	0.5618	0.6209	0.6410	0.6096	0.5294	0.4345	0.0				
10	0.0	0.5614	0.6786	0.7882	0.8699	0.8973	0.8536	0.7443	0.6135	0.0				
9	0.0	0.7030	0.8481	0.9827	1.0834	1.1169	1.0623	0.9279	0.7661	0.0				
8	0.0	0.8221	0.9898	1.1446	1.2605	1.2986	1.2350	1.0800	0.8932	0.0				
7	0.0	0.9181	1.1025	1.2719	1.3989	1.4401	1.3693	1.1992	0.9941	0.0				
6	0.0	0.9884	1.1827	1.3606	1.4939	1.5361	1.4601	1.2811	1.0656	0.0				
5	0.0	1.0262	1.2230	1.4025	1.5368	1.5772	1.4978	1.3175	1.1007	0.0				
4	0.0	1.0173	1.2087	1.3830	1.5126	1.5477	1.4668	1.2934	1.0856	0.0				
3	0.0	0.9239	1.1134	1.2745	1.3936	1.4211	1.3417	1.1839	0.9870	0.0				
2	0.0	0.7171	0.8701	1.0067	1.1108	1.1304	1.0553	0.9232	0.7619	0.0				
1	0.0	0.4156	0.5244	0.6079	0.6924	0.7029	0.6341	0.5542	0.4403	0.0				

EXPOSURE 0.0 CYCLE 9 S(I,J,K) BY BANK

(3)

	1	2	3	4	5	6	7	8	9	10	11	12	13	14
12	0.0	0.2574	0.3043	0.3313	0.3566	0.3815	0.3789	0.3423	0.2837	0.0				
11	0.0	0.4815	0.5530	0.5996	0.6436	0.6875	0.6837	0.6204	0.5294	0.0				
10	0.0	0.6786	0.7768	0.8404	0.9001	0.9604	0.9558	0.8694	0.7443	0.0				
9	0.0	0.8481	0.9705	1.0487	1.1218	1.1959	1.1900	1.0836	0.9279	0.0				
8	0.0	0.9898	1.1321	1.2219	1.3057	1.3908	1.3838	1.2610	1.0800	0.0				
7	0.0	1.1025	1.2592	1.3568	1.4478	1.5409	1.5333	1.3984	1.1992	0.0				
6	0.0	1.1827	1.3473	1.4478	1.5413	1.6386	1.6310	1.4900	1.2811	0.0				
5	0.0	1.2230	1.3880	1.4854	1.5750	1.6703	1.6632	1.5248	1.3175	0.0				
4	0.0	1.2087	1.3668	1.4543	1.5323	1.6126	1.6062	1.4866	1.2934	0.0				
3	0.0	1.1134	1.2573	1.3302	1.3906	1.4458	1.4392	1.3506	1.1839	0.0				
2	0.0	0.8701	0.9958	1.0489	1.0931	1.1239	1.1162	1.0624	0.9232	0.0				
1	0.0	0.5244	0.6172	0.6502	0.6752	0.6890	0.6831	0.6537	0.5542	0.0				

(4)

	1	2	3	4	5	6	7	8	9	10	11	12	13	14
12	0.0	0.3011	0.3313	0.2335	0.2453	0.3885	0.4030	0.3789	0.3274	0.0				
11	0.0	0.5618	0.5996	0.4256	0.4466	0.6996	0.7252	0.6837	0.6096	0.0				
10	0.0	0.7882	0.8404	0.5996	0.6286	0.9774	1.0126	0.9558	0.8536	0.0				
9	0.0	0.9827	1.0487	0.7528	0.7887	1.2178	1.2611	1.1900	1.0623	0.0				
8	0.0	1.1446	1.2219	0.8830	0.9246	1.4178	1.4677	1.3838	1.2350	0.0				
7	0.0	1.2719	1.3568	0.9869	1.0325	1.5726	1.6280	1.5333	1.3693	0.0				
6	0.0	1.3606	1.4478	1.0583	1.1050	1.6735	1.7337	1.6310	1.4601	0.0				
5	0.0	1.4025	1.4854	1.0859	1.1279	1.7027	1.7677	1.6632	1.4978	0.0				
4	0.0	1.3830	1.4543	1.0531	1.0782	1.6183	1.6886	1.6062	1.4668	0.0				
3	0.0	1.2745	1.3302	0.9285	0.9268	1.1158	1.1800	1.4392	1.3417	0.0				
2	0.0	1.0067	1.0489	0.7070	0.6883	0.7148	0.7617	1.1162	1.0553	0.0				
1	0.0	0.6079	0.6502	0.4282	0.4105	0.4196	0.4498	0.6831	0.6341	0.0				

(5)

	1	2	3	4	5	6	7	8	9	10	11	12	13	14
12	0.2359	0.3432	0.3566	0.2453	0.2478	0.3743	0.3885	0.3815	0.3545	0.2393				
11	0.4581	0.6209	0.6436	0.4466	0.4510	0.6744	0.6996	0.6875	0.6410	0.4645				
10	0.6462	0.8699	0.9001	0.6286	0.6347	0.9429	0.9774	0.9604	0.8973	0.6550				
9	0.8062	1.0834	1.1218	0.7887	0.7964	1.1754	1.2178	1.1959	1.1169	0.8169				
8	0.9395	1.2605	1.3057	0.9246	0.9336	1.3688	1.4178	1.3908	1.2986	0.9516				
7	1.0455	1.3989	1.4478	1.0325	1.0420	1.5179	1.5726	1.5409	1.4401	1.0584				
6	1.1216	1.4939	1.5413	1.1050	1.1129	1.6129	1.6735	1.6386	1.5361	1.1348				
5	1.1616	1.5368	1.5750	1.1279	1.1292	1.6339	1.7027	1.6703	1.5772	1.1742				
4	1.1527	1.5126	1.5323	1.0782	1.0618	1.5372	1.6183	1.6126	1.5477	1.1639				
3	1.0686	1.3936	1.3906	0.9268	0.8835	1.0339	1.1158	1.4458	1.4211	1.0777				
2	0.8355	1.1108	1.0931	0.6883	0.6374	0.6505	0.7148	1.1239	1.1304	0.8422				
1	0.4846	0.6924	0.6752	0.4105	0.3726	0.3765	0.4196	0.6890	0.7029	0.4881				

JAERI-M 86-063

EXPOSURE 0.0 CYCLE 9 S(I,J,K) BY BANK

(6)

	1	2	3	4	5	6	7	8	9	10	11	12	13	14
12	0.2393	0.3545	0.3815	0.3885	0.3743	0.2478	0.2453	0.3566	0.3432	0.2359				
11	0.4645	0.6410	0.6875	0.6996	0.6744	0.4510	0.4466	0.6436	0.6209	0.4581				
10	0.6550	0.8973	0.9604	0.9774	0.9429	0.6347	0.6286	0.9001	0.8699	0.6462				
9	0.8169	1.1169	1.1959	1.2178	1.1754	0.7964	0.7887	1.1218	1.0834	0.8062				
8	0.9516	1.2986	1.3908	1.4178	1.3688	0.9336	0.9246	1.3057	1.2605	0.9395				
7	1.0584	1.4401	1.5409	1.5726	1.5179	1.0420	1.0325	1.4478	1.3989	1.0455				
6	1.1348	1.5361	1.6386	1.6735	1.6129	1.1129	1.1050	1.5413	1.4939	1.1216				
5	1.1742	1.5772	1.6703	1.7027	1.6339	1.1292	1.1279	1.5750	1.5368	1.1616				
4	1.1639	1.5477	1.6126	1.6183	1.5372	1.0618	1.0782	1.5323	1.5126	1.1527				
3	1.0777	1.4211	1.4458	1.1158	1.0339	0.8835	0.9268	1.3906	1.3936	1.0686				
2	0.8422	1.1304	1.1239	0.7148	0.6505	0.6374	0.6883	1.0931	1.1108	0.8355				
1	0.4881	0.7029	0.6890	0.4196	0.3765	0.3726	0.4105	0.6752	0.6924	0.4846				

(7)

	1	2	3	4	5	6	7	8	9	10	11	12	13	14
12	0.0	0.3274	0.3789	0.4030	0.3885	0.2453	0.2335	0.3313	0.3011	0.0				
11	0.0	0.6096	0.6837	0.7252	0.6996	0.4466	0.4256	0.5996	0.5618	0.0				
10	0.0	0.8536	0.9558	1.0126	0.9774	0.6286	0.5996	0.8404	0.7882	0.0				
9	0.0	1.0623	1.1900	1.2611	1.2178	0.7887	0.7528	1.0487	0.9827	0.0				
8	0.0	1.2350	1.3838	1.4677	1.4178	0.9246	0.8830	1.2219	1.1446	0.0				
7	0.0	1.3693	1.5333	1.6280	1.5726	1.0325	0.9869	1.3568	1.2719	0.0				
6	0.0	1.4601	1.6310	1.7337	1.6735	1.1050	1.0583	1.4478	1.3606	0.0				
5	0.0	1.4978	1.6632	1.7677	1.7027	1.1279	1.0859	1.4854	1.4025	0.0				
4	0.0	1.4668	1.6062	1.6886	1.6183	1.0782	1.0531	1.4543	1.3830	0.0				
3	0.0	1.3417	1.4392	1.1800	1.1158	0.9268	0.9285	1.3302	1.2745	0.0				
2	0.0	1.0553	1.1162	0.7617	0.7148	0.6883	0.7070	1.0489	1.0067	0.0				
1	0.0	0.6341	0.6831	0.4498	0.4196	0.4105	0.4282	0.6502	0.6079	0.0				

(8)

	1	2	3	4	5	6	7	8	9	10	11	12	13	14
12	0.0	0.2837	0.3423	0.3789	0.3815	0.3566	0.3313	0.3043	0.2574	0.0				
11	0.0	0.5294	0.6204	0.6837	0.6875	0.6436	0.5996	0.5530	0.4815	0.0				
10	0.0	0.7443	0.8694	0.9558	0.9604	0.9001	0.8404	0.7768	0.6786	0.0				
9	0.0	0.9279	1.0836	1.1900	1.1959	1.1218	1.0487	0.9705	0.8481	0.0				
8	0.0	1.0800	1.2610	1.3838	1.3908	1.3057	1.2219	1.1321	0.9898	0.0				
7	0.0	1.1992	1.3984	1.5333	1.5409	1.4478	1.3568	1.2592	1.1025	0.0				
6	0.0	1.2811	1.4900	1.6310	1.6386	1.5413	1.4478	1.3473	1.1827	0.0				
5	0.0	1.3175	1.5248	1.6632	1.6703	1.5750	1.4854	1.3880	1.2230	0.0				
4	0.0	1.2934	1.4866	1.6062	1.6126	1.5323	1.4543	1.3668	1.2087	0.0				
3	0.0	1.1839	1.3506	1.4392	1.4458	1.3906	1.3302	1.2573	1.1134	0.0				
2	0.0	0.9232	1.0624	1.1162	1.1239	1.0931	1.0489	0.9958	0.8701	0.0				
1	0.0	0.5542	0.6537	0.6831	0.6890	0.6752	0.6502	0.6172	0.5244	0.0				

EXPOSURE 0.0 CYCLE 9 S(I,J,K) BY BANK

	1	2	3	4	5	6	7	8	9	10	11	12	13	14
(9)														
12	0.0	0.2243	0.2837	0.3274	0.3545	0.3432	0.3011	0.2574	0.2042	0.0				
11	0.0	0.4345	0.5294	0.6096	0.6410	0.6209	0.5618	0.4815	0.3966	0.0				
10	0.0	0.6135	0.7443	0.8536	0.8973	0.8699	0.7882	0.6786	0.5614	0.0				
9	0.0	0.7661	0.9279	1.0623	1.1169	1.0834	0.9827	0.8481	0.7030	0.0				
8	0.0	0.8932	1.0800	1.2350	1.2986	1.2605	1.1446	0.9898	0.8221	0.0				
7	0.0	0.9941	1.1992	1.3693	1.4401	1.3989	1.2719	1.1025	0.9181	0.0				
6	0.0	1.0656	1.2811	1.4601	1.5361	1.4939	1.3606	1.1827	0.9884	0.0				
5	0.0	1.1007	1.3175	1.4978	1.5772	1.5368	1.4025	1.2230	1.0262	0.0				
4	0.0	1.0856	1.2934	1.4668	1.5477	1.5126	1.3830	1.2087	1.0173	0.0				
3	0.0	0.9870	1.1839	1.3417	1.4211	1.3936	1.2745	1.1134	0.9239	0.0				
2	0.0	0.7619	0.9232	1.0553	1.1304	1.1108	1.0067	0.8701	0.7171	0.0				
1	0.0	0.4403	0.5542	0.6341	0.7029	0.6924	0.6079	0.5244	0.4156	0.0				
(10)														
12	0.0	0.0	0.0	0.0	0.2393	0.2359	0.0	0.0	0.0	0.0				
11	0.0	0.0	0.0	0.0	0.4645	0.4581	0.0	0.0	0.0	0.0				
10	0.0	0.0	0.0	0.0	0.6550	0.6462	0.0	0.0	0.0	0.0				
9	0.0	0.0	0.0	0.0	0.8169	0.8062	0.0	0.0	0.0	0.0				
8	0.0	0.0	0.0	0.0	0.9516	0.9395	0.0	0.0	0.0	0.0				
7	0.0	0.0	0.0	0.0	1.0584	1.0455	0.0	0.0	0.0	0.0				
6	0.0	0.0	0.0	0.0	1.1348	1.1216	0.0	0.0	0.0	0.0				
5	0.0	0.0	0.0	0.0	1.1742	1.1616	0.0	0.0	0.0	0.0				
4	0.0	0.0	0.0	0.0	1.1639	1.1527	0.0	0.0	0.0	0.0				
3	0.0	0.0	0.0	0.0	1.0777	1.0686	0.0	0.0	0.0	0.0				
2	0.0	0.0	0.0	0.0	0.8422	0.8355	0.0	0.0	0.0	0.0				
1	0.0	0.0	0.0	0.0	0.4881	0.4846	0.0	0.0	0.0	0.0				

EXPOSURE 0.0 CYCLE 9 U(I,J) BY CHANNEL

	1	2	3	4	5	6	7	8	9	10	11	12	13	14
(0)														
1	0.0	0.0	0.0	0.0	0.2391	0.2411	0.0	0.0	0.0	0.0				
2	0.0	0.2008	0.2364	0.2549	0.2749	0.2795	0.2670	0.2505	0.2137	0.0				
3	0.0	0.2364	0.2633	0.2659	0.2766	0.2862	0.2851	0.2804	0.2505	0.0				
4	0.0	0.2549	0.2659	0.2038	0.2068	0.2646	0.2731	0.2851	0.2670	0.0				
5	0.2391	0.2749	0.2766	0.2068	0.2023	0.2541	0.2646	0.2862	0.2795	0.2411				
6	0.2411	0.2795	0.2862	0.2646	0.2541	0.2023	0.2068	0.2766	0.2749	0.2391				
7	0.0	0.2670	0.2851	0.2731	0.2646	0.2068	0.2038	0.2659	0.2549	0.0				
8	0.0	0.2505	0.2804	0.2851	0.2862	0.2766	0.2659	0.2633	0.2364	0.0				
9	0.0	0.2137	0.2505	0.2670	0.2795	0.2749	0.2549	0.2364	0.2008	0.0				
10	0.0	0.0	0.0	0.0	0.2411	0.2391	0.0	0.0	0.0	0.0				
11	0.0	0.0	0.0	0.0	0.0	0.0	0.0	0.0	0.0	0.0				

JAERI-M 86-063

EXPOSURE 0.0 CYCLE 9 U(I,J,K) BY BANK

	1	2	3	4	5	6	7	8	9	10	11	12	13	14
(1)														
12	0.0	0.0	0.0	0.0	0.4215	0.4242	0.0	0.0	0.0	0.0				
11	0.0	0.0	0.0	0.0	0.4127	0.4154	0.0	0.0	0.0	0.0				
10	0.0	0.0	0.0	0.0	0.3979	0.4006	0.0	0.0	0.0	0.0				
9	0.0	0.0	0.0	0.0	0.3771	0.3797	0.0	0.0	0.0	0.0				
8	0.0	0.0	0.0	0.0	0.3493	0.3519	0.0	0.0	0.0	0.0				
7	0.0	0.0	0.0	0.0	0.3129	0.3154	0.0	0.0	0.0	0.0				
6	0.0	0.0	0.0	0.0	0.2650	0.2675	0.0	0.0	0.0	0.0				
5	0.0	0.0	0.0	0.0	0.2018	0.2041	0.0	0.0	0.0	0.0				
4	0.0	0.0	0.0	0.0	0.1184	0.1204	0.0	0.0	0.0	0.0				
3	0.0	0.0	0.0	0.0	0.0121	0.0137	0.0	0.0	0.0	0.0				
2	0.0	0.0	0.0	0.0	0.0	0.0	0.0	0.0	0.0	0.0				
1	0.0	0.0	0.0	0.0	0.0	0.0	0.0	0.0	0.0	0.0				
(2)														
12	0.0	0.3729	0.4185	0.4413	0.4656	0.4722	0.4579	0.4374	0.3911	0.0				
11	0.0	0.3641	0.4096	0.4322	0.4561	0.4625	0.4484	0.4282	0.3822	0.0				
10	0.0	0.3493	0.3948	0.4172	0.4409	0.4471	0.4331	0.4132	0.3673	0.0				
9	0.0	0.3282	0.3740	0.3963	0.4197	0.4257	0.4117	0.3920	0.3460	0.0				
8	0.0	0.2998	0.3461	0.3684	0.3919	0.3977	0.3835	0.3639	0.3174	0.0				
7	0.0	0.2624	0.3096	0.3321	0.3558	0.3615	0.3469	0.3270	0.2799	0.0				
6	0.0	0.2135	0.2615	0.2844	0.3087	0.3142	0.2988	0.2787	0.2307	0.0				
5	0.0	0.1501	0.1980	0.2211	0.2461	0.2513	0.2349	0.2145	0.1664	0.0				
4	0.0	0.0689	0.1147	0.1370	0.1620	0.1668	0.1496	0.1297	0.0835	0.0				
3	0.0	0.0	0.0095	0.0290	0.0517	0.0556	0.0391	0.0217	0.0	0.0				
2	0.0	0.0	0.0	0.0	0.0	0.0	0.0	0.0	0.0	0.0				
1	0.0	0.0	0.0	0.0	0.0	0.0	0.0	0.0	0.0	0.0				
(3)														
12	0.0	0.4185	0.4513	0.4559	0.4706	0.4846	0.4832	0.4750	0.4374	0.0				
11	0.0	0.4096	0.4420	0.4464	0.4609	0.4745	0.4732	0.4652	0.4282	0.0				
10	0.0	0.3948	0.4270	0.4313	0.4453	0.4585	0.4572	0.4496	0.4132	0.0				
9	0.0	0.3740	0.4061	0.4101	0.4237	0.4364	0.4352	0.4280	0.3920	0.0				
8	0.0	0.3461	0.3784	0.3820	0.3953	0.4075	0.4063	0.3997	0.3639	0.0				
7	0.0	0.3096	0.3422	0.3455	0.3585	0.3703	0.3690	0.3630	0.3270	0.0				
6	0.0	0.2615	0.2948	0.2975	0.3103	0.3216	0.3203	0.3150	0.2787	0.0				
5	0.0	0.1980	0.2317	0.2339	0.2461	0.2566	0.2552	0.2511	0.2145	0.0				
4	0.0	0.1147	0.1476	0.1490	0.1601	0.1691	0.1676	0.1652	0.1297	0.0				
3	0.0	0.0095	0.0387	0.0394	0.0484	0.0549	0.0534	0.0529	0.0217	0.0				
2	0.0	0.0	0.0	0.0	0.0	0.0	0.0	0.0	0.0	0.0				
1	0.0	0.0	0.0	0.0	0.0	0.0	0.0	0.0	0.0	0.0				

```
OUTPUT OF SCOPERS-2 PROGRAM     NS MUTSU BOL,FULL POWER,NO XENON,G1,G2 INSERTED, MAY 1976 *FOR J     PAGE      1

                                                    INPUT CARDS          TIME 20 HRS  16 MIN  54 SEC
                    1     2     3     4     5     6     7     8     9     10    11    12    13    14    15    16

KD B/P BRN-LST    E(O)  EMAX    DE    PTH   PRATED  DX    DZ     RODCEL  BC     IMAX  JMAX  KMAX  BORN
 1  1   0              * 0.0 0.0 0.0 36.0 36.0 8.98 8.667 -2 -1 12 12 12 0.0                *              (  PWR     )

KD PCH KPCH       DSIJK  NS  DL(S)   NU     DL(U)  DL(SH)  DSHNK  LMBDA   JP  JS  JU  JK
 2  0   0              * 0.00009 4 0.0 20 0.00004 0.0 0.0 1.0 0 0 0 0                       *              (          )

KD                      ALBEDO  CONSTANTS  ( TOP , BOTTOM , PERIPHERAL )
 4  0   0              *  3.0 0.25 0.236 25.0 3.0 0.25 0.236 25.0 3.0 0.35 0.236 36.0     *              (          )

KD KZ   T              CONSTANTS  BY  FUEL  TYPE       B(T,KZ,J)  J=1,28(BWR) , J=1,30(PWR)
 5  1   1              * 52.98 0.169 4.0812 0.01204 1.2489 0.0 0.0 -0.00023 0.0 0.0          *              (          )
 5  1   1              * 1.0700 0.0 0.0 -2.00E-4 0.0 0.0 0.7962 0.0 0.0 -1.45E-4 0.0        *              (          )
 5  1   1              * 0.0 0.0 0.0 0.01 0.0 +0.00808 0.0 1.0 1.0 3.4614                   *              (          )
 5  0   1              * 53.74 0.172 3.6448 0.01072 1.1657 0.0 0.0 -0.00023 0.0 0.0         *              (          )
 5  0   1              * 1.0044 0.0 0.0 -2.00E-4 0.0 0.0 0.7533 0.0 0.0 -1.50E-4 0.0        *              (          )
 5  0   1              * 0.0 0.0 0.0 0.01 0.035 +0.0060 .035 3.5 1.0                        *              (          )
 5 -1   1              * 52.98 0.169 4.0812 0.01204 1.2489 0.0 0.0 -0.00023 0.0 0.0         *              (          )
 5 -1   1              * 1.0700 0.0 0.0 -2.00E-4 0.0 0.0 0.7962 0.0 0.0 -1.45E-4 0.0        *              (          )
 5 -1   1              * 0.0 0.0 0.0 0.01 0.0 +0.00808 0.0 1.0 1.0 1.1538                   *              (          )
 5  1   2              * 52.75 0.167 3.3336 0.00946 1.3365 0.0 0.0 -0.000275 0.0 0.0        *              (          )
 5  1   2              * 1.1601 0.0 0.0 -2.40E-4 0.0 0.0 0.8813 0.0 0.0 -1.80E-4 0.0        *              (          )
 5  1   2              * 0.0 0.0 0.0 0.01 0.0 +0.00742 0.0 1.0 1.0 3.4614                   *              (          )
 5  0   2              * 53.30 0.170 2.9131 0.00826 1.2268 0.0 0.0 -0.000280 0.0 0.0        *              (          )
 5  0   2              * 1.0718 0.0 0.0 -2.45E-4 0.0 0.0 0.8218 0.0 0.0 -1.90E-4 0.0        *              (          )
 5  0   2              * 0.0 0.0 0.0 0.01 0.021 +0.0036 .021 3.3 1.0                        *              (          )
 5 -1   2              * 52.75 0.167 3.3336 0.00946 1.3365 0.0 0.0 -0.000275 0.0 0.0        *              (          )
 5 -1   2              * 1.1601 0.0 0.0 -2.40E-4 0.0 0.0 0.8813 0.0 0.0 -1.80E-4 0.0        *              (          )
 5 -1   2              * 0.0 0.0 0.0 0.01 0.0 +0.00742 0.0 1.0 1.0 1.1538                   *              (          )

KD      I                        FUEL  TYPE          T(I,J)  J=1,JMAX
 6  0   1              *  0 0 2 2 2 2 2 2 2 2 0 0                                          *              (          )
 6  0   2              *  0 0 2 2 2 2 2 2 2 2 0 0                                          *              (          )
 6  0   3              *  2 2 2 2 1 1 1 1 2 2 2 2                                          *              (          )
 6  0   4              *  2 2 2 2 1 1 1 1 2 2 2 2                                          *              (          )
 6  0   5              *  2 2 1 1 1 1 1 1 1 1 2 2                                          *              (          )
 6  0   6              *  2 2 1 1 1 1 1 1 1 1 2 2                                          *              (          )
 6  0   7              *  2 2 1 1 1 1 1 1 1 1 2 2                                          *              (          )
 6  0   8              *  2 2 1 1 1 1 1 1 1 1 2 2                                          *              (          )
 6  0   9              *  2 2 2 2 1 1 1 1 2 2 2 2                                          *              (          )
 6  0  10              *  2 2 2 2 1 1 1 1 2 2 2 2                                          *              (          )
 6  0  11              *  0 0 2 2 2 2 2 2 2 2 0 0                                          *              (          )
 6  0  12              *  0 0 2 2 2 2 2 2 2 2 0 0                                          *              (          )

KD      I              CONTROL ROD POSITION          R(I,J)  J=1,JMAX
 8  0   1              *   S12                                                            *              (          )
 8  0   2              *   S12                                                            *              (          )
 8  0   3              *   S12                                                            *              (          )
 8  0   4              *   S12                                                            *              (          )
 8  0   5              *   S6 12.0 S5                                                     *              (          )
```

INPUT CARDS

```
                  1     2     3     4     5     6     7     8     9     10    11    12    13    14    15    16
 8  0   6              *   S12                                                          *                 (           )
 8  0   7              *   S4 12.0 S3 12.0 S3                                           *                 (           )
 8  0   8              *   S12                                                          *                 (           )
 8  0   9              *   S6 12.0 S5                                                   *                 (           )
 8  0  10              *   S12                                                          *                 (           )
 8  0  11              *   S12                                                          *                 (           )
 8  0  12              *   S12                                                          *                 (           )

KD   IACCEL        ACCELERATION FACTORS          ACCEL(NS) ,  NS=1,16
14  0   0              * 0.375 R4                                                       *                 (           )

KD  K IED             THERMAL-HYDRAULIC CONST.        C(J)       J=1,18(BWR) , J=1,15(PWR)
15  0   0              * 1610. 0.0 0.0 1.0 287.0 -9.615 0.0 1.0 34.3 0.8333 0.0  0.0 0.0*                 (           )
15  0   0              * 278.8 1.0                                                      *                 (           )

KD      T             ETA-E ETA-T ETA-TH KS
20  0   1              *   1.0 0.0 0.23 1.0                                           *                 (           )
20  0   2              *   1.0 0.0 0.23 1.0                                           *                 (           )
99  0   0              *                                                              *                 (           )
```

BASIC ALBEDO FOR TOP 0.38914

BASIC ALBEDO FOR BOTTOM 0.38914

BASIC ALBEDO FOR PERIPHERAL 0.24785

ALBEDOS IN GEOMETRIC CONSIDERATION --- (XBRHL/XBRHLC/AVL/AHS/AHL)

J=	1	2	3	4	5	6	7	8	9	10	11	12
I=	1											
	0.0	0.0	3.0000	2.0000	2.0000	2.0000	2.0000	2.0000	2.0000	3.0000	0.0	0.0
	0.0	0.0	1.0000	0.0	0.0	0.0	0.0	0.0	0.0	1.0000	0.0	0.0
	0.0	0.0	0.9914	0.4957	0.4957	0.4957	0.4957	0.4957	0.4957	0.9914	0.0	0.0
	0.0	0.0	0.4957	0.2478	0.2478	0.2478	0.2478	0.2478	0.2478	0.4957	0.0	0.0
	0.0	0.0	0.4957	0.4957	0.4957	0.4957	0.4957	0.4957	0.4957	0.4957	0.0	0.0
I=	2											
	0.0	0.0	1.0000	0.0	0.0	0.0	0.0	0.0	0.0	1.0000	0.0	0.0
	0.0	0.0	0.0	0.0	0.0	0.0	0.0	0.0	0.0	0.0	0.0	0.0
	0.0	0.0	0.6613	0.0	0.0	0.0	0.0	0.0	0.0	0.6613	0.0	0.0
	0.0	0.0	0.3306	0.0	0.0	0.0	0.0	0.0	0.0	0.3306	0.0	0.0
	0.0	0.0	0.2478	0.0	0.0	0.0	0.0	0.0	0.0	0.2478	0.0	0.0
I=	3											
	3.0000	1.0000	1.0000	0.0	0.0	0.0	0.0	0.0	0.0	1.0000	1.0000	3.0000
	1.0000	0.0	1.0000	0.0	0.0	0.0	0.0	0.0	0.0	1.0000	0.0	1.0000
	0.9914	0.6613	0.0	0.0	0.0	0.0	0.0	0.0	0.0	0.0	0.6613	0.9914
	0.4957	0.3306	0.0	0.0	0.0	0.0	0.0	0.0	0.0	0.0	0.3306	0.4957
	0.4957	0.2478	0.0	0.0	0.0	0.0	0.0	0.0	0.0	0.0	0.2478	0.4957
I=	4											
	2.0000	0.0	0.0	0.0	0.0	0.0	0.0	0.0	0.0	0.0	0.0	2.0000
	0.0	0.0	0.0	0.0	0.0	0.0	0.0	0.0	0.0	0.0	0.0	0.0
	0.4957	0.0	0.0	0.0	0.0	0.0	0.0	0.0	0.0	0.0	0.0	0.4957
	0.2478	0.0	0.0	0.0	0.0	0.0	0.0	0.0	0.0	0.0	0.0	0.2478
	0.4957	0.0	0.0	0.0	0.0	0.0	0.0	0.0	0.0	0.0	0.0	0.4957
I=	5											
	2.0000	0.0	0.0	0.0	0.0	0.0	0.0	0.0	0.0	0.0	0.0	2.0000
	0.0	0.0	0.0	0.0	0.0	0.0	0.0	0.0	0.0	0.0	0.0	0.0
	0.4957	0.0	0.0	0.0	0.0	0.0	0.0	0.0	0.0	0.0	0.0	0.4957
	0.2478	0.0	0.0	0.0	0.0	0.0	0.0	0.0	0.0	0.0	0.0	0.2478
	0.4957	0.0	0.0	0.0	0.0	0.0	0.0	0.0	0.0	0.0	0.0	0.4957
I=	6											
	2.0000	0.0	0.0	0.0	0.0	0.0	0.0	0.0	0.0	0.0	0.0	2.0000
	0.0	0.0	0.0	0.0	0.0	0.0	0.0	0.0	0.0	0.0	0.0	0.0
	0.4957	0.0	0.0	0.0	0.0	0.0	0.0	0.0	0.0	0.0	0.0	0.4957
	0.2478	0.0	0.0	0.0	0.0	0.0	0.0	0.0	0.0	0.0	0.0	0.2478
	0.4957	0.0	0.0	0.0	0.0	0.0	0.0	0.0	0.0	0.0	0.0	0.4957
I=	7											
	2.0000	0.0	0.0	0.0	0.0	0.0	0.0	0.0	0.0	0.0	0.0	2.0000
	0.0	0.0	0.0	0.0	0.0	0.0	0.0	0.0	0.0	0.0	0.0	0.0
	0.4957	0.0	0.0	0.0	0.0	0.0	0.0	0.0	0.0	0.0	0.0	0.4957
	0.2478	0.0	0.0	0.0	0.0	0.0	0.0	0.0	0.0	0.0	0.0	0.2478
	0.4957	0.0	0.0	0.0	0.0	0.0	0.0	0.0	0.0	0.0	0.0	0.4957

ALBEDOS IN GEOMETRIC CONSIDERATION --- (XBRHL/XBRHLC/AVL/AHS/AHL)

J=	1	2	3	4	5	6	7	8	9	10	11	12
I=	8											
	2.0000	0.0	0.0	0.0	0.0	0.0	0.0	0.0	0.0	0.0	0.0	2.0000
	0.0	0.0	0.0	0.0	0.0	0.0	0.0	0.0	0.0	0.0	0.0	0.0
	0.4957	0.0	0.0	0.0	0.0	0.0	0.0	0.0	0.0	0.0	0.0	0.4957
	0.2478	0.0	0.0	0.0	0.0	0.0	0.0	0.0	0.0	0.0	0.0	0.2478
	0.4957	0.0	0.0	0.0	0.0	0.0	0.0	0.0	0.0	0.0	0.0	0.4957
I=	9											
	2.0000	0.0	0.0	0.0	0.0	0.0	0.0	0.0	0.0	0.0	0.0	2.0000
	0.0	0.0	0.0	0.0	0.0	0.0	0.0	0.0	0.0	0.0	0.0	0.0
	0.4957	0.0	0.0	0.0	0.0	0.0	0.0	0.0	0.0	0.0	0.0	0.4957
	0.2478	0.0	0.0	0.0	0.0	0.0	0.0	0.0	0.0	0.0	0.0	0.2478
	0.4957	0.0	0.0	0.0	0.0	0.0	0.0	0.0	0.0	0.0	0.0	0.4957
I=	10											
	3.0000	1.0000	1.0000	0.0	0.0	0.0	0.0	0.0	0.0	1.0000	1.0000	3.0000
	1.0000	0.0	1.0000	0.0	0.0	0.0	0.0	0.0	0.0	1.0000	0.0	1.0000
	0.9914	0.6613	0.0	0.0	0.0	0.0	0.0	0.0	0.0	0.0	0.6613	0.9914
	0.4957	0.3306	0.0	0.0	0.0	0.0	0.0	0.0	0.0	0.0	0.3306	0.4957
	0.4957	0.2478	0.0	0.0	0.0	0.0	0.0	0.0	0.0	0.0	0.2478	0.4957
I=	11											
	0.0	0.0	1.0000	0.0	0.0	0.0	0.0	0.0	0.0	1.0000	0.0	0.0
	0.0	0.0	0.0	0.0	0.0	0.0	0.0	0.0	0.0	0.0	0.0	0.0
	0.0	0.0	0.6613	0.0	0.0	0.0	0.0	0.0	0.0	0.6613	0.0	0.0
	0.0	0.0	0.3306	0.0	0.0	0.0	0.0	0.0	0.0	0.3306	0.0	0.0
	0.0	0.0	0.2478	0.0	0.0	0.0	0.0	0.0	0.0	0.2478	0.0	0.0
I=	12											
	0.0	0.0	3.0000	2.0000	2.0000	2.0000	2.0000	2.0000	2.0000	3.0000	0.0	0.0
	0.0	0.0	1.0000	0.0	0.0	0.0	0.0	0.0	0.0	1.0000	0.0	0.0
	0.0	0.0	0.9914	0.4957	0.4957	0.4957	0.4957	0.4957	0.4957	0.9914	0.0	0.0
	0.0	0.0	0.4957	0.2478	0.2478	0.2478	0.2478	0.2478	0.2478	0.4957	0.0	0.0
	0.0	0.0	0.4957	0.4957	0.4957	0.4957	0.4957	0.4957	0.4957	0.4957	0.0	0.0

EXPOSURE 0.0 CYCLE 0 R(I,J) BY CHANNEL

	1	2	3	4	5	6	7	8	9	10	11	12	13	14
(0)														
1	0.0	0.0	0.0	0.0	0.0	0.0	0.0	0.0	0.0	0.0	0.0	0.0		
2	0.0	0.0	0.0	0.0	0.0	0.0	0.0	0.0	0.0	0.0	0.0	0.0		
3	0.0	0.0	0.0	0.0	0.0	0.0	0.0	0.0	0.0	0.0	0.0	0.0		
4	0.0	0.0	0.0	0.0	0.0	0.0	0.0	0.0	0.0	0.0	0.0	0.0		
5	0.0	0.0	0.0	0.0	0.0	0.0	12.0000	0.0	0.0	0.0	0.0	0.0		
6	0.0	0.0	0.0	0.0	0.0	0.0	0.0	0.0	0.0	0.0	0.0	0.0		
7	0.0	0.0	0.0	0.0	12.0000	0.0	0.0	0.0	12.0000	0.0	0.0	0.0		
8	0.0	0.0	0.0	0.0	0.0	0.0	0.0	0.0	0.0	0.0	0.0	0.0		
9	0.0	0.0	0.0	0.0	0.0	0.0	12.0000	0.0	0.0	0.0	0.0	0.0		
10	0.0	0.0	0.0	0.0	0.0	0.0	0.0	0.0	0.0	0.0	0.0	0.0		
11	0.0	0.0	0.0	0.0	0.0	0.0	0.0	0.0	0.0	0.0	0.0	0.0		
12	0.0	0.0	0.0	0.0	0.0	0.0	0.0	0.0	0.0	0.0	0.0	0.0		
13	0.0	0.0	0.0	0.0	0.0	0.0	0.0	0.0	0.0	0.0	0.0	0.0		

NC	NU	NS	DELTA L S	DELTA L U	DELTA L C	ACCEL S TOT	MAX REL CHG IN SOURCE	SOURCE TOT	LAMBDA
1	1	1	-0.099806	-0.099806	-0.099806	1536.05225	0.512099 1 3 12	1456.78711	0.900194
1	1	2	0.027072	-0.072735	-0.072735	1535.98267	0.179761 6 6 1	1554.31079	0.927265
1	1	3	0.012160	-0.060575	-0.060575	1536.00586	0.169768 1 3 1	1545.81982	0.939425
1	1	4	0.007082	-0.053493	-0.053493	1535.98584	0.117875 6 6 1	1543.74609	0.946507
1	2	1	0.002987	0.002987	-0.050506	1536.00366	0.082578 6 6 1	1541.12671	0.949494
1	2	2	0.002097	0.005084	-0.048409	1536.00244	0.072251 6 6 1	1539.94946	0.951591
1	2	3	0.001732	0.006816	-0.046677	1536.00879	0.053943 6 6 1	1539.18018	0.953323
1	2	4	0.001240	0.008056	-0.045437	1536.00879	0.047383 6 6 1	1538.43799	0.954563
1	3	1	0.000829	0.000829	-0.044608	1535.99316	0.037533 6 6 1	1537.81006	0.955392
1	3	2	0.000726	0.001554	-0.043882	1535.98633	0.032714 6 6 1	1537.43555	0.956118
1	3	3	0.000624	0.002179	-0.043258	1535.98657	0.026875 6 6 1	1537.20020	0.956742
1	3	4	0.000494	0.002673	-0.042764	1535.99072	0.023418 6 6 1	1536.91870	0.957236
CONVERGENCE			1 LAMBDA	0.957236	SHANK 0.958578	SHANK SQ 0.0	DEL LMB 0.001342	DEL SH SQ 0.0	
1	4	1	0.000341	0.000341	-0.042423	1536.00098	0.019888 6 7 1	1536.68774	0.957577
1	4	2	0.000324	0.000665	-0.042099	1535.99976	0.017285 6 6 1	1536.54907	0.957901
1	4	3	0.000312	0.000978	-0.041787	1535.99854	0.014928 6 6 1	1536.48682	0.958213
1	4	4	0.000246	0.001223	-0.041541	1535.98975	0.013005 6 6 1	1536.37671	0.958459
CONVERGENCE			1 LAMBDA	0.958459	SHANK 0.959490	SHANK SQ 0.0	DEL LMB 0.001031	DEL SH SQ 0.0	
1	5	1	0.000164	0.000164	-0.041376	1536.00952	0.011458 6 6 1	1536.27612	0.958624
1	5	2	0.000187	0.000351	-0.041190	1536.00562	0.010037 7 6 1	1536.24780	0.958810
1	5	3	0.000150	0.000501	-0.041039	1535.99316	0.008934 6 6 1	1536.20337	0.958961
1	5	4	0.000136	0.000638	-0.040903	1535.99756	0.007868 6 6 1	1536.18799	0.959097
CONVERGENCE			1 LAMBDA	0.959097	SHANK 0.960583	SHANK SQ 0.951974	DEL LMB 0.0	DEL SH SQ 0.008609	
1	6	1	0.000106	0.000106	-0.040797	1535.99829	0.007109 6 6 1	1536.14209	0.959203
1	6	2	0.000099	0.000205	-0.040698	1535.99023	0.006319 7 6 1	1536.11792	0.959302
1	6	3	0.000090	0.000295	-0.040608	1536.00220	0.005746 6 6 1	1536.11768	0.959392
1	6	4	0.000088	0.000383	-0.040520	1535.98560	0.005141 7 6 1	1536.10254	0.959480
CONVERGENCE			1 LAMBDA	0.959480	SHANK 0.962694	SHANK SQ 0.957768	DEL LMB 0.0	DEL SH SQ 0.004926	
1	7	1	0.000061	0.000061	-0.040460	1535.99683	0.004727 6 6 1	1536.07788	0.959540
1	7	2	0.000056	0.000117	-0.040403	1535.98755	0.004272 7 6 1	1536.07666	0.959597
1	7	3	0.000057	0.000174	-0.040347	1535.99097	0.003939 6 7 1	1536.06909	0.959653
1	7	4	0.000048	0.000222	-0.040298	1535.98535	0.003578 6 6 1	1536.07227	0.959702
CONVERGENCE			1 LAMBDA	0.959702	SHANK 0.964286	SHANK SQ 0.970324	DEL LMB 0.0	DEL SH SQ 0.006039	
1	8	1	0.000050	0.000050	-0.040249	1535.97314	0.003326 5 5 1	1536.06714	0.959751
1	8	2	0.000031	0.000081	-0.040218	1535.98828	0.003047 6 6 1	1536.05054	0.959782
1	8	3	0.000035	0.000115	-0.040183	1535.99878	0.002833 6 7 1	1536.05664	0.959817
1	8	4	0.000035	0.000151	-0.040147	1535.99878	0.002603 6 6 1	1536.04248	0.959853
CONVERGENCE			1 LAMBDA	0.959853	SHANK 0.963835	SHANK SQ 0.964216	DEL LMB 0.0	DEL SH SQ 0.000381	
1	9	1	0.000016	0.000016	-0.040131	1535.98682	0.002440 8 8 1	1536.03125	0.959869
1	9	2	0.000038	0.000055	-0.040093	1535.99170	0.002251 6 6 1	1536.06641	0.959907
1	9	3	0.000017	0.000072	-0.040076	1536.01196	0.002105 6 6 1	1536.02124	0.959924

JAERI—M 86—063

NC	NU	NS	DELTA L S	DELTA L U	DELTA L C	ACCEL S TOT	MAX REL CHG IN SOURCE			SOURCE TOT	LAMBDA
1	9	4	0.000019	0.000091	-0.040057	1536.01147	0.001947	7	7 1	1536.02417	0.959943
CONVERGENCE	1	LAMBDA	0.959943	SHANK	0.969849	SHANK SQ	0.964147	DEL LMB	0.0	DEL SH SQ	0.005702
1	10	1	0.000025	0.000025	-0.040031	1536.02466	0.001828	5	5 1	1536.02148	0.959969
1	10	2	0.000036	0.000062	-0.039995	1535.98535	0.001701	7	7 1	1536.03345	0.960005
1	10	3	0.000019	0.000081	-0.039976	1535.98779	0.001599	6	7 1	1536.03442	0.960024
1	10	4	-0.000000	0.000081	-0.039976	1536.02051	0.001490	6	6 1	1536.00537	0.960024
CONVERGENCE	1	LAMBDA	0.960024	SHANK	0.994048	SHANK SQ	0.961834	DEL LMB	0.0	DEL SH SQ	0.032214
1	11	1	0.000019	0.000019	-0.039957	1535.99634	0.001399	7	6 1	1536.02417	0.960043
1	11	2	0.000012	0.000031	-0.039945	1535.99146	0.001303	6	6 1	1536.02051	0.960055
1	11	3	0.000012	0.000043	-0.039933	1536.01318	0.001226	7	7 1	1536.02075	0.960067
1	11	4	0.000021	0.000064	-0.039912	1535.99072	0.001142	6	7 1	1536.02051	0.960088
CONVERGENCE	1	LAMBDA	0.960088	SHANK	0.981685	SHANK SQ	0.985898	DEL LMB	0.0	DEL SH SQ	0.004213
1	12	1	-0.000004	-0.000004	-0.039916	1536.00098	0.001076	6	6 1	1536.00659	0.960084
1	12	2	0.000018	0.000014	-0.039898	1535.99146	0.001007	7	6 1	1536.03247	0.960102
1	12	3	0.000008	0.000022	-0.039890	1536.01465	0.000944	6	7 1	1536.01196	0.960110
1	12	4	0.000012	0.000034	-0.039878	1535.99487	0.000884	6	6 1	1536.01392	0.960122
CONVERGENCE	1	LAMBDA	0.960122	SHANK	0.975410	SHANK SQ	0.968866	DEL LMB	0.0	DEL SH SQ	0.006544

POWER								QUALITY/TEMP.	
THERMAL	RELATIVE	PEAK	I	J	K	S(K)	LEVEL	U(K)	INLET	EXIT
36.0000	1.00000	2.03139	4	3	9				277.3850	296.6240
						0.64639	12	281.04541		
						1.07259	11	279.90039		
						1.34163	10	278.29297		
						1.37051	9	276.48511		
						1.30367	8	274.70190		
						1.25807	7	272.99219		
						1.18609	6	271.35913		
						1.08500	5	269.83984		
						0.95301	4	268.47583		
						0.78965	3	267.30762		
						0.60313	2	266.37329		
						0.39144	1	265.70581		
						AVG S		AVG U		AVG K
						1.00010		272.70654		1.13628

EXPOSURE 0.0 CYCLE 12 S(I,J) BY CHANNEL

	1	2	3	4	5	6	7	8	9	10	11	12	13	14
(0)														
1	0.0	0.0	0.5679	0.8293	0.9354	0.9669	0.9669	0.9354	0.8293	0.5679	0.0	0.0		
2	0.0	0.0	0.9885	1.2746	1.3445	1.3498	1.3498	1.3445	1.2746	0.9885	0.0	0.0		
3	0.5679	0.9885	1.3371	1.4861	1.0566	1.0046	1.0046	1.0566	1.4861	1.3371	0.9885	0.5679		
4	0.8293	1.2746	1.4861	1.4741	0.9619	0.8710	0.8710	0.9619	1.4741	1.4861	1.2746	0.8293		
5	0.9354	1.3445	1.0566	0.9619	0.5517	0.4799	0.4799	0.5517	0.9619	1.0566	1.3445	0.9354		
6	0.9669	1.3498	1.0046	0.8710	0.4799	0.4066	0.4066	0.4799	0.8710	1.0046	1.3498	0.9669		
7	0.9669	1.3498	1.0046	0.8710	0.4799	0.4066	0.4066	0.4799	0.8710	1.0046	1.3498	0.9669		
8	0.9354	1.3445	1.0566	0.9619	0.5517	0.4799	0.4799	0.5517	0.9619	1.0566	1.3445	0.9354		
9	0.8293	1.2746	1.4861	1.4741	0.9619	0.8710	0.8710	0.9619	1.4741	1.4861	1.2746	0.8293		
10	0.5679	0.9885	1.3371	1.4861	1.0566	1.0046	1.0046	1.0566	1.4861	1.3371	0.9885	0.5679		
11	0.0	0.0	0.9885	1.2746	1.3445	1.3498	1.3498	1.3445	1.2746	0.9885	0.0	0.0		
12	0.0	0.0	0.5679	0.8293	0.9354	0.9669	0.9669	0.9354	0.8293	0.5679	0.0	0.0		
13	0.0	0.0	0.0	0.0	0.0	0.0	0.0	0.0	0.0	0.0	0.0	0.0		

EXPOSURE 0.0 CYCLE 12 S(I,J,K) BY BANK

	1	2	3	4	5	6	7	8	9	10	11	12	13	14
(1)														
12	0.0	0.0	0.3701	0.5479	0.6163	0.6351	0.6351	0.6163	0.5479	0.3701	0.0	0.0		
11	0.0	0.0	0.6339	0.9189	1.0314	1.0630	1.0630	1.0314	0.9189	0.6339	0.0	0.0		
10	0.0	0.0	0.7912	1.1452	1.2856	1.3258	1.3258	1.2856	1.1452	0.7912	0.0	0.0		
9	0.0	0.0	0.7920	1.1496	1.2930	1.3350	1.3350	1.2930	1.1496	0.7920	0.0	0.0		
8	0.0	0.0	0.7376	1.0744	1.2112	1.2521	1.2521	1.2112	1.0744	0.7376	0.0	0.0		
7	0.0	0.0	0.7054	1.0296	1.1627	1.2031	1.2031	1.1627	1.0296	0.7054	0.0	0.0		
6	0.0	0.0	0.6619	0.9675	1.0937	1.1323	1.1323	1.0937	0.9675	0.6619	0.0	0.0		
5	0.0	0.0	0.6039	0.8837	0.9997	1.0352	1.0352	0.9997	0.8837	0.6039	0.0	0.0		
4	0.0	0.0	0.5296	0.7759	0.8781	0.9094	0.9094	0.8781	0.7759	0.5296	0.0	0.0		
3	0.0	0.0	0.4388	0.6435	0.7284	0.7543	0.7543	0.7284	0.6435	0.4388	0.0	0.0		
2	0.0	0.0	0.3357	0.4936	0.5590	0.5788	0.5788	0.5590	0.4936	0.3357	0.0	0.0		
1	0.0	0.0	0.2148	0.3220	0.3652	0.3781	0.3781	0.3652	0.3220	0.2148	0.0	0.0		
(2)														
12	0.0	0.0	0.6514	0.8481	0.8883	0.8872	0.8872	0.8883	0.8481	0.6514	0.0	0.0		
11	0.0	0.0	1.0934	1.3952	1.4604	1.4598	1.4598	1.4604	1.3952	1.0934	0.0	0.0		
10	0.0	0.0	1.3615	1.7366	1.8206	1.8221	1.8221	1.8206	1.7366	1.3615	0.0	0.0		
9	0.0	0.0	1.3670	1.7518	1.8430	1.8482	1.8482	1.8430	1.7518	1.3670	0.0	0.0		
8	0.0	0.0	1.2787	1.6468	1.7388	1.7472	1.7472	1.7388	1.6468	1.2787	0.0	0.0		
7	0.0	0.0	1.2268	1.5836	1.6759	1.6860	1.6860	1.6759	1.5836	1.2268	0.0	0.0		
6	0.0	0.0	1.1539	1.4918	1.5802	1.5905	1.5905	1.5802	1.4918	1.1539	0.0	0.0		
5	0.0	0.0	1.0550	1.3655	1.4469	1.4565	1.4565	1.4469	1.3655	1.0550	0.0	0.0		
4	0.0	0.0	0.9273	1.2013	1.2728	1.2809	1.2809	1.2728	1.2013	0.9273	0.0	0.0		
3	0.0	0.0	0.7699	0.9982	1.0570	1.0632	1.0632	1.0570	0.9982	0.7699	0.0	0.0		
2	0.0	0.0	0.5916	0.7677	0.8120	0.8159	0.8159	0.8120	0.7677	0.5916	0.0	0.0		
1	0.0	0.0	0.3859	0.5090	0.5380	0.5397	0.5397	0.5380	0.5090	0.3859	0.0	0.0		

EXPOSURE 0.0 CYCLE 12 S(I,J,K) BY BANK

	1	2	3	4	5	6	7	8	9	10	11	12	13	14
(3)														
12	0.3701	0.6514	0.8894	0.9801	0.6685	0.6291	0.6291	0.6685	0.9801	0.8894	0.6514	0.3701		
11	0.6339	1.0934	1.4614	1.6082	1.1058	1.0427	1.0427	1.1058	1.6082	1.4614	1.0934	0.6339		
10	0.7912	1.3615	1.8186	2.0042	1.3854	1.3102	1.3102	1.3854	2.0042	1.8186	1.3615	0.7912		
9	0.7920	1.3670	1.8351	2.0314	1.4403	1.3677	1.3677	1.4403	2.0314	1.8351	1.3670	0.7920		
8	0.7376	1.2787	1.7261	1.9199	1.3919	1.3268	1.3268	1.3919	1.9199	1.7261	1.2787	0.7376		
7	0.7054	1.2268	1.6609	1.8529	1.3458	1.2853	1.2853	1.3458	1.8529	1.6609	1.2268	0.7054		
6	0.6619	1.1539	1.5654	1.7490	1.2694	1.2128	1.2128	1.2694	1.7490	1.5654	1.1539	0.6619		
5	0.6039	1.0550	1.4336	1.6028	1.1611	1.1090	1.1090	1.1611	1.6028	1.4336	1.0550	0.6039		
4	0.5296	0.9273	1.2618	1.4111	1.0194	0.9729	0.9729	1.0194	1.4111	1.2618	0.9273	0.5296		
3	0.4388	0.7699	1.0490	1.1728	0.8440	0.8043	0.8043	0.8440	1.1728	1.0490	0.7699	0.4388		
2	0.3357	0.5916	0.8074	0.9020	0.6411	0.6091	0.6091	0.6411	0.9020	0.8074	0.5916	0.3357		
1	0.2148	0.3859	0.5361	0.5987	0.4072	0.3853	0.3853	0.4072	0.5987	0.5361	0.3859	0.2148		
(4)														
12	0.5479	0.8481	0.9801	0.9587	0.5968	0.5326	0.5326	0.5968	0.9587	0.9801	0.8481	0.5479		
11	0.9189	1.3952	1.6082	1.5759	0.9908	0.8870	0.8870	0.9908	1.5759	1.6082	1.3952	0.9189		
10	1.1452	1.7366	2.0042	1.9708	1.2479	1.1220	1.1220	1.2479	1.9708	2.0042	1.7366	1.1452		
9	1.1496	1.7519	2.0314	2.0089	1.3072	1.1819	1.1819	1.3072	2.0089	2.0314	1.7519	1.1496		
8	1.0744	1.6468	1.9199	1.9093	1.2722	1.1561	1.1561	1.2722	1.9093	1.9199	1.6468	1.0744		
7	1.0296	1.5836	1.8529	1.8487	1.2349	1.1251	1.1251	1.2349	1.8487	1.8529	1.5836	1.0296		
6	0.9675	1.4918	1.7490	1.7472	1.1663	1.0632	1.0632	1.1663	1.7472	1.7490	1.4918	0.9675		
5	0.8837	1.3655	1.6028	1.6014	1.0666	0.9718	0.9718	1.0666	1.6015	1.6028	1.3655	0.8837		
4	0.7759	1.2013	1.4111	1.4090	0.9353	0.8511	0.8511	0.9353	1.4090	1.4111	1.2013	0.7759		
3	0.6435	0.9982	1.1728	1.1693	0.7724	0.7013	0.7013	0.7724	1.1693	1.1728	0.9982	0.6435		
2	0.4936	0.7677	0.9020	0.8967	0.5839	0.5280	0.5280	0.5839	0.8967	0.9020	0.7677	0.4936		
1	0.3220	0.5090	0.5987	0.5927	0.3684	0.3312	0.3312	0.3684	0.5927	0.5987	0.5090	0.3220		
(5)														
12	0.6163	0.8883	0.6685	0.5968	0.3309	0.2833	0.2833	0.3309	0.5968	0.6685	0.8883	0.6163		
11	1.0314	1.4604	1.1058	0.9908	0.5542	0.4761	0.4761	0.5542	0.9908	1.1058	1.4604	1.0314		
10	1.2856	1.8206	1.3854	1.2479	0.7032	0.6069	0.6069	0.7032	1.2479	1.3854	1.8206	1.2856		
9	1.2930	1.8430	1.4403	1.3072	0.7483	0.6496	0.6496	0.7483	1.3072	1.4403	1.8430	1.2930		
8	1.2112	1.7388	1.3919	1.2722	0.7383	0.6443	0.6443	0.7383	1.2722	1.3919	1.7388	1.2112		
7	1.1627	1.6759	1.3458	1.2349	0.7191	0.6294	0.6294	0.7191	1.2349	1.3458	1.6759	1.1627		
6	1.0937	1.5802	1.2694	1.1663	0.6793	0.5951	0.5951	0.6793	1.1663	1.2694	1.5802	1.0937		
5	0.9997	1.4469	1.1611	1.0666	0.6202	0.5431	0.5431	0.6202	1.0666	1.1611	1.4469	0.9997		
4	0.8781	1.2728	1.0194	0.9353	0.5422	0.4743	0.4743	0.5422	0.9353	1.0194	1.2728	0.8781		
3	0.7284	1.0570	0.8440	0.7724	0.4458	0.3891	0.3891	0.4458	0.7724	0.8440	1.0570	0.7284		
2	0.5590	0.8120	0.6411	0.5839	0.3337	0.2901	0.2901	0.3337	0.5839	0.6411	0.8120	0.5590		
1	0.3652	0.5380	0.4072	0.3684	0.2054	0.1776	0.1776	0.2054	0.3684	0.4072	0.5380	0.3652		

JAERI-M 86-063

EXPOSURE 0.0 CYCLE 12 S(I,J,K) BY BANK

(6)

	1	2	3	4	5	6	7	8	9	10	11	12	13	14
12	0.6351	0.8872	0.6291	0.5326	0.2833	0.2360	0.2360	0.2833	0.5326	0.6291	0.8872	0.6351		
11	1.0630	1.4598	1.0427	0.8870	0.4761	0.3981	0.3981	0.4761	0.8870	1.0427	1.4598	1.0630		
10	1.3258	1.8221	1.3102	1.1220	0.6069	0.5099	0.5099	0.6069	1.1220	1.3102	1.8221	1.3258		
9	1.3350	1.8482	1.3677	1.1819	0.6496	0.5491	0.5491	0.6496	1.1819	1.3677	1.8482	1.3350		
8	1.2521	1.7472	1.3268	1.1561	0.6443	0.5476	0.5476	0.6443	1.1561	1.3268	1.7472	1.2521		
7	1.2031	1.6860	1.2853	1.1251	0.6294	0.5366	0.5366	0.6294	1.1251	1.2853	1.6860	1.2031		
6	1.1323	1.5905	1.2128	1.0632	0.5951	0.5079	0.5079	0.5951	1.0632	1.2128	1.5905	1.1323		
5	1.0352	1.4565	1.1090	0.9718	0.5431	0.4635	0.4635	0.5431	0.9718	1.1090	1.4565	1.0352		
4	0.9094	1.2809	0.9729	0.8511	0.4743	0.4043	0.4043	0.4743	0.8511	0.9729	1.2809	0.9094		
3	0.7543	1.0632	0.8043	0.7013	0.3891	0.3308	0.3308	0.3891	0.7013	0.8043	1.0632	0.7543		
2	0.5788	0.8159	0.6091	0.5280	0.2901	0.2457	0.2457	0.2901	0.5280	0.6091	0.8159	0.5788		
1	0.3781	0.5397	0.3853	0.3312	0.1776	0.1496	0.1496	0.1776	0.3312	0.3853	0.5397	0.3781		

(7)

	1	2	3	4	5	6	7	8	9	10	11	12	13	14
12	0.6351	0.8872	0.6291	0.5326	0.2833	0.2360	0.2360	0.2833	0.5326	0.6291	0.8872	0.6351		
11	1.0630	1.4598	1.0427	0.8870	0.4761	0.3981	0.3981	0.4761	0.8870	1.0427	1.4598	1.0630		
10	1.3258	1.8221	1.3102	1.1220	0.6069	0.5099	0.5099	0.6069	1.1220	1.3102	1.8221	1.3258		
9	1.3350	1.8482	1.3677	1.1819	0.6496	0.5491	0.5491	0.6496	1.1819	1.3677	1.8482	1.3350		
8	1.2521	1.7472	1.3268	1.1561	0.6443	0.5476	0.5476	0.6443	1.1561	1.3268	1.7472	1.2521		
7	1.2031	1.6860	1.2853	1.1251	0.6294	0.5366	0.5366	0.6294	1.1251	1.2853	1.6860	1.2031		
6	1.1323	1.5905	1.2128	1.0632	0.5951	0.5079	0.5079	0.5951	1.0632	1.2128	1.5905	1.1323		
5	1.0352	1.4565	1.1090	0.9718	0.5431	0.4635	0.4635	0.5431	0.9718	1.1090	1.4565	1.0352		
4	0.9094	1.2809	0.9729	0.8511	0.4743	0.4043	0.4043	0.4743	0.8511	0.9729	1.2809	0.9094		
3	0.7543	1.0632	0.8043	0.7013	0.3891	0.3308	0.3308	0.3891	0.7013	0.8043	1.0632	0.7543		
2	0.5788	0.8159	0.6091	0.5280	0.2901	0.2457	0.2457	0.2901	0.5280	0.6091	0.8159	0.5788		
1	0.3781	0.5397	0.3853	0.3312	0.1776	0.1496	0.1496	0.1776	0.3312	0.3853	0.5397	0.3781		

(8)

	1	2	3	4	5	6	7	8	9	10	11	12	13	14
12	0.6163	0.8883	0.6685	0.5968	0.3309	0.2833	0.2833	0.3309	0.5968	0.6685	0.8883	0.6163		
11	1.0314	1.4604	1.1058	0.9908	0.5542	0.4761	0.4761	0.5542	0.9908	1.1058	1.4604	1.0314		
10	1.2856	1.8206	1.3854	1.2479	0.7032	0.6069	0.6069	0.7032	1.2479	1.3854	1.8206	1.2856		
9	1.2930	1.8430	1.4403	1.3072	0.7483	0.6496	0.6496	0.7483	1.3072	1.4403	1.8430	1.2930		
8	1.2112	1.7388	1.3919	1.2722	0.7383	0.6443	0.6443	0.7383	1.2722	1.3919	1.7388	1.2112		
7	1.1627	1.6759	1.3458	1.2349	0.7191	0.6294	0.6294	0.7191	1.2349	1.3458	1.6759	1.1627		
6	1.0937	1.5802	1.2694	1.1663	0.6793	0.5951	0.5951	0.6793	1.1663	1.2694	1.5802	1.0937		
5	0.9997	1.4469	1.1611	1.0666	0.6202	0.5431	0.5431	0.6202	1.0666	1.1611	1.4469	0.9997		
4	0.8781	1.2728	1.0194	0.9353	0.5422	0.4743	0.4743	0.5422	0.9353	1.0194	1.2728	0.8781		
3	0.7284	1.0570	0.8440	0.7724	0.4458	0.3891	0.3891	0.4458	0.7724	0.8440	1.0570	0.7284		
2	0.5590	0.8120	0.6411	0.5839	0.3337	0.2901	0.2901	0.3337	0.5839	0.6411	0.8120	0.5590		
1	0.3652	0.5380	0.4072	0.3684	0.2054	0.1776	0.1776	0.2054	0.3684	0.4072	0.5380	0.3652		

EXPOSURE 0.0 CYCLE 12 S(I,J,K) BY BANK

	1	2	3	4	5	6	7	8	9	10	11	12	13	14
(9)														
12	0.5479	0.8481	0.9801	0.9587	0.5968	0.5326	0.5326	0.5968	0.9587	0.9801	0.8481	0.5479		
11	0.9189	1.3952	1.6082	1.5759	0.9908	0.8870	0.8870	0.9908	1.5759	1.6082	1.3952	0.9189		
10	1.1452	1.7366	2.0042	1.9708	1.2479	1.1220	1.1220	1.2479	1.9708	2.0042	1.7366	1.1452		
9	1.1496	1.7519	2.0314	2.0089	1.3072	1.1819	1.1819	1.3072	2.0089	2.0314	1.7519	1.1496		
8	1.0744	1.6468	1.9199	1.9093	1.2722	1.1561	1.1561	1.2722	1.9093	1.9199	1.6468	1.0744		
7	1.0296	1.5836	1.8529	1.8487	1.2349	1.1251	1.1251	1.2349	1.8487	1.8529	1.5836	1.0296		
6	0.9675	1.4918	1.7490	1.7472	1.1663	1.0632	1.0632	1.1663	1.7472	1.7490	1.4918	0.9675		
5	0.8837	1.3655	1.6028	1.6015	1.0666	0.9718	0.9718	1.0666	1.6014	1.6028	1.3655	0.8837		
4	0.7759	1.2013	1.4111	1.4090	0.9353	0.8511	0.8511	0.9353	1.4090	1.4111	1.2013	0.7759		
3	0.6435	0.9982	1.1728	1.1693	0.7724	0.7013	0.7013	0.7724	1.1693	1.1728	0.9982	0.6435		
2	0.4936	0.7677	0.9020	0.8967	0.5839	0.5280	0.5280	0.5839	0.8967	0.9020	0.7677	0.4936		
1	0.3220	0.5090	0.5987	0.5927	0.3684	0.3312	0.3312	0.3684	0.5927	0.5987	0.5090	0.3220		
(10)														
12	0.3701	0.6514	0.8894	0.9801	0.6685	0.6291	0.6291	0.6685	0.9801	0.8894	0.6514	0.3701		
11	0.6339	1.0934	1.4614	1.6082	1.1058	1.0427	1.0427	1.1058	1.6082	1.4614	1.0934	0.6339		
10	0.7912	1.3615	1.8186	2.0042	1.3854	1.3102	1.3102	1.3854	2.0042	1.8186	1.3615	0.7912		
9	0.7920	1.3670	1.8351	2.0314	1.4403	1.3677	1.3677	1.4403	2.0314	1.8351	1.3670	0.7920		
8	0.7376	1.2787	1.7261	1.9199	1.3919	1.3268	1.3268	1.3919	1.9199	1.7261	1.2787	0.7376		
7	0.7054	1.2268	1.6609	1.8529	1.3458	1.2853	1.2853	1.3458	1.8529	1.6609	1.2268	0.7054		
6	0.6619	1.1539	1.5654	1.7490	1.2694	1.2128	1.2128	1.2694	1.7490	1.5654	1.1539	0.6619		
5	0.6039	1.0550	1.4336	1.6028	1.1611	1.1090	1.1090	1.1611	1.6028	1.4336	1.0550	0.6039		
4	0.5296	0.9273	1.2618	1.4111	1.0194	0.9729	0.9729	1.0194	1.4111	1.2618	0.9273	0.5296		
3	0.4388	0.7699	1.0490	1.1728	0.8440	0.8043	0.8043	0.8440	1.1728	1.0490	0.7699	0.4388		
2	0.3357	0.5916	0.8074	0.9020	0.6411	0.6091	0.6091	0.6411	0.9020	0.8074	0.5916	0.3357		
1	0.2148	0.3859	0.5361	0.5987	0.4072	0.3853	0.3853	0.4072	0.5987	0.5361	0.3859	0.2148		
(11)														
12	0.0	0.0	0.6514	0.8481	0.8883	0.8872	0.8872	0.8883	0.8481	0.6514	0.0	0.0		
11	0.0	0.0	1.0934	1.3952	1.4604	1.4598	1.4598	1.4604	1.3952	1.0934	0.0	0.0		
10	0.0	0.0	1.3615	1.7366	1.8206	1.8221	1.8221	1.8206	1.7366	1.3615	0.0	0.0		
9	0.0	0.0	1.3670	1.7518	1.8430	1.8482	1.8482	1.8430	1.7519	1.3670	0.0	0.0		
8	0.0	0.0	1.2787	1.6468	1.7388	1.7472	1.7472	1.7388	1.6468	1.2787	0.0	0.0		
7	0.0	0.0	1.2268	1.5836	1.6759	1.6860	1.6860	1.6759	1.5836	1.2268	0.0	0.0		
6	0.0	0.0	1.1539	1.4918	1.5802	1.5905	1.5905	1.5802	1.4918	1.1539	0.0	0.0		
5	0.0	0.0	1.0550	1.3655	1.4469	1.4565	1.4565	1.4469	1.3655	1.0550	0.0	0.0		
4	0.0	0.0	0.9273	1.2013	1.2728	1.2809	1.2809	1.2728	1.2013	0.9273	0.0	0.0		
3	0.0	0.0	0.7699	0.9982	1.0570	1.0632	1.0632	1.0570	0.9982	0.7699	0.0	0.0		
2	0.0	0.0	0.5916	0.7677	0.8120	0.8159	0.8159	0.8120	0.7677	0.5916	0.0	0.0		
1	0.0	0.0	0.3859	0.5090	0.5380	0.5397	0.5397	0.5380	0.5090	0.3859	0.0	0.0		

JAERI-M 86-063

EXPOSURE 0.0 CYCLE 12 S(I,J,K) BY BANK

	1	2	3	4	5	6	7	8	9	10	11	12	13	14
(12)														
12	0.0	0.0	0.3701	0.5479	0.6163	0.6351	0.6351	0.6163	0.5479	0.3701	0.0	0.0		
11	0.0	0.0	0.6339	0.9189	1.0314	1.0630	1.0630	1.0314	0.9189	0.6339	0.0	0.0		
10	0.0	0.0	0.7912	1.1452	1.2856	1.3258	1.3258	1.2856	1.1452	0.7912	0.0	0.0		
9	0.0	0.0	0.7920	1.1496	1.2930	1.3350	1.3350	1.2930	1.1496	0.7920	0.0	0.0		
8	0.0	0.0	0.7376	1.0744	1.2112	1.2521	1.2521	1.2112	1.0744	0.7376	0.0	0.0		
7	0.0	0.0	0.7054	1.0296	1.1627	1.2031	1.2031	1.1627	1.0296	0.7054	0.0	0.0		
6	0.0	0.0	0.6619	0.9675	1.0937	1.1323	1.1323	1.0937	0.9675	0.6619	0.0	0.0		
5	0.0	0.0	0.6039	0.8837	0.9997	1.0352	1.0352	0.9997	0.8837	0.6039	0.0	0.0		
4	0.0	0.0	0.5296	0.7759	0.8781	0.9094	0.9094	0.8781	0.7759	0.5296	0.0	0.0		
3	0.0	0.0	0.4388	0.6435	0.7284	0.7543	0.7543	0.7284	0.6435	0.4388	0.0	0.0		
2	0.0	0.0	0.3357	0.4936	0.5590	0.5788	0.5788	0.5590	0.4936	0.3357	0.0	0.0		
1	0.0	0.0	0.2148	0.3220	0.3652	0.3781	0.3781	0.3652	0.3220	0.2148	0.0	0.0		

EXPOSURE 0.0 CYCLE 12 U(I,J) BY CHANNEL

	1	2	3	4	5	6	7	8	9	10	11	12	13	14
(0)														
1	0.0	0.0	269.52	271.41	272.19	272.42	272.42	272.19	271.41	269.52	0.0	0.0		
2	0.0	0.0	272.57	274.66	275.19	275.24	275.24	275.19	274.66	272.57	0.0	0.0		
3	269.52	272.57	275.12	276.23	273.16	272.79	272.79	273.16	276.23	275.12	272.57	269.52		
4	271.41	274.66	276.23	276.17	272.49	271.84	271.84	272.49	276.17	276.23	274.66	271.41		
5	272.19	275.19	273.16	272.49	269.51	268.99	268.99	269.51	272.49	273.16	275.19	272.19		
6	272.42	275.24	272.79	271.84	268.99	268.45	268.45	268.99	271.84	272.79	275.24	272.42		
7	272.42	275.24	272.79	271.84	268.99	268.45	268.45	268.99	271.84	272.79	275.24	272.42		
8	272.19	275.19	273.16	272.49	269.51	268.99	268.99	269.51	272.49	273.16	275.19	272.19		
9	271.41	274.66	276.23	276.17	272.49	271.84	271.84	272.49	276.17	276.23	274.66	271.41		
10	269.52	272.57	275.12	276.23	273.16	272.79	272.79	273.16	276.23	275.12	272.57	269.52		
11	0.0	0.0	272.57	274.66	275.19	275.24	275.24	275.19	274.66	272.57	0.0	0.0		
12	0.0	0.0	269.52	271.41	272.19	272.42	272.42	272.19	271.41	269.52	0.0	0.0		
13	0.0	0.0	0.0	0.0	0.0	0.0	0.0	0.0	0.0	0.0	0.0	0.0		

EXPOSURE 0.0 CYCLE 12 U(I,J,K) BY BANK

	1	2	3	4	5	6	7	8	9	10	11	12	13	14
(1)														
12	0.0	0.0	274.30	278.37	280.03	280.52	280.52	280.03	278.37	274.30	0.0	0.0		
11	0.0	0.0	273.63	277.40	278.93	279.39	279.39	278.93	277.40	273.63	0.0	0.0		
10	0.0	0.0	272.68	276.02	277.39	277.80	277.80	277.39	276.02	272.68	0.0	0.0		
9	0.0	0.0	271.63	274.49	275.67	276.03	276.03	275.67	274.49	271.63	0.0	0.0		
8	0.0	0.0	270.61	273.01	274.00	274.30	274.30	274.00	273.01	270.61	0.0	0.0		
7	0.0	0.0	269.65	271.61	272.42	272.66	272.66	272.42	271.61	269.65	0.0	0.0		
6	0.0	0.0	268.73	270.27	270.91	271.10	271.10	270.91	270.27	268.73	0.0	0.0		
5	0.0	0.0	267.89	269.03	269.51	269.65	269.65	269.51	269.03	267.89	0.0	0.0		
4	0.0	0.0	267.13	267.92	268.25	268.35	268.35	268.25	267.92	267.13	0.0	0.0		
3	0.0	0.0	266.48	266.97	267.17	267.24	267.24	267.17	266.97	266.48	0.0	0.0		
2	0.0	0.0	265.96	266.21	266.31	266.34	266.34	266.31	266.21	265.96	0.0	0.0		
1	0.0	0.0	265.59	265.66	265.69	265.70	265.70	265.69	265.66	265.59	0.0	0.0		

Acknowledgements

The SCOPERS-2 has been developed to be incorporated into the fuel management calculation code system for Nuclear Ship MUTSU. Thanks are due to all members of the Japan Nuclear Ship Development Agency (now joined to JAERI) who have supported the authors during this course of study.

References

1) D.L. Delp, et al., "FLARE, A Three-Dimensional Boiling Water Reactor Simulator," GEAP-4598, General Electric, Atomic Power Equipment Department (1964)
2) T. Shimooke, "The Studies on the Reactor Nodal Theory in terms of the Migration Kernel," JAERI-M 5805, Japan Atomic Energy Research Institute (1974)
3) Z. Weiss, Nucl. Sci. & Eng., 48, 235 (1972)
4) T. Shimooke, "A Generalized FLARE-Type Nodal Equation," Trans. Am. Nucl. Soc., 21, 501 (1975)
5) S. Glasstone and M.C. Edlund, "The Elements of Nuclear Reactor Theory," p.186, D. Van Nostrand Co., Inc., New York (1960)

APPENDIX

Derivation of Migration Kernel from Node to Node ——— An Approximate Method to Integrate Analytically a Point Kernel by Six Space-Variables in Cartesian Co-oridinates. ———

I. General Expression of the Migration Kernel

A. Definition of the Kernel

In the one-energy-group nodal reactor theory a reactor core is devided into a uniform array of the rectangular parallelepipeds (hereafter called the "node") that have long edges in three directions comparable to the migration length, and the neutronic reactions in the core are described in terms of the production rate of the fission energy neutrons, Ψ_ℓ (neutrons/cm^3·sec), in a node ℓ. If we introduce the absorption rate of neutrons, A_ℓ (neutrons/cm^3·sec), for the node ℓ, then, Ψ_ℓ can be written as:

$$\Psi_\ell = k_{\infty\ell} \cdot A_\ell \tag{A1}$$

where $k_{\infty\ell}$ is the infinite multiplication factor for the medium of which the node ℓ is made.

Slowing down and diffusion of the neutrons are described together in terms of the migration kernel, $K_{\ell m}$, which is defined as the probability that a fission neutron born in the node m suffers slowing down and diffuses until it is absorbed in another node ℓ. According to this definition of the kernel, A_ℓ can be given as

$$A_\ell = \sum_{m=1}^{18} K_{\ell m} \cdot \Psi_m + K_{\ell\ell} \cdot \Psi_\ell . \tag{A2}$$

Since the spacing between nodes is large in comparison with the square root of the age of thermal neutrons, the migration kernel is supposed to be non-zero only between two adjacent nodes in any directions. Moreover, the kernels between the two nodes that are positioned in a point contact to each other as shown in Fig. A3, will be neglected because they are

small compared with those for the nodes that are positioned in a line or a surface contact. In these approximations, the summation in Eq. (A2) is extended to 18 neighboured nodes, examples of which are given in Figs. A1 and A2. The summation in Eq. (A2) is, in the original FLARE equation, made only for 6 neighbouring nodes which are in a surface contact to the source node. In this report, the summation in Eq. (A2) is enlarged to the seential amount and the kernel between the two nodes in a line contact to each other will be also estimated.

Equations (A1) and (A2) are combined to give the FLARE nodal equation (1), shown in Chapter III, for Ψ_ℓ's of the internal nodes ℓ's.

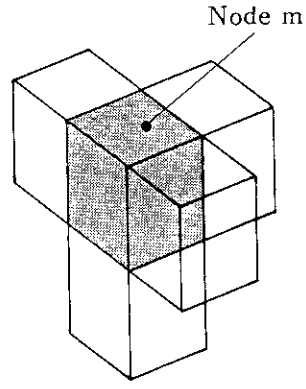

Fig. A1
Four of the nodes that are positioned in a surface contact to the node m (there are all six nodes of this kind).

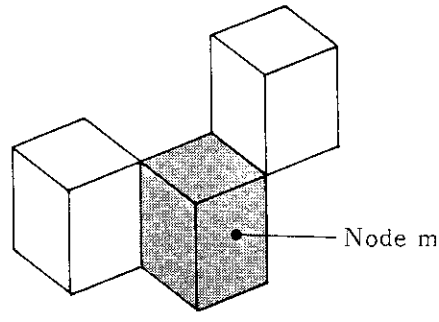

Fig. A2
Two of the nodes that are positioned in a line contact to the node m (there are all 12 nodes of this kind).

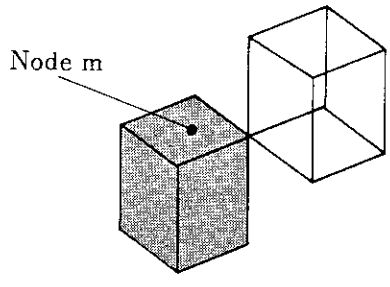

Fig. A3
One of the nodes that are positioned in a point contact to the node m (there are all 8 nodes of this kind).

B. Slowing Down and Diffusion of the Fission Neutrons emerged from a Point Source in an Infinite Medium

We will first calculate the number of neutrons that are absorbed per unit volume and per sec. at the distance r from the origin where there is a point source emitting one fission neutron per sec. The thermal neutron slowing down density at a distance r from this source is given according to the Fermi age theory as follows:

$$q\ (r,\tau) = \frac{e^{-r^2/4\tau}}{(4\pi\tau)^{3/2}} \tag{A3}$$

where τ is the age of the thermal neutrons for the medium concerned, which is considered as infinite temporarily. Consequently, in an element of volume $d\mathbf{r}'$, at the position $\mathbf{r}'$, the source of thermal neutrons is

$$S(\mathbf{r}')d\mathbf{r}' = \frac{e^{-\mathbf{r}'^2/4\tau}}{(4\pi\tau)^{3/2}}\, d\mathbf{r}' \ . \tag{A4}$$

On the other hand, it follows by the elementary diffusion theory that the point source diffusion kernel in an infinite medium is

$$G_{pt}(\mathbf{r},\mathbf{r}') = \frac{e^{-\kappa|\mathbf{r}-\mathbf{r}'|}}{4\pi D|\mathbf{r}-\mathbf{r}'|} \ , \tag{A5}$$

where κ is the reciprocal of the diffusion length and D is the diffusion coefficient. Combining the two expressions (A4) and (A5), we can get the thermal flux $\phi(\mathbf{r})$ at the point $\mathbf{r}$ as

$$\begin{aligned}\phi(\mathbf{r}) &= \int_{\text{all space}} G_{pt}(\mathbf{r},\mathbf{r}')\cdot S(\mathbf{r}')d\mathbf{r}' \\ &= \frac{1}{4\pi D}\cdot\frac{1}{(4\pi\tau)^{3/2}}\int_{\text{all space}} \frac{\exp(-\kappa|\mathbf{r}-\mathbf{r}'|-\mathbf{r}'^2/4\tau)}{|\mathbf{r}-\mathbf{r}'|}\, d\mathbf{r}'.\end{aligned} \tag{A6}$$

To obtain the integral (A6), take the direction $\mathbf{r}$ as the z-axis of the spherical coordinate system (see Fig. A4); then

$$\begin{aligned}\phi(r) = \frac{1}{(4\pi D)\cdot(4\pi\tau)^{3/2}} \iiint \frac{\exp(-\kappa\sqrt{r^2+r'^2-2rr'\cos\theta'})}{\sqrt{r^2+r'^2-2rr'\cos\theta'}} \\ \times \exp(-r'^2/4\tau)r'^2dr'\sin\theta'd\theta'd\psi' \ .\end{aligned} \tag{A7}$$

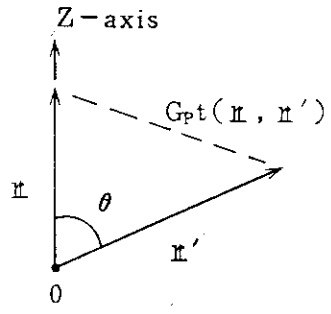

Fig. A4
Spherical coordinates system for integration of the kernel $G_{pt}(r,r')$.

Integrating Eq. (A7) by ψ' at first, then transforming the integral variable θ' to $p \equiv \sqrt{r^2+r'^2-2rr'\cos\theta'}$, we can integrate Eq. (A7) as follows:

$$\phi(r) = \frac{1}{4\pi D}\cdot\frac{2\pi}{(4\pi\tau)^{3/2}}\int\frac{e^{-r'^2/4\tau}}{rr'}\left(\int_{|r-r'|}^{|r+r'|} e^{-\kappa p}dp\right)r'^2dr'$$

$$= \frac{1}{2\pi D}\cdot\frac{1}{(4\pi\tau)^{3/2}}\cdot\frac{1}{r}\int_0^\infty r'e^{-r'^2/4\tau}\left(e^{-\kappa|r-r'|} - e^{-\kappa|r+r'|}\right)dr'. \quad (A8)$$

The integral (A8) can be carried out in a similar manner to that described in a textbook[5]. The solution is

$$\phi(r) = \frac{e^{\kappa^2\tau}}{8\pi D}\left[\frac{e^{-\kappa r}}{r}\left\{1+\mathrm{erf}\left(\frac{r}{2\sqrt{\tau}} - \kappa\sqrt{\tau}\right)\right\} - \frac{e^{\kappa r}}{r}\left\{1-\mathrm{erf}\left(\frac{r}{2\sqrt{\tau}} + \kappa\sqrt{\tau}\right)\right\}\right], \quad (A9)$$

which is the thermal flux distribution for the point source emitting one fission neutron per sec. at the origin. Notice that this expression can be applied at the distance r from the origin in any direction, since the flux distirbution should be isotropic for a point source.

Then, multiplying $\phi(r)$ by the macroscopic absorption cross section Σ_a*), we can get the number of neutorns absorbed per unit volume per sec. at the distance r from the origin with unit source;

$$K(r) = \Sigma_a\phi(r)$$

$$= \frac{\kappa^2 e^{\kappa^2\tau}}{8\pi}\left[\frac{e^{-\kappa r}}{r}\left\{1+\mathrm{erf}\left(\frac{r}{2\sqrt{\tau}} - \kappa\sqrt{\tau}\right)\right\} - \frac{e^{\kappa r}}{r}\left\{1-\mathrm{erf}\left(\frac{r}{2\sqrt{\tau}} + \kappa\sqrt{\tau}\right)\right\}\right]$$

$$= \frac{\kappa^2}{2\pi}\sqrt{\frac{\tau}{\pi}}\left\{\frac{1}{2\kappa\tau - r}\,f\left(\kappa\sqrt{\tau} - \frac{r}{2\sqrt{\tau}}\right) - \frac{1}{2\kappa\tau + r}\,f\left(\kappa\sqrt{\tau} + \frac{r}{2\sqrt{\tau}}\right)\right\}\frac{e^{-r^2/4\tau}}{r} \quad (A10)$$

*) Remember the medium is considered uniform and infinite.

where f(x) is the complementary error function multiplied by $\sqrt{\pi}/2$, i.e.,

$$f(x) \equiv \frac{\sqrt{\pi}}{2} \times e^{x^2} \operatorname{erfc}(x). \tag{A11}$$

This result can be put in a more general form so as to express the absorption probability after slowing down at a field point denoted by the vector $\mathbf{r}$, for the fast neutrons emerging isotropically from a point source at the vector $\mathbf{r}'$; thus,

$$K(|\mathbf{r}-\mathbf{r}'|) = \frac{\kappa^2}{2\pi}\sqrt{\frac{\tau}{\pi}}\left\{\frac{1}{2\kappa\tau-|\mathbf{r}-\mathbf{r}'|} f\left(\kappa\sqrt{\tau}-\frac{|\mathbf{r}-\mathbf{r}'|}{2\sqrt{\tau}}\right) - \frac{1}{2\kappa\tau+|\mathbf{r}-\mathbf{r}'|} f\left(\kappa\sqrt{\tau}+\frac{|\mathbf{r}-\mathbf{r}'|}{2\sqrt{\tau}}\right)\right\} \times \frac{e^{-\frac{(\mathbf{r}-\mathbf{r}')^2}{4\tau}}}{|\mathbf{r}-\mathbf{r}'|}$$

C. Nodal Integration Form

Now we will evaluate the migration kernel $K_{\ell m}$ in nodal theory, or the probability that the neutrons, born by fission in the node m, is absorbed in the node ℓ.

Consider the three-dimensional array of nodes in a neutron-multiplying medium, each having L_x, L_y and L_z cm long three edges. Let one neutron be born per unit sec. in a node (hereafter, denoted as m), then the source density will be 1/V within the node, where $V=L_x L_y L_z$. In the volume element $d\mathbf{x}'$ about $\mathbf{x}'$ within the node m, there are $\frac{1}{V} d\mathbf{x}'$ neutrons emitted per second. For these source neutrons, dK neutrons are absorbed per cm^3 per sec. at $\mathbf{x}$, and hence from Eq. (A12),

$$dK = K(|\mathbf{x}-\mathbf{x}'|) \frac{d\mathbf{x}'}{V} . \tag{A13}$$

Since the source is distributed uniformly within the node m, the total number of neutrons absorbed per unit volume per sec. at $\mathbf{x}$ is obtained by integrating the expression (A13) over the space within the node m; thus;

$$K(\mathbf{x})_m = \int_{\text{node m}} K(|\mathbf{x}-\mathbf{x}'|) \frac{d\mathbf{x}'}{V} . \tag{A14}$$

Futhermore, take the position $\mathbf{x}$ within the node ℓ. Then, by integrating

$K(\mathbf{x})_m$ over $\mathbf{x}$ within the node ℓ, the total number of neutrons absorbed in the node ℓ is

$$K_{\ell m} = \frac{1}{V} \int_{\text{node } \ell} \int_{\text{node } m} K(|\mathbf{x}-\mathbf{x}'|) d\mathbf{x}' d\mathbf{x} ,$$

or explicitly,

$$K_{\ell m} = \frac{1}{V} \frac{\kappa^2}{2\pi} \sqrt{\frac{\tau}{\pi}} \iint_{\ell\, m} \left[\frac{1}{2\kappa\tau - R} f\left(\kappa\sqrt{\tau} - \frac{R}{2\sqrt{\tau}}\right) - \frac{1}{2\kappa\tau + R} f\left(\kappa\sqrt{\tau} + \frac{R}{2\sqrt{\tau}}\right) \right] \frac{e^{-R^2/4\tau}}{R} \times dx'dy'dz'dxdydz \qquad \text{(A15)}$$

$$\text{with } R \equiv \sqrt{(x-x')^2 + (y-y')^2 + (z-z')^2} .$$

Equation (A15) is nothing but the integral expression for the migration kernel, between the nodes ℓ and m, which is defined in Section II-A.

In derivation of the kernel described above, it is implicitly supposed that the medium is the same for both nodes ℓ and m, and furthermore it is also the same for other nodes which are adjacent both to the nodes ℓ and m, if any (e.g., Ⓐ and Ⓑ in the case shown in the Fig. A5).

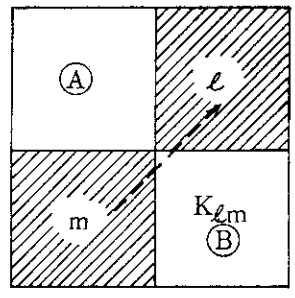

Fig. A5
Source node m, absorption node ℓ and their neighbouring nodes.

It is obvious that this is not a good assumption, because the medium generally varies node by node in a reactor-core, even though the medium is roughly approximated to be uniform within a node in the present model. In such cases, the nuclear constants in the migration kernel (A15) should be chosen as identical to one of those of different nodes, or to some sort of averaged value.

II. Six-Multiple Integration over Source and Absorption Nodes

It is necessary to make the integration of Eq. (A15) over six variables in a multiple way, in order to evaluate the from-node-to-node migration kernel. It is no wise way to try to do so in straightforward. A hint emerges from the fact that the probability represented by Eq. (A12) may essentially vanish, if the two points, i.e., the source and absorption points, are apart from each other by more than a certain length, e.g., L_c cm. The critical length L_c depends on the medium concerned, being on the order of the migration length in the case of a thermal reactor.

In the following will be described how to approximate and perform the six-multiple integration given by Eq. (A15) to obtain some analytical expression of the results, which are useful for computer-aided evaluation of nodal theory. The method described will be applied for the nodal multiple integrations of a general physical quantity that has a similar property to that the migration kernel has.

A. Details of the Procedure; Integration over y' and z'

Meanwhile, we will confine our interest to such a case in which two nodes ℓ and m are adjacent in a surface contact to each other as shown in Fig. A6. Take the rectangular coordinate systems for each node, as shown also in Fig. A6.

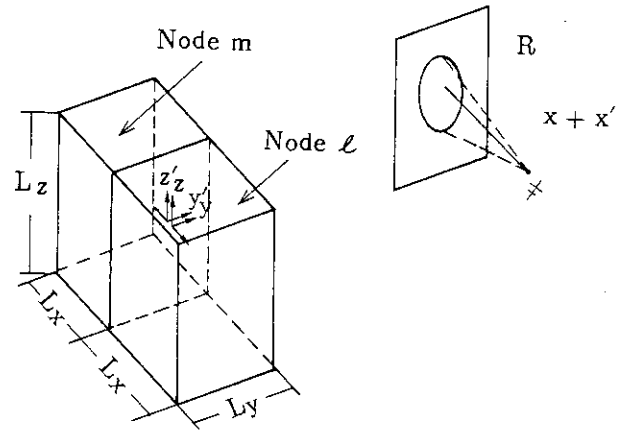

Fig. A6
Rectangular coordinate systems for two nodes ℓ and m which are adjacent in a surface contact to each other.

We first perform the integration over y' and z' with the certain x' fixed in the source-node, fixing also the counter point x(x,y,z) in the absorption-node ℓ. This is physically equivalent to evaluating the contributions to the absorption at the point x by the source on the plane (y',z'). Then, it is obvious that the largest contribution to the point x is from the source point on the plane (y',z'), whose coordinates are such that y'=y and z'=z, i.e. the point with the shortest distance from the point x. The contribution decreases gradually as the source point spreads on the plane outwards from this center of the strongest contribution, because the plane has the uniform source, each isotropic; and each source in the plane gives the contribution to the point x as a function only of the R that is the separation distance between the two points. Hence, we can replace the integration over the square-plane (y',z') by that over a certain circle of radius r_c, neglecting the contributions from outside the circle. The critical radius r_c should be given as

$$r_c^2 + (x+x')^2 = L_c^2 \quad \text{or} \quad r_c = \sqrt{L_c^2 - (x+x')^2} \quad . \tag{A16}$$

Let

$$A(x,y,z;x')$$

$$= \iint_{\text{plane}(y',z')} \left[\frac{1}{2\kappa\tau - R} f\left(\kappa\sqrt{\tau} - \frac{R}{2\sqrt{\tau}}\right) - \frac{1}{2\kappa\tau + R} f\left(\kappa\sqrt{\tau} + \frac{R}{2\sqrt{\tau}}\right)\right] \times \frac{e^{-R^2/4\tau}}{R} dy'dz', \tag{A17}$$

i.e., the integrations over y' and z' in Eq. (A15). Then, according to the above argument,

$$A(x,y,z;x')$$

$$\equiv g(y,z;x+x') \int_0^{r_c}\int_0^{2\pi} \left[\frac{1}{2\kappa\tau - \sqrt{r'^2+(x+x')^2}} f\left(\kappa\sqrt{\tau} - \frac{\sqrt{r'^2+(x+x')^2}}{2\sqrt{\tau}}\right) - \frac{1}{2\kappa\tau + \sqrt{r'^2+(x+x')^2}} f\left(\kappa\sqrt{\tau} + \frac{\sqrt{r'^2+(x+x')^2}}{2\sqrt{\tau}}\right)\right] \frac{e^{-\frac{r'^2+(x+x')^2}{4\tau}}}{\sqrt{r'^2+(x-x')^2}} \times r'dr'd\psi' \tag{A18}$$

where r' and ϕ' are the radial and azimuthal coordinates on the plate with the origin at the point (y,z). g (y,z; x+x') is a correction factor for the overestimated integral in Eq. (A18), when the circle of radius r_c exceeds the boundary of the square-plane (y',z') as illustrated in Fig. A7.

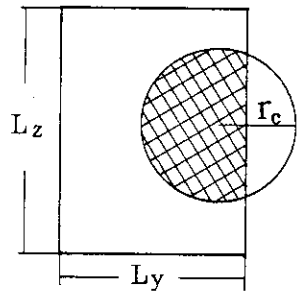

Fig. A7
The circle of radius r_c extends over the node boundary.

The exceeding occurs generally if the absorption point x near the node boundary is considered and/or if the distance (x+x') is short. For the latter case, the circle of contribution becomes large (see Eq. (A16)) and exceeds the square boundary. In these circumstances, however, the integration over the circle is carried out as if there is no boundary, and then the ratio of real integral area to the full circle will be applied to the value integrated. Thus, g (y,z; x+x') is given as

$$g\ (y,z;\ x+x') = 1$$

when the circle of radius r_c is within the square and

$$g\ (y,z;\ x+x') = \frac{\text{the real integral area (hatched in Fig. A7)}}{\pi r_c^2}$$

when a part of the circle of radius r_c is outside the square. It is obvious, from this argument, that A (x,y,z; x') will be underestimated compared with the true value when it is approximated by Eq. (A18).

The integral appeared in Eq. (A18), B(x+x'), can be easily evaluated as follows:

Putting $R \equiv \sqrt{r'^2+(x+x')^2}$ and $dR = r'dr'/\sqrt{r'^2+(x+x')^2}$; then

$$B(x+x') = 2\pi\int_{x+x'}^{L_c} \left[\frac{1}{2\kappa\tau-R}\, f\left(\kappa\sqrt{\tau}-\frac{R}{2\sqrt{\tau}}\right) - \frac{1}{2\kappa\tau+R}\, f\left(\kappa\sqrt{\tau}+\frac{R}{2\sqrt{\tau}}\right)\right] e^{-R^2/4\tau} dR$$

$$= \frac{2\pi}{\kappa}\left[\left\{\frac{1}{2\kappa\tau-(x+x')}\, f\left(\kappa\sqrt{\tau}-\frac{x+x'}{2\sqrt{\tau}}\right) + \frac{1}{2\kappa\tau+(x+x')}\, f\left(\kappa\sqrt{\tau}+\frac{x+x'}{2\sqrt{\tau}}\right)\right\} e^{-\frac{(x+x')^2}{4\tau}}\right.$$

$$-\left\{\frac{1}{2\kappa\tau-L_c} f\left(\kappa\sqrt{\tau}-\frac{L_c}{2\sqrt{\tau}}\right)+\frac{1}{2\kappa\tau+L_c} f\left(\kappa\sqrt{\tau}+\frac{L_c}{2\sqrt{\tau}}\right)\right\} e^{-\frac{L_c^2}{4\tau}}\Big] \quad . \tag{A19}$$

Interest is in the thermal reactor for which it is well assumed that

$$2\kappa\tau \gg x+x' \quad \text{and} \quad \kappa\sqrt{\tau} \gg 1.$$

Then it is put that

$$f\left(\kappa\sqrt{\tau} \pm \frac{x+x'}{2\sqrt{\tau}}\right) \simeq f\left(\kappa\sqrt{\tau}\right) \simeq \frac{1}{2} \quad .$$

Therefore, we can make the expression of $B(x+x')$ simpler for the later convenience as follows:

$$B(x+x') = 4\pi\tau\left[-\frac{1}{(2\kappa\tau)^2-(x+x')^2} e^{-\frac{(x+x')^2}{4\tau}} - \frac{1}{(2\kappa\tau)^2-L_c^2} e^{-\frac{L_c^2}{4\tau}}\right]$$

$$\simeq \frac{\pi}{\kappa^2\tau}\left[\left(1+\frac{(x+x')^2}{(2\kappa\tau)^2}\right) e^{-\frac{(x+x')^2}{4\tau}} - \left(1+\frac{L_c^2}{(2\kappa\tau)^2}\right) e^{-\frac{L_c^2}{4\tau}}\right]. \tag{A20}$$

Notice that the second step in Eq. (A20) is not necessarily required for the final purpose of performing the integration, but the approximation is made to have the simpler final results than otherwise. A simple expression of the kernel will be disirable for achieving economic computer calculations when it is applied. Hence, using the $g\ (y,z\ ;\ x+x')$ factor and Eq. (A20), it is given finally that

$$A(x,y,z\ ;\ x') = g(y,z\ ;\ x+x')\cdot B(x+x'). \tag{A21}$$

Now we will consider the integration of $A\ (x,y,z\ ;\ x')$ over y and z. As $A\ (x,y,z\ ;\ x')$ is given by Eq. (A21), it is sufficient for us to integrate the factor $g\ (y,z\ ;\ x+x')$ over y and z. This integration of g will be discussed below.

B. Evaluation of the g-Factor and Integration over y and z

1. $0 \leq r_c \leq \frac{L_y}{2}$

We will first consider the case where the critical radius r_c is shorter than the shorter edge of the rectangle, e.g., L_y cm, of the two edges, i.e. L_y and L_z cm. These circumstances occur when the two points, i.e., the source point and the absorption point, are far apart from each other; hence, the distance $x+x' \simeq L_c$.

To consider whether the circle of radius r_c is within the rectangle ABCD, divide the rectangle into four regions of small rectangles, as specified in Fig. A8. In the figure, only a quarter of the rectangle is considered because of symmetrical property of the problem.

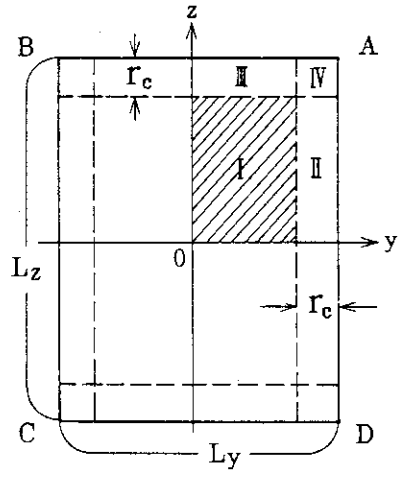

Fig. A8
Division of the node rectangle section ABCD into four regions.

When the center of the circle is on the region I, the whole circle is completely within the rectangle ABCD. Therefore,

$$g\ (y,z\ ;x+x') = g_1(y,z) = 1, \tag{A22}$$

when $o \leq y \leq \frac{L_y}{2} - r_c$ and $o \leq z \leq \frac{L_z}{2} - r_c$.

When the center of the circle is on the region II, a part of the circle is beyond the boundary AD, as shown in Fig. A9. In this case, it is easy to show that

$$g(y,z;x+x') = g_2(y,z)$$

$$= \frac{1}{\pi r_c^2}\left\{\left(\frac{L_y}{2}-y\right)\sqrt{r_c^2-\left(\frac{L_y}{2}-y\right)^2} + r_c^2\left(\pi - \cos^{-1}\frac{\frac{L_y}{2}-y}{r_c}\right)\right\}, \tag{A23}$$

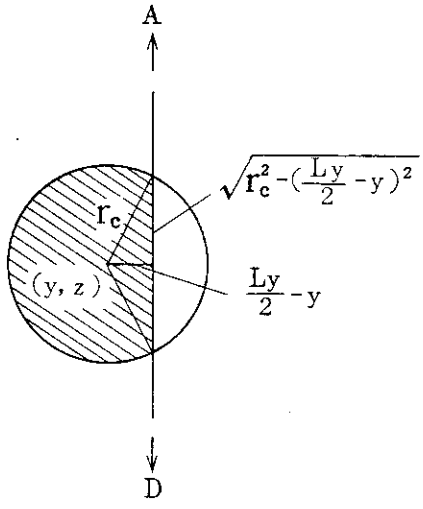

Fig. A9
The center of the circle (radius r_c) is on the region II.

if $\frac{L_y}{2} - r_c < y \leq \frac{L_y}{2}$ and $o \leq z \leq \frac{L_z}{2} - r_c$.

The situation is similar if the center of the circle is on the region III. In this case, a part of the circle is beyond the boundary AB insetead of AD, and

$$g(y,z;x+x') = g_3(y,z)$$

$$= \frac{1}{\pi r_c^2}\{(\frac{L_z}{2} - z)\sqrt{r_c^2 - (\frac{L_z}{2}-z)^2} + r_c^2(\pi - \cos^{-1}\frac{\frac{L_z}{2}-z}{r_c})\}\ , \qquad \text{(A24)}$$

if $o \leq y \leq \frac{L_y}{2} - r_c$ and $\frac{L_z}{2} - r_c < z \leq \frac{L_z}{2}$.

When the center of the circle is on the corner region IV, the circle goes beyond both edges AB and AD (see Fig. A10). In this case

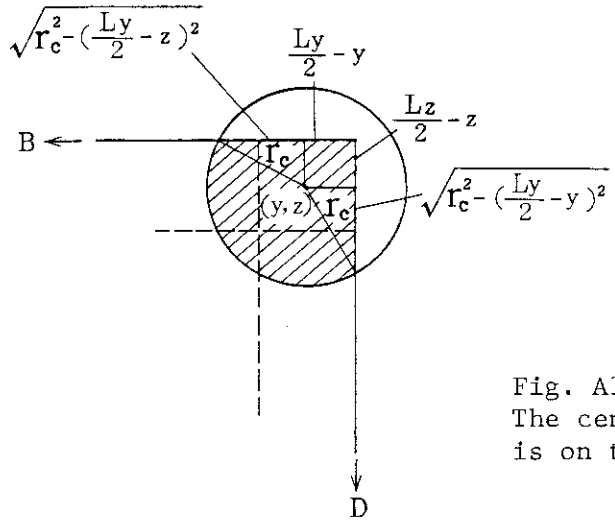

Fig. A10
The center of the circle (radius r_c) is on the corner region IV.

$$g(y,z;x+x') = g_4(y,z)$$

$$= \frac{1}{\pi r_c^2}\{(\frac{L_y}{2}-y)\cdot(\frac{L_z}{2}-z) + \frac{1}{2}(\frac{L_y}{2}-y)\cdot\sqrt{r_c^2-(\frac{L_y}{2}-y)^2} + \frac{1}{2}(\frac{L_z}{2}-z)\cdot\sqrt{r_c^2-(\frac{L_z}{2}-z)^2}$$

$$+ \frac{r_c^2}{2}(\frac{\pi}{2} + \sin^{-1}\frac{\frac{L_y}{2}-y}{r_c} + \sin^{-1}\frac{\frac{L_z}{2}-z}{r_c})\}\ , \qquad \text{(A25)}$$

if $\frac{L_y}{2} - r_c < y \le \frac{L_y}{2}$ and $\frac{L_z}{2} - r_c < z \le \frac{L_z}{2}$.

Hence, taking into consideration the symmetrical property of the g-factor, the integration of g over y and z can be performed as follows:

$$\int\int_{ABCD} g(y,z;x+x')dydz$$

$$= 4\int_0^{\frac{L_y}{2}}\int_0^{\frac{L_z}{2}} g(y,z;x+x')dydz$$

$$=4[\int_0^{\frac{L_y}{2}-r_c}\int_0^{\frac{L_z}{2}-r_c} g_1(y,z)dydz + \int_{\frac{L_y}{2}-r_c}^{\frac{L_y}{2}}\int_0^{\frac{L_z}{2}-r_c} g_2(y,z)dydz$$

$$+ \int_0^{\frac{L_y}{2}-r_c}\int_{\frac{L_z}{2}-r_c}^{\frac{L_z}{2}} g_3(y,z)dydz + \int_{\frac{L_y}{2}-r_c}^{\frac{L_y}{2}}\int_{\frac{L_z}{2}-r_c}^{\frac{L_z}{2}} g_4(y,z)dydz] \ . \qquad \text{(A26)}$$

Introducing the equation (A22), (A23), (A24) and (A25) into the integrands in Eq. (A26), we can get the following final solution for the integral:

$$\int\int_{ABCD} g(y,z;x+x')dydz = L_yL_z - \frac{4}{3\pi}(L_y+L_z)r_c + (\frac{11}{3\pi}-1)r_c, \qquad \text{(A27)}$$

where $r_c = \sqrt{L_c^2 - (x+x')^2}$.

The result given by Eq. (A27) is without approximations.

2. $\frac{L_y}{2} < r_c \le \frac{L_z}{2}$

Here, we will consider the case where the critical radius r_c is intermediate between $L_y/2$ and $L_z/2$, provided that L_z is longer than L_y. To evaluate where the circle of radius r_c exists relative to the rectangle as a function of the circle center, we divide the rectangle area into six

regions, as shown in Fig. A11. Because of the symmetrical property of the problem, only a quarter of the rectangle is considered here.

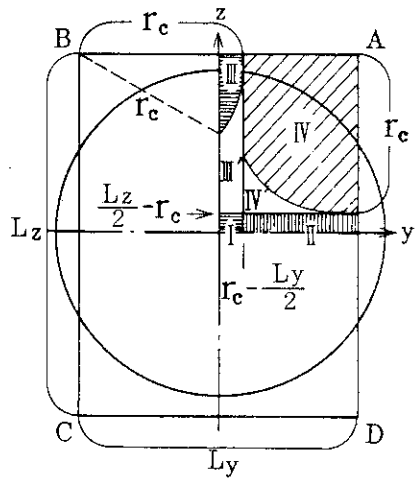

Fig. A11
Division of the node rectangle section ABCD into six regions.

The region I is specified as the rectangle having the widths of $r_c - \frac{L_y}{2}$ and $\frac{L_z}{2} - r_c$. Hence, the circle cuts the edges AD and BC at two points for each, if the circle center is on the region I (see Fig. A12). It follows, therefore, that

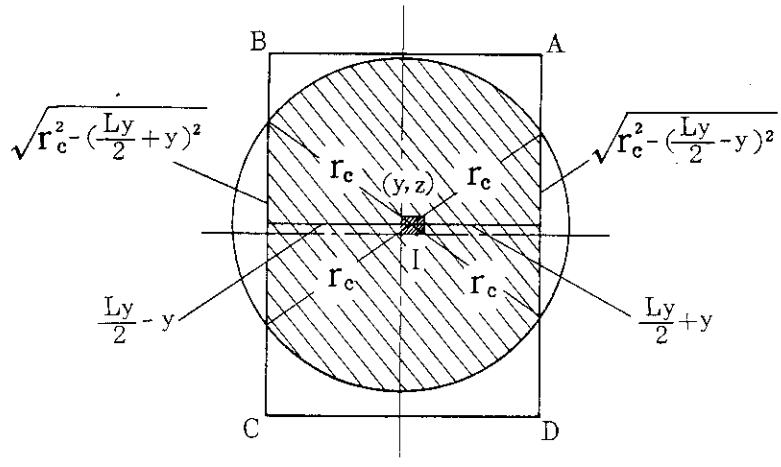

Fig. A12
The center of the circle (radius r_c) is on the region I.

$$g(y,z;x+x') = g_1(y,z)$$

$$= \frac{1}{\pi r_c^2}\left\{\left(\frac{L_y}{2}-y\right)\cdot\sqrt{r_c^2-\left(\frac{L_y}{2}-y\right)^2}+\left(\frac{L_y}{2}+y\right)\cdot\sqrt{r_c^2-\left(\frac{L_y}{2}+y\right)^2}\right.$$

$$\left.+\ r_c^2\left(\pi-\cos^{-1}\frac{\frac{L_y}{2}-y}{r_c}-\cos^{-1}\frac{\frac{L_y}{2}+y}{r_c}\right)\right\}, \qquad \text{(A28)}$$

if $o \le y \le r_c - \frac{L_y}{2}$ and $o \le z \le \frac{L_z}{2} - r_c$.

If the center of the circle is on the region II, the circle cuts only the edge AD at two points (see Fig. A13). In this case, it follows that

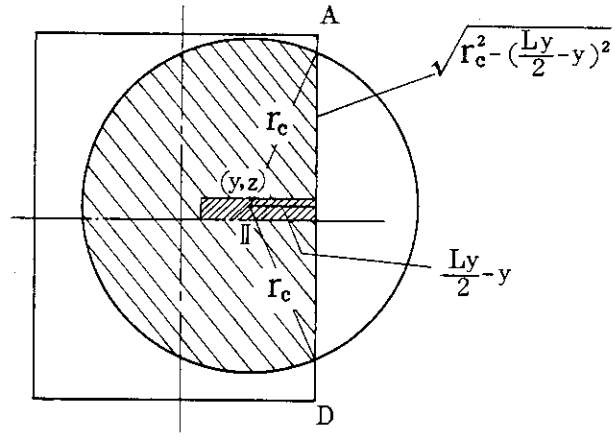

Fig. A13
The center of the circle (radius r_c) is on the region II.

$$g(y,z;x+x') = g_2(y,z)$$

$$= \frac{1}{\pi r_c^2}\left\{\left(\frac{L_y}{2}-y\right)\cdot\sqrt{r_c^2-\left(\frac{L_y}{2}-y\right)^2}+r_c^2\left(\pi-\cos^{-1}\frac{\frac{L_z}{2}-y}{r_c}\right)\right\}, \qquad \text{(A29)}$$

where $r_c - \frac{L_y}{2} < y \le \frac{L_y}{2}$ and $o \le z \le \frac{L_z}{2} - r_c$.

The region III is an area enclosed by three boundaries, i.e., z-axis, edge AB and a part of the circle whose center is on the corner B and whose radius is r_c. When the circle center is on this region, the circle never cuts the edge AB; instead, it cuts the edges BC and AD, at a point for each. The situation is shown in Fig. A14. Then, it follows that

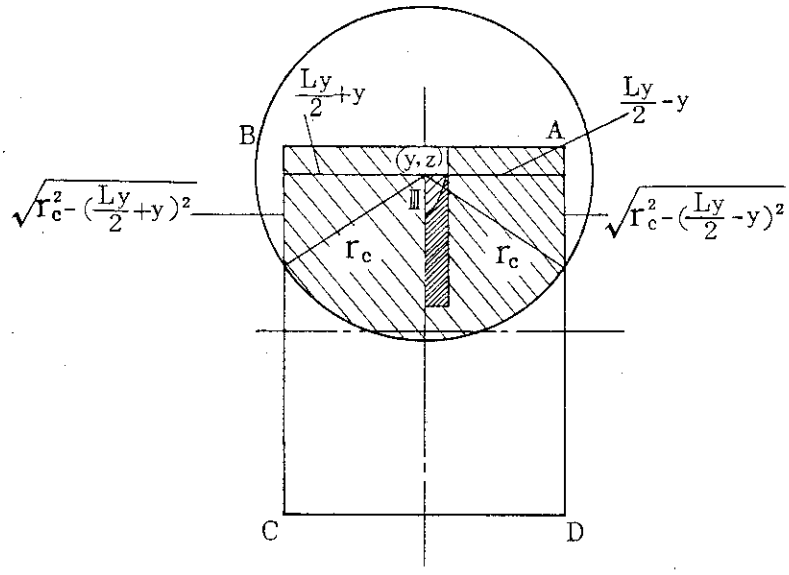

Fig. A14
The center of the circle (radius r_c) is on the region Ⅲ.

$$g(y,z;x+x') = g_3(y,z)$$

$$= \frac{1}{\pi r_c^2}\{L_y(\frac{L_z}{2}-z) + \frac{1}{2}(\frac{L_y}{2}-y)\cdot\sqrt{r_c^2-(\frac{L_y}{2}-y)^2} + \frac{1}{2}(\frac{L_y}{2}+y)\cdot\sqrt{r_c^2-(\frac{L_y}{2}+y)^2}$$

$$+ \frac{r_c^2}{2}(\pi - \cos^{-1}\frac{\frac{L_y}{2}-y}{r_c} - \cos^{-1}\frac{\frac{L_y}{2}+y}{r_c})\}. \qquad (A30)$$

Strictly speaking, this is valid if the coordinate (y,z) is within the region Ⅲ. However, we will make an approximation and suppose that the expression (A30) is valid also when the coordinate (y,z) is within the region Ⅲ'. Under this approximation, Eq. (A30) is valid when

$$o \le y \le r_c - \frac{L_y}{2} \quad \text{and} \quad \frac{L_z}{2} - r_c < z \le \frac{L_z}{2}.$$

The region IV is an area enclosed by four boundaries, i.e., edge AB, edge AD, the vertical line specified by the equation $y = r_c - \frac{L_y}{2}$, and a part of the circle whose center is on the corner A and whose radius is r_c. When the circle center is on this region, the circle cuts the edges AB and AD at only a point for each (see Fig. A15). Then it follows that

$$g(y,z;x+x') = g_4(y,z)$$

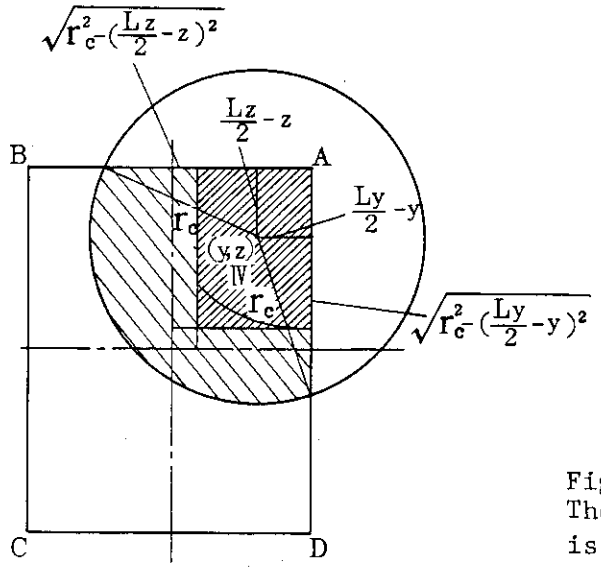

Fig. A15
The center of the circle (radius r_c) is on the region IV.

$$= \frac{1}{\pi r_c^2}\left\{\left(\frac{L_y}{2}-y\right)\cdot\left(\frac{L_z}{2}-z\right)+\frac{1}{2}\left(\frac{L_y}{2}-y\right)\sqrt{r_c^2-\left(\frac{L_y}{2}-y\right)^2}+\frac{1}{2}\left(\frac{L_z}{2}-z\right)\sqrt{r_c^2-\left(\frac{L_z}{2}-z\right)^2}\right.$$

$$\left.+\frac{r_c^2}{2}\left(\frac{\pi}{2}+\sin^{-1}\frac{\frac{L_y}{2}-y}{r_c}+\sin^{-1}\frac{\frac{L_z}{2}-z}{r_c}\right)\right\}, \qquad \text{(A31)}$$

if the coordinate (y,z) is within the region IV. We make an approximation in the same way as above; that is, Eq. (A31) is applied also in the small region IV'. Hence, Eq. (A31) is valid when

$$r_c-\frac{L_y}{2} < y \le \frac{L_y}{2} \quad \text{and} \quad \frac{L_z}{2}-r_c < z \le \frac{L_z}{2}.$$

This assumption is good because the additional region IV' is small in area and it is located adjacent to the region IV.

Now we can integrate g (y,z ; x+x') over y and z in the rectangle ABCD as follows:

$$\int_{ABCD}\int g(y,z;x+x')dydz = 4\int_0^{\frac{L_y}{2}}\int_0^{\frac{L_z}{2}} g(y,z;x+x')dydz$$

$$= 4\left[\int_0^{r_c-\frac{L_y}{2}}\int_0^{\frac{L_z}{2}-r_c} g_1(y,z)dydz+\int_{r_c-\frac{L_y}{2}}^{\frac{L_y}{2}}\int_0^{\frac{L_z}{2}-r_c} g_2(y,z)dydz\right.$$

$$+\int_0^{r_c-\frac{L_y}{2}}\int_{\frac{L_z}{2}-r_c}^{\frac{L_z}{2}} g_3(y,z)\,dydz+\int_{r_c-\frac{L_y}{2}}^{\frac{L_y}{2}}\int_{\frac{L_z}{2}-r_c}^{\frac{L_z}{2}} g_4(y,z)\,dydz\Big]. \qquad (A32)$$

Introducing Eq. (A28), (A29), (A30) and (A31) into the integrands in Eq. (A32), the following solution is finally obtained:

$$\int_{ABCD}\int g(y,z;x+x')\,dydz = L_yL_z-\frac{4}{3\pi}(L_y+L_z)r_c+(\frac{11}{3\pi}-1)r_c^2\ , \qquad (A33)$$

where $r_c=\sqrt{L_c^2-(x+x')^2}$.

It should be noticed that this result for $\frac{L_y}{2} < r_c \le \frac{L_z}{2}$ has the same form as the result (A27) for $0 \le r_c \le \frac{L_y}{2}$.

3. $\frac{L_z}{2} < r_c \le \frac{1}{2}\sqrt{L_y^2+L_z^2}$

Next we consider the case in which $\frac{L_z}{2} < r_c \le \frac{1}{2}\sqrt{L_y^2+L_z^2}$, i.e., the critical radius r_c is longer than half the length L_z and shorter than half the diagonal length of the rectangle ABCD. In this case, in order to evaluate the relative positions of the circle to the rectangle ABCD, the latter can be divided into the four regions and the three additional ones as specified in Fig. A16 (typically, a quarter part of the rectangle is considered here).

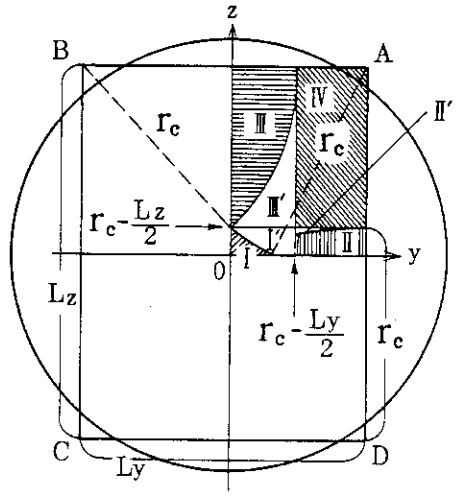

Fig. A16
Division of the node rectangle section into seven regions.

If the circle center is on the region I which is enclosed by the four boundaries, i.e., y-axis, z-axis, the line specified by the equation $z = r_c - \frac{L_z}{2}$, and a part of the circle whose center is on A and whose radius is r_c, the circle then surely cuts the four edges at two points for each. We will ignore, however, the part of the circle beyond the edges AB and CD, because the exceeding area is small compared with the other exceeding over the lines AD and BC*). And make one more approximation that the region I' is considered as a part of the region I.

Under the similar approximation also for the regions II and III, we can integrate the g-factor over y and z in the rectangle area; and it follows finally that

$$\int_{ABCD}\int g(y,z;x+x')dydz = L_yL_z - \frac{4}{3\pi}(L_y+L_z)r_c + (\frac{11}{3\pi}-1)r_c^2 , \qquad (A34)$$

for

$$\frac{L_z}{2} < r_c \leq \frac{1}{2}\sqrt{L_y^2 + L_z^2}.$$

Again, this result has the same expression of r_c as the previous cases. It should be noticed that the integrations for a certain region differs from each other in different cases but the cancellation occurs in their sum, resulting in the same function of r_c for any case.

4. $\frac{1}{2}\sqrt{L_y^2 + L_z^2} < r_c \leq L_y$

This case occurs when the x-coordinates of the two opposite points, i.e., of the source point and of the absorption one, are near to each other; and the source region, from which non-negligible contributions come to the absorption point x, extends itself over almost entire area of the rectangle-section of the node.

In this case, taking the same approximation as the case 3, it follows that

$$\int_{ABCD}\int g(y,z;x+x')dydz = L_yL_z - \frac{4}{3\pi}(L_y+L_z)r_c + (\frac{11}{3\pi}-1)r_c^2 , \qquad (A35)$$

which is the same function of r_c as the previous cases.

In conclusion up to this point, we can state that

---

*) This means the small exceeding areas are included in the g-factor.

$$\int\int_{ABCD} g(y,z;x+x')dydz = L_yL_z - \frac{4}{3\pi}(L_y+L_z)r_c + (\frac{11}{3\pi}-1)r_c^2 \qquad (A36)$$

for all $r_c \leq L_y$, where $r_c = \sqrt{L_c^2 - (x+x')^2}$.

Notice that Eq. (A36) is symmetrical in L_y and L_z. So, the condition supposed before the evaluation in this section, that L_z is longer than L_y, is no longer restrictive hereafter for application of the results given by Eq. (A36).

We made approximations in this section, especially for large value of r_c, to carry out the integration of g-factor. Generally, these approximations produce overestimated g-factors, and hence the overestimated solution for the integration given by Eq. (A36).

5. $L_y < r_c \leq L_c$

In the limit that r_c is much larger than L_y, it can be written by definition that

$$g(y,z;x+x') = L_yL_z/\pi r_c^2 \text{ for any value of } (y,z).$$

Then,

$$\int\int_{ABCD} g(y,z;x+x')dydz = \frac{L_yL_z}{\pi r_c^2} L_yL_z. \qquad (A37)$$

Setting $r_c = L_y$, Eq. (A37) becomes $\frac{L_yL_z}{\pi L_y^2} L_yL_z = \frac{L_z^2}{\pi} \simeq \frac{L_yL_z}{\pi}$, taking into consideration that $L_y \simeq L_z$. On the other hand, Eq. (A36) given for $r_c \leq L_y$ becomes, at $r_c = L_y$,

$$\simeq L_yL_z - \frac{8}{3\pi} L_zL_y + (\frac{11}{3\pi} - 1) L_y^2$$

$$\simeq L_yL_z(1 - \frac{8}{3\pi} + \frac{11}{3\pi} - 1) = \frac{1}{\pi} L_yL_z.$$

This fact shows that Eq. (A36) and Eq. (A37) coincide with each other at $r_c = L_y$. So we can combine both the equations in order to cover the whole range of $r_c (0 \leq r_c \leq L_c = 2L_y)$. Meantime, L_c is put arbitrarily equal to $2\ L_y$.

Now we will assume that Eq. (A36) tends to $L_yL_z/4\pi$ that is the limit value of Eq. (A37) at $r_c = L_c(=2L_y)$, modifying the quadratic term of r_c in Eq. (A36) (the smallest term in Eq. (A36) for the range $o \leq r_c < L_y$). Then,

$$L_yL_z - \frac{4}{3\pi}(L_y+L_z)r_c + \delta(\frac{11}{3\pi}-1)r_c^2 \to \frac{L_yL_z}{4\pi} \text{ , when } r_c \to L_c(=2L_y).$$

This equating leads to

$$\delta(\frac{11}{3\pi} - 1) = \frac{1}{4}(\frac{67}{12\pi} - 1).$$

Hence, the integration of g-factor finally becomes

$$\int\int_{ABCD} g(y,z;x+x')dydz = L_yL_z - \frac{4}{3\pi}(L_y+L_z)r_c + \frac{1}{4}(\frac{67}{12\pi}-1)r_c^2 \qquad (A38)$$

for all values of $r_c = \sqrt{L_c^2 - (x+x')^2} \leq L_c$.

C. Integration over x and x' and the Final Results

The migration kernel $K_{\ell m}$, whose solution we are looking for, is now written as

$$K_{\ell m} = \frac{1}{V}\frac{\kappa^2}{2\pi}\sqrt{\frac{\tau}{\pi}}\iiiint A(x,y,z;x')dxdydzdx'$$

$$= \frac{1}{V}\frac{\kappa^2}{2\pi}\sqrt{\frac{\tau}{\pi}}\iint\{\iint g(y,z;x+x')dydz\}\cdot B(x+x')dxdx' , \qquad (A39)$$

where A (x,y,z;x') is defined by Eq. (A17) and is approximated by Eq. (A18) or (A21).

Using the solution for B (x+x') given by Eq. (A20), and the solution for the integral $\iint g(y,z;x+x')dydz$ given by Eq. (A38), $K_{\ell m}$ can be modified to

$$K_{\ell m} = \frac{1}{V}\frac{1}{2\tau}\sqrt{\frac{\tau}{\pi}}\int_0^{L_x}\int_0^{L_x}\{a + b\sqrt{L_c^2 - (x+x')^2} + c(L_c^2 - (x+x')^2)\}$$

$$\times [\{1+\frac{(x+x')^2}{(2\kappa\tau)^2}\}e^{-\frac{(x+x')^2}{4\tau}} - \{1+\frac{L_c^2}{(2\kappa\tau)^2}\}e^{-\frac{L_c^2}{4\tau}}]dxdx', \qquad (A40)$$

where $a \equiv L_yL_z$, $b \equiv -\frac{4}{3\pi}(L_y+L_z)$ and $c \equiv \frac{1}{4}(\frac{67}{12\pi}-1)$.

In order to integrate this function analytically, we must approximate the factor $\sqrt{L_c^2 - (x+x')^2}$ in the integrand by a polynomial of $(x+x')$. The quadratic function of $(x+x')$ was taken to approximate the part of the circle-function; then,

$$\sqrt{L_c^2 - (x+x')^2} = L_c\left(1 - \frac{\alpha}{2L_c^2}(x+x')^2\right) ,$$

where $\alpha = \frac{8}{7}(9\sqrt{3} - 4\pi - 2) = 1.1681$. The α was determined by equating the integrated values of both sides of the equation, that is,

$$\int_0^{L_x}\int_0^{L_x} \sqrt{L_c^2 - (x+x')^2}\, dxdx' = L_c \int_0^{L_x}\int_0^{L_x} \left(1 - \frac{\alpha}{2L_c^2}(x+x')^2\right)dxdx'$$

with L_c consistently put to $2L_y(=2L_x)$.

Notice that the 2nd factor in the integrand in Eq. (A40), i.e., the exponential function part has the largest value at $x+x' = 0$, decreasing gradually as $x+x' \to L_c$ and vanishing to zero at $x+x' = L_c$. Therefore, main contribution from the integrand to the integral is expected for the range $x+x' \ll L_c$. If we took this drastic approximation, the α were unity. Hence, the approximation taken above may be better than the drastic one.

Let

$$A_1 = \frac{1}{2\tau}\int_0^{L_x}\int_0^{L_x} \left[\left(1 + \frac{(x+x')^2}{(2\kappa\tau)^2}\right)e^{-\frac{(x+x')^2}{4\tau}} - \left(1 + \frac{L_c^2}{(2\kappa\tau)^2}\right)e^{-\frac{L_c^2}{4\tau}}\right]dxdx'. \tag{A41}$$

This can be easily evaluated by partial integration, using the formula;

$$\int e^{ax}\mathrm{erf}(bx)dx = \frac{1}{a}\left\{e^{ax}\mathrm{erf}(bx) - e^{\frac{a^2}{4b^2}}\mathrm{erf}\left(bx - \frac{a}{2b}\right)\right\} \tag{A42}$$

and

$$\int \mathrm{erf}(x)dx = x\,\mathrm{erf}(x) + \frac{1}{\sqrt{\pi}}e^{-x^2}. \tag{A43}$$

The solution becomes

$$A_1 = A_1(L_x)$$

$$\equiv \left(1+\frac{1}{\kappa^2\tau}\right) + \left\{4\left(1+\frac{1}{2\kappa^2\tau}\right) f\left(\frac{L_x}{2\sqrt{\tau}}\right) - 2\left(1+\frac{1}{\kappa^2\tau}\right)\right\} e^{-\frac{L_x^2}{4\tau}}$$

$$- \left\{2\left(1+\frac{1}{2\kappa^2\tau}\right) f\left(\frac{L_x}{\sqrt{\tau}}\right) - \left(1+\frac{1}{\kappa^2\tau}\right) + \frac{L_x^2}{2\tau}\left(1+\frac{1}{\kappa^2\tau}\frac{L_x^2}{\tau}\right)\right\} e^{-\frac{L_x^2}{\tau}}, \qquad (A44)$$

where f(x) is the complementary error function multiplied by $\sqrt{\pi}/2$, given by Eq. (A11). In Eq. (A44), L_c is put equal to $2L_x$ for simplicity.

$$\text{Let } A_2 = \frac{1}{8\tau^2}\int_0^{L_x}\int_0^{L_x}(x+x')^2\left[\left(1+\frac{(x+x')^2}{(2\kappa\tau)^2}\right)e^{-\frac{(x+x')^2}{4\tau}} - \left(1+\frac{L_c^2}{(2\kappa\tau)^2}\right)e^{-\frac{L_c^2}{4\tau}}\right]dxdx'. \qquad (A45)$$

Then, in the same manner as above, we can get

$$A_2 = A_2(L_x)$$

$$\equiv \left(1+\frac{2}{\kappa^2\tau}\right)+\left\{2\left(1+\frac{3}{2\kappa^2\tau}\right) f\left(\frac{L_x}{2\sqrt{\tau}}\right) - 2\left(1+\frac{2}{\kappa^2\tau}\right) - \frac{1}{\kappa^2\tau}\frac{L_x^2}{4\tau}\right\} e^{-\frac{L_x^2}{4\tau}}$$

$$- \left\{\left(1+\frac{3}{2\kappa^2\tau}\right) f\left(\frac{L_x}{\sqrt{\tau}}\right) - \left(1+\frac{2}{\kappa^2\tau}\right) - \frac{1}{2\kappa^2\tau}\frac{L_x^2}{t}\right.$$

$$\left. + \frac{7}{48}\left(1+\frac{1}{\kappa^2\tau}\frac{L_x^2}{\tau}\right)\frac{L_x^4}{\tau^2}\right\} e^{-\frac{L_x^2}{\tau}}. \qquad (A46)$$

Using Eqs. (A44) and (A46) for the solutions of the integrals, and also introducing explicitly the values for a, b and c, with $L_c = 2L_x$, the migration kernel $K_{\ell m}$ becomes

$$K_{\ell m} = \frac{1}{V}\sqrt{\frac{\tau}{\pi}}\left[\left\{L_yL_z - \frac{8}{3\pi}L_x(L_y+L_z) + \left(\frac{67}{12\pi}-1\right)L_x^2\right\}\cdot A_1(L_x)\right.$$

$$\left. + \left\{\frac{4\alpha}{3\pi}\frac{L_y+L_z}{L_x} - \left(\frac{67}{12\pi}-1\right)\right\}\tau\cdot A_2(L_x)\right]. \qquad (A47)$$

III. Derivation of the Kernels for Different Directions

In this section, the kernels will be derived for directions other than x-direction.

A. Kernel for z-Direction

It is sufficient for us to replace L_y by L_x, L_z by L_y and L_x by L_z in the result obtained above, in order to have the kernel for the node which is in a surface contact to the source node in z-direction. The result is

$$K_{\ell m} = \frac{1}{V}\sqrt{\frac{\tau}{\pi}}\left[\{L_xL_y - \frac{8}{3\pi}L_z(L_x+L_y) + (\frac{67}{12\pi}-1)L_z^2\}\cdot A_1(L_z)\right.$$
$$\left. + \{\frac{4\alpha}{3\pi}\frac{L_x+L_y}{L_z} - (\frac{67}{12\pi}-1)\}\tau\cdot A_2(L_z)\right], \qquad (A48)$$

where $A_1(L_z)$ and $A_2(L_z)$ are given by Eq. (A44) and (A46) substituting L_z for L_x.

Remember that the node length L_x is equal to L_y in our simple assumption, so that the kernel for the y-direction is the same as that for the x-direction which is already derived.

B. Kernel for the Diagonal Direction in x-y Plane

In this subsection we will consider the migration kernel between the nodes which are positioned as in Fig. A17. Let $K_{(\alpha,\beta)\to(\gamma,\delta)}$ be the kernel from the region of the two nodes α and β to that of the two nodes γ and δ. These nodes are relatively positioned as shown in Fig. A18. Then, by definition, it follows that

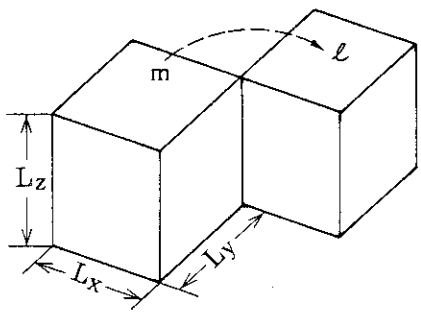

Fig. A17
Two nodes adjacent in a contact to each other in the diagonal direction on X-Y plane.

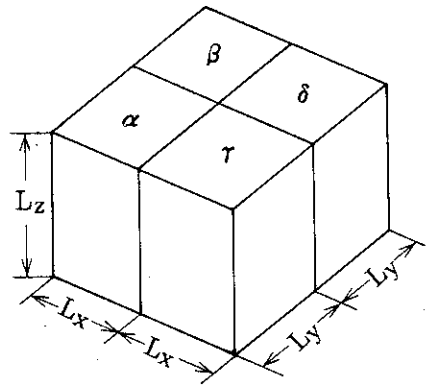

Fig. 18
Four nodes adjacent in
a contact to each other.

$$K_{(\alpha,\beta)\to(\gamma,\delta)} = \frac{1}{2}\,(K_{\alpha\to\gamma}+K_{\alpha\to\delta}) + \frac{1}{2}\,(K_{\beta\to\gamma}+K_{\beta\to\delta}) = K_{\alpha\to\gamma}+K_{\alpha\to\delta}. \qquad (A49)$$

It is assumed in this equation that the nodes α and β are the same in material, and also the nodes γ and δ. Hence, the kernel to be derived are given by the following equation:

$$K_{\alpha\to\delta} = K_{(\alpha,\beta)\to(\gamma,\delta)} - K_{\alpha\to\gamma}. \qquad (A50)$$

Since $K_{\alpha\to\gamma}$ in Eq. (A50) has been already solved, it is sufficient to have $K_{(\alpha,\beta)\to(\gamma,\delta)}$ here in order to get the kernel $K_{\alpha\to\delta}$.

Replacing L_z by $2L_y$, and L_y by L_z (with L_x and L_c unchanged), we can argue in the same way as described previously to derive the kernel $K_{\ell m}$. Then we can have

$$\int g\,dydz = 2L_yL_z - \frac{4}{3\pi}\,(2L_y+L_z)r_c + \frac{1}{4}\,(\frac{67}{12\pi}-1)r_c^2\ ,$$

and

$$K_{(\alpha,\beta)\to(\gamma,\delta)}$$

$$= \frac{1}{2V}\,\frac{1}{2\tau}\sqrt{\frac{\tau}{\pi}}\int_0^{L_x}\int_0^{L_x}\,[2L_yL_z - \frac{4}{3\pi}(2L_y+L_z)r_c + \frac{1}{4}\,(\frac{67}{12\pi}-1)r_c^2]$$

$$\times\,[\{1+\frac{(x+x')^2}{(2\kappa\tau)^2}\}e^{-\frac{(x+x')^2}{4\tau}} - \{1+\frac{L_c^2}{(2\kappa\tau)^2}\}\,e^{-\frac{L_c^2}{4\tau}}]dxdx'. \qquad (A51)$$

Substracting $K_{\alpha\to\gamma}$ given by combined Eqs. (A38) and (A39) from Eq. (A51), we can get $K_{\alpha\to\delta}$ as follows:

$$K_{\alpha\to\delta}$$

$$= \frac{1}{V}\frac{1}{2\tau}\sqrt{\frac{\tau}{\pi}}\int_0^{L_x}\int_0^{L_x}\left[\frac{2}{3\pi}L_z r_c - \frac{1}{8}\left(\frac{67}{12\pi}-1\right)r_c^2\right]\cdot\left[\left\{1+\frac{(x+x')^2}{(2\kappa\tau)^2}\right\}e^{-\frac{(x+x')^2}{4\tau}}\right.$$

$$\left. - \left\{1+\frac{L_c^2}{(2\kappa\tau)^2}\right\}e^{-\frac{L_c^2}{4\tau}}\right]dxdx'.$$

Thus finally, it follows that

$$K_{\alpha\to\delta} = \frac{1}{2}\frac{1}{V}\sqrt{\frac{\tau}{\pi}}\left[\left\{\frac{8}{3\pi}L_xL_z - \left(\frac{67}{12\pi}-1\right)L_x^2\right\}\cdot A_1(L_x) + \left\{-\frac{4\alpha}{3\pi}\frac{L_z}{L_x} + \left(\frac{67}{12\pi}-1\right)\right\}\tau\right.$$

$$\left. \times A_2(L_x)\right]. \qquad \text{(A52)}$$

This is the migration kernel in the diagonal direction on x-y plane.

The kernel for the diagonal direction in x-z plane can be derived in the same way as above. The four kinds of kernels so far derived are independent of each other in the simple assumption that $L_x = L_y$, and the kernels of other directions coincide with one of these four. All of these kernels derived are summarized in TAble 3.1. In Table 3.1, the factor q multiplied to the kernels is a correction factor for the escaped neutrons beyond the absorption nodes (see below for details).

C. Correction for Escaped Neutrons beyond the Absorption Nodes

It should be noticed that some neutrons reach the outside region, i.e., the region which surrounds the absorption nodes on the outside, even when the dimensions of the node are large. The probability that neutrons reach one of these third nodes is small, much less than 1% for a typical case. But the sum of these probabilities becomes large because the third nodes are many in number, and the sum cannot be neglected.

In the framework of the coarse-mesh approximation in which the kernels are considered only for the adjacent nodes, the probability that neutrons go beyond the absorption nodes should be in some way included in these kernels for adjacent nodes. In order to estimate these effects, we will consider three regions devided spherically (see Fig. A19); i.e., the

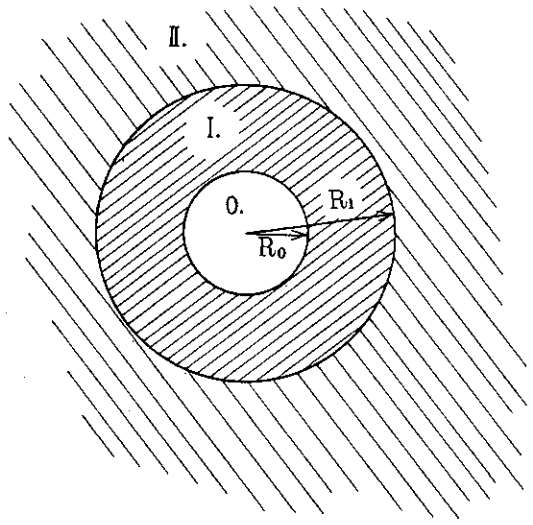

Fig. A19
Three regions divided spherically.

center sphere (radius R_0) that represents the source node; the middle shell (outer radius R_1), the total of adjacent nodes; and the outward region, the total of surrounding nodes. Then, the probability that neutrons are absorbed in all the adjacent nodes are approximately given as

$$P_1 = 4\pi\int_{R_0}^{R_1} K(r)r^2dr$$

$$= \left[\mathrm{erf}\left(\frac{r}{2\sqrt{\tau}}\right) - 2\sqrt{\frac{\tau}{\pi}}\left\{\frac{\kappa r+1}{2\kappa\tau-r} f\left(\kappa\sqrt{\tau}-\frac{r}{2\sqrt{\tau}}\right) + \frac{\kappa r-1}{2\kappa\tau+r} f\left(\kappa\sqrt{\tau}+\frac{r}{2\sqrt{\tau}}\right)\right\}e^{-\frac{r^2}{4\tau}}\right]_{R_0}^{R_1} \tag{A53}$$

using Eq. (12) for K(r). In this equation, R_0 and R_1 may be taken as

$$R_0 = \left(\frac{3}{4\pi}\right)^{1/3}\sqrt{(L_x^2+L_y^2+L_z^2)/3}\ *) \quad \text{and} \quad R_1 = R_0 + L_x. \tag{A54}$$

Since $f\left(\kappa\sqrt{\tau} \pm \frac{r}{2\sqrt{\tau}}\right) \simeq f(\kappa\sqrt{\tau}) \simeq \frac{1}{2}$, P_I can be made simpler i.e.,

$$P_I = \left[\mathrm{erf}\left(\frac{r}{2\sqrt{\tau}}\right) - 2\sqrt{\frac{\tau}{\pi}}\frac{r(2\kappa^2\tau+1)}{(2\kappa\tau)^2-r^2}e^{-\frac{r^2}{4\tau}}\right]_{R_0}^{R_1}$$

$$= 2\sqrt{\frac{\tau}{\pi}}\left\{\frac{2}{R_0} f\left(\frac{R_0}{2\sqrt{\tau}}\right) + \frac{R_0(2\kappa^2\tau+1)}{(2\kappa\tau)^2-R_0^2}\right\}e^{-\frac{R_0^2}{4\tau}}$$

$$- 2\sqrt{\frac{\tau}{\pi}}\left\{\frac{2}{R_1} f\left(\frac{R_1}{2\sqrt{\tau}}\right) + \frac{R_1(2\kappa^2\tau+1)}{(2\kappa\tau)^2-R_1^2}\right\}e^{-\frac{R_1^2}{4\tau}}. \tag{A55}$$

*) The volume of the sphere of the radius R_0 is taken equal to the node, when $L_x = L_y = L_z$.

In the same way, the probability that neutrons are absorbed in the region consisting of the third nodes is

$$P_{II} = 2\sqrt{\frac{\tau}{\pi}}\left\{\frac{2}{R_1} f\left(\frac{R_1}{2\sqrt{\tau}}\right) + \frac{R_1(2\kappa^2\tau+1)}{(2\kappa\tau)^2 - R_1^2}\right\} e^{-\frac{R_1^2}{4\tau}} . \tag{A56}$$

Thus, the probability that neutrons are absorbed at the region behind the adjacent node ℓ is on the order of $K_{\ell m} \times \frac{P_{II}}{P_I}$. When this probability is added to the kernel $K_{\ell m}$, we can finally obtain the kernel $K'_{\ell m}$ in the coarse-mesh approximation; i.e.,

$$K'_{\ell m} = K_{\ell m} + K_{\ell m}\frac{P_{II}}{P_I} = K_{\ell m}\frac{P_I + P_{II}}{P_I} .$$

The correction factir $(P_I + P_{II})/P_I$, denoted as q hereafter, can be written as follows using Eqs. (A55) and (A56),

$$q \equiv \frac{P_I + P_{II}}{P_I} = \frac{\left\{\frac{2}{R_0} f\left(\frac{R_0}{2\sqrt{\tau}}\right) + \frac{R_0(2\kappa^2\tau+1)}{(2\kappa\tau)^2 - R_0^2}\right\} e^{-\frac{R_0^2}{4\tau}}}{\left\{\frac{2}{R_0} f\left(\frac{R_0}{2\sqrt{\tau}}\right) + \frac{R_0(2\kappa^2\tau+1)}{(2\kappa\tau)^2 - R_0^2}\right\} e^{-\frac{R_0^2}{4\tau}} - \left\{\frac{2}{R_1} f\left(\frac{R_1}{2\sqrt{\tau}}\right) + \frac{R_1(2\kappa^2\tau+1)}{(2\kappa\tau)^2 - R_1^2}\right\} e^{-\frac{R_1^2}{4\tau}}} \tag{A57}$$

where R_0 and R_1 are given by Eq. (A54).